

CHAPTER ONE

INTRODUCTION

1.1 Background to the study

Environmental protection and sustainability is one of the millennium development goals and groundwater quality management is very much connected with this goal (Environmental Protection Agency, 2011). Environmental protection and safety can only be achieved when there is flexible and cost effective earth resistivity measuring devices to access the status of groundwater. The advent of technology has made the quest for water for all purposes in life to drift from ordinary search for surface water to prospecting for steady and reliable subsurface or groundwater from boreholes. Groundwater is the part of precipitation that seeps down through the soil until it reaches rock material that is saturated with water (Dingman, 2002). Soil is a sort of ecosystem, and it is relatively sensitive to foreign matter being applied to it. Soil health is defined as the continued capacity of soil to function as a vital living system, by recognizing that it contains biological elements that are key to ecosystem function within land-use boundaries (Doran and Zeiss, 2000). These functions are able to sustain biological productivity of soil, maintain the quality of surrounding air and water environments, as well as promote plant, animal, and human health (Doran *et al.*, 1996). Soil pollution happens when chemicals adhere to the soil, either from being directly spilled onto the soil or through contact with soil that has already been contaminated. As the world becomes more industrialized, the long term effects of soil pollution are becoming more of a problem all over the world. In Africa, three quarters of farm land is severely degraded (Eswaran *et al.*, 1997). These devastating effects on soil had over the years gradually led to groundwater pollution which have resulted to putting severe stress on the quality and quantity of water resources worldwide. Each year about two million people die as a result of poor sanitation and contaminated water, ninety percent (90%) of the victims are children (Anon, 2009). These

hazardous effects emanate from the presence of toxic elements of environmental concern in the waste; elements such as Lead, Cyanide, Arsenic and Chromium. Many of these metals have been found to act as biological poisons even at low concentration (parts per billion-ppb) levels (Okoronkwo *et al.*, 2005). Groundwater is considered a very important natural resource. It provides a reasonable percentage of public water supplies. In Nigeria, most rural population supply their own drinking water from groundwater and this has rescued the citizenry from acute shortage of water. As such, groundwater preservation and conservation is of paramount importance. Groundwater monitoring is a process used to determine the effects of human activities or operations on the groundwater aquifers and the soil layers bearing such water resource (Depountist *et al.*, 2005). It provides the data to measure improvement in environmental performance through surface measurement and groundwater equally served as a medium of contact between the subsurface and field equipment. Electrical and electromagnetic methods have gradually and systematically made their way to the top in the successful search of groundwater pollution. Electromagnetic survey utilizes the principle of the subsurface response to the propagation of alternating current and magnetic force. Among all the types of electromagnetic procedures, the Very Low Frequency (VLF) electromagnetic method has a unique acceptance in the exploration industries because of its accuracy, low power consumption, processing and presentation of data and eventually its ease of use. Thus, VLF measures the field strength and phase displacement around conductive geologic structures such as faults and fractures. The VLF was used to delineate the conductive zones and non-conductive zones. The purpose of electrical surveys is to determine the subsurface resistivity distribution by making measurements on the ground surface. Variation in resistance due to current flow at depth causes distinctive variations in the potential difference which provides information about subsurface structure and materials (Loke, 2001). From these measurements, the true resistivity of the subsurface can be estimated. But, the ground resistivity is

related to various geological parameters such as the mineral and fluid content, porosity and degree of water saturation in rock. The impact of pollutants like solid and liquid wastes produced by different sources (like domestic and different industries, pesticides used in agriculture) on our environment can be studied by resistivity survey. Groundwater contamination is increasing continuously by different types of pollutants (Nwankwo, 2011). Electrical resistivity methods have been used for decades in hydrogeological, mining and geotechnical investigations. More recently, it has been used for environmental surveys. The electrical resistivity method is the most commonly applied geophysical tool for groundwater exploration as it can determine aquifer thickness and depth to bedrock (Majumdar and Das, 2011). It is also capable of determining the quality of groundwater i.e., whether the water is saline, fresh or contaminated (Froese and Clement, 2005). The method is also capable of determining the subsurface flow of contaminated groundwater resulting from pollution if the polluted water has a distinctive resistivity. Characterizing and imaging the underground conditions of landfills and location of subsurface contamination has always been a challenge. Conventional environmental monitoring is used to determine the spread and fate of groundwater contamination/subsurface condition and it is performed by the expensive task of drilling closely spaced boreholes for point sampling (Adeoti *et al.*, 2010). However, this type of approach is time consuming and labour intensive (Zume *et al.*, 2006) and has led to the development of instruments and systems which collect data much more rapidly. Geophysical methods by themselves will not discover groundwater or pollution plumes but they offer invaluable assistance in determining subsurface conditions that are susceptible to groundwater or pollution plumes. It also reduces the incidence of abortive boreholes with resultant savings in cost (Olawofela *et al.*, 2012). The electrical resistivity imaging involves the injection of current into a body using dipole-dipole electrode arrangements or other configuration patterns to image the internals of the medium under investigation. Imaging techniques allows the generation of

two/three-dimensional (2D/3D) images of electrical conductivity for a given profile or volume of the ground. The technique is suitable for non-invasive investigation of landfill due to its sensitivity to high electrical contrast. The geophysical techniques deployed at every site include very low frequency electromagnetic (VLF-EM) device and electrical resistivity imaging (ERI). The decision to choose very low frequency electromagnetic and electrical resistivity imaging technique surveys as primary technique in this study are due to the reasons developed in the following discussion.

- i) The resistivity imaging technique and ground conductivity techniques map the physical property of material (electrical conductivity) in the survey. Easy correlation can be made between the data provided by each method.
- ii) Resistivity results are in the form of 2D profiles where the X-axis is a length on the ground surface and Y-axis represent the depth of investigation. Generally the resistivity profile represents a vertical slice of the resistivity value of the ground material.
- iii) The density of the data provided by these two techniques is very good. The VLF-EM survey as an example can provide about 20-30 thousand data points in a one hour survey. While the resistivity can give about 600 - 700 data points in an hour. Compared to other conventional techniques such as drilling and soil sampling, the geophysical technique provides a high density data coverage in a short time. By using parallel 2D resistivity profiles in the dumpsites and integrating the results a 3D visualization of the subsurface can be developed.

The study, tries evaluating the status of groundwater within Benin City metropolis to ascertain if the inhabitants are consuming contaminated water since most of the populace depend on groundwater because of its abundance, stable quality and quantity, and inexpensive nature to exploit. Consumption of contaminated water has resulted in epidemics and loss of many lives in many developing countries.

1.2 Water Cycle

Water is one of the most common substances known. It is a good solvent for many substances and rarely occurs in its pure form in nature. Water that is evaporated from the ocean or land surface (surface water) goes back into the atmosphere and forms cloud. Precipitation from these clouds falls over land areas and eventually flows into streams then to the sea and ocean while some infiltrates underground and becomes groundwater. Surface water is also called runoff water such as, water from the ponds, streams, rivers, seas, oceans. Surface water movement is influenced by the topography of the land surface due to the tendency of its flow from high relief (high contour values) to areas of low relief (low contour values). Groundwater is the part of the rainfall that does not immediately flow off across the land surface but sinks into the ground; this constitutes underground water or groundwater (Todd and Mays, 2005).

1.3 Sources of Groundwater Pollution

Groundwater pollution can be divided into two types, which are related to human activities and industrial activities. Pollution caused by human activities can be divided into two other sub sections: point source pollution and non point source (diffuse) pollution. Point source pollution by human activities refers to contamination originating from a single tank, disposal sites and industrial activities. Waste disposal sites, accidental spills, leaking gasoline storage tank, and dump or landfill are examples of point sources. Whereas the chemicals used in agricultural activities such as fertilizers, pesticides and herbicides are examples of non point source (diffuse) pollution (Doran *et al.*, 1996).

1.3.1 Nature of Contaminants

Contaminants can be natural or human-induced. Naturally occurring contaminants are present in the rocks and sediments. As groundwater flows through sediments, metals such as iron and

manganese are dissolved and may later be found in high concentrations in the water. Industrial discharge, urban activities, agriculture, ground-water pumpage, and disposal of waste all can affect groundwater quality. Contaminants from leaking fuel tanks or fuel or toxic chemical spills may enter the groundwater and contaminate the aquifer. Pesticides and fertilizers applied to lawns and crops can accumulate and migrate to the water table. The physical properties of an aquifer, such as thickness, rock or sediment type, and location, play a large part in determining whether contaminants from the land surface will reach the groundwater. The risk of contamination is greater for unconfined (water-table) aquifers than for confined aquifers because they usually are nearer to land surface and lack an overlying confining layer to impede the movement of contaminants. Because groundwater moves slowly in the subsurface and many contaminants are absorbed to the sediments, restoration of a contaminated aquifer is difficult and may require years, decades, centuries, or even millennia (Doran and Zeiss, 2000).

1.3.2 Soil and Groundwater Pollution Problems

Soil pollution harms plants that feed people. Chemicals can sometimes be absorbed into food like lettuce and be ingested. Other times, the pollutants simply kill the plants, which have created widespread crop destruction and famine in other parts of the world. The entire ecosystem changes when new materials are added to the soil, as microorganisms die off or move away from contaminants. Even when soil is not being used for food, the matter of its contamination can be of health concern. This is especially so when that soil is found in parks, neighbourhoods or other places where people spend time. Health effects will be different depending on what kind of pollutant is in the soil. It can range from developmental problems, such as in children exposed to lead, to cancer from chromium and some chemicals found in fertilizer, whether those chemicals are still used or have been banned but are still found in the soil. Some soil contaminants increase

the risk of leukemia, while others can lead to kidney damage, liver problems and changes in the central nervous system. Those are just the long term effects of soil pollution. In the short term, exposure to chemicals in the soil can lead to headaches, nausea, fatigue and skin rashes at the site of exposure (Klaassen, 2001). If contaminated soil is used to grow food, the land will usually produce lower yields than it would if it were not contaminated. This, in turn, can cause even more harm because lack of plants on the soil will cause more erosion, spreading the contaminants onto land that might not have been contaminated before. In addition, the pollutants will change the makeup of the soil and the types of microorganisms that will live in it. If certain organisms die off in the area, the larger predator animals will also have to move away or die because they have lost their food supply. Thus it is possible for soil pollution to change whole ecosystems. Studies have revealed that the effects of cadmium pollution in soil are significantly increasing lung cancer risk (Environmental Protection Agency, 2011). It is difficult to evaluate the health implications of the various substances found in ground water. It is obvious that ground water contain a wide variety of substances that have health implications. In addition, it is also possible that even deficiencies of certain elements may pose serious health implications (Foster *et al.*, 1986). Water contaminants may be subdivided into four major classes; physical, microbiological, chemical, and radionuclide. Though many of these chemical contaminants are unique in that some are essential in maintaining human health: whilst others are a major threat to man. Amongst the elements that are believed to play an essential role in human nutrition are calcium, chlorine, chromium, copper, fluorine, iodine, iron, magnesium, manganese, molybdenum, nickel, phosphorus, potassium, selenium, silicon, sodium, strontium, sulphur, tin, vanadium and zinc (Kirschmann and Dunne, 1984). In contrast, aluminum, cadmium, lead and mercury are definitely toxic, but in widely varying concentrations. Arsenic, however, may be an essential trace element at low concentrations, despite the fact that it is clearly harmful when ingested at higher doses. Similarly, boron may be critical in calcium

utilization by the body (Nielsen *et al.*, 1987). The quantity of human intake of any of these chemical substances obtained from drinking water is influenced by both their solubility and the nature of local bedrock geology and soils. The growing pollution posed by these chemical substances calls for public health concern. In many countries of the world studies identify health problems linked to environmental contaminants. In 2012 World Health Organization (WHO) published the results of an innovative study of the causes of cholera in most African countries, attributing it to drinking of contaminated water. In developing countries today the old killers are still around-tuberculosis, malaria, and diarrhea diseases. But joining these as important cause of death and ill health are cancers and chronic diseases caused by industrial and agricultural chemicals and other pollutants in the atmosphere, soil, and water. Lead, mercury, copper, arsenic, and other heavy metals used in industry have caused many deaths. A number of pesticides and other chemicals, known as persistent organic pollutants, which are used both in agriculture and in industry, can cause cancer and genetic abnormalities in humans. Contaminated drinking water contributes to diseases in developing and developed countries worldwide. The rising rates of diseases such as Asthma, cancers, reproductive disorders and neurological illnesses (Klaassen, 2001) are due to consumption of contaminated groundwater. According to Environmental Protection Agency (2011), the number of children and the total numbers of people with asthma are doubled every year. The percentage of women developing breast cancer and men been diagnosed with prostate cancer is on the increase. Hence, the role of people exposure to environmental contaminants is coming under increasing rate. Today, increased activities within the study area which includes industrial waste from breweries, dead and decayed organic matter in contact with the rivers, and the effect of buried pipes (rust) as well as the numerous chemical waste within the Local Government Area have drastically polluted the sources of water supply to the region and rendered it unhygienic and unsafe for drinking. Unfortunately, these were the only available

sources of water, despite the increased demand for potable water in the region due to increase in the population within the last few years. A better knowledge of the near surface aquifer distribution, formation and type in this area is therefore important so as to ascertain whether the aquifer is prone to contamination or not since the surface water have been polluted (Oseji *et al.*, 2006). Most of the side effects of industrial wastes are the possible pollution of water and the destruction of aquatic lives. These prospecting/production activities have caused several damages on vegetation, death of marine and terrestrial organisms as well as toxic effects, distributive acid rains and serious contamination of air, water and land. In many large cities and villages in the developing countries, the soil and surface water are contaminated as presented in Fig. 1.1 due to the indiscriminate dumping of contaminants.



Fig. 1.1: Snap shot of a contaminated dumpsite in Benin City

1.3.3 Safe and Wholesome Water

Water is an excellent solvent. It can contain lots of dissolved chemicals. Since groundwater moves through rocks and subsurface soil, it has a lot of opportunity to dissolve substances as it moves. For that reason, groundwater will often have more dissolved substances than surface water will (Doran and Zeiss, 2000).

Even though the ground is an excellent mechanism for filtering out particulate matter, such as leaves, soil, and bugs, dissolved chemicals and gases can still occur in large concentrations in groundwater to cause problems. Groundwater can get contaminated from industrial, domestic, and agricultural chemicals from the surface. This includes chemicals such as pesticides and herbicides that many homeowners apply to their lawns. Contamination of groundwater by salt spread on road is of major concern in northern areas of the United State (Environmental Protection Agency, 2011). Salt is spread on roads to melt ice and with salt being so soluble in water, excess sodium and chloride is easily transported into the subsurface groundwater. The most common water-quality problem in rural water supplies is bacterial contamination from septic tanks, which are often used in rural areas that don't have a sewage-treatment system. Effluent (overflow and leakage) from a septic tank can percolate (seep) down to the water table and maybe in a homeowner's own well. Just as with urban water supplies, chlorination may be necessary to kill the dangerous bacteria. Internationally water intended for human consumption should not only be 'safe' but must also be 'wholesome'. Safe drinking water is one that can protect the consumer from harmful substances, even when taken over a prolonged period. Water may be safe, but if it has an unpleasant taste or appearance it may drive the consumer to other safer sources. Drinking water therefore, should be completely safe and must also be agreeable to use or wholesome. Safe and wholesome water is defined as water free from harmful and chemical substances, from pathogenic agents and finally pleasant to the taste and fit for use for other domestic purposes. Water is said to be contaminated when it contains toxic or harmful substances above the maximum contamination level (Environmental Protection Agency, 2011).

1.4 Study Area - Benin City

Benin City consists of three senatorial districts (Edo North, Edo Central and Edo South) with eighteen Local Government Areas as shown in Fig. 1.2.



Fig. 1.3: Snap Shot of Ikhueniro Dumpsite



Fig. 1.4: Snap Shot of Capitol Dumpsite



Fig. 1.5: Snap Shot of Oluku Dumpsite

1.4.1 Climate and Vegetation of Benin Land

The vegetation over a geographical area is essentially a response to the climate in that area. Benin land in Edo State falls within the tropical rain forest zone of Nigeria which subsequently gave way to very thick vegetation that is stratified with the much thicker vegetation occurring along river channels and this normally typifies primary vegetation while the presence of grassland with sparse trees and shrubs typifies the secondary vegetation pattern within the vegetation belt. The vegetation has been destroyed by the activities of man such as bush burning, farming, construction and local mining. Benin land is drained by the meandering river Ikpoba in the South with some which flows in the southwest direction. The elevation contrast observed resulted into the generation of pressure as the river flows and this had subsequently led to the formation of sheet erosion that was noticed in the western part of the area. The Southern part of Ikpoba land is flooded seasonally while in the other parts that are not prone to flood the nature/shape of the surface is related to the drainage characteristics. The Eastern and Southern part of the study area is characterized by brownish clay formation. Edo land is accessible through numerous road network and footpaths, which also serve as links to the neighboring villages. There is no visible rock outcrop within the area. During rainfall, there is a relatively high rate of infiltration into the subsurface through the unconsolidated soil in the Northern, Western and Central part of the study area as shown in Benin region geological formation Fig. 1.6. This reduces surface run-off. The inhabitants of the area are mostly subsistent and peasant farmers. However, with the advent of the companies (breweries) within Ikpoba Okhia, other micro-businesses within Benin land and the establishments of Government institutions, most people diverted from farming to working in these companies and Government parastatals (Akujieze, 2004).

1.4.2 General Geology of Study Area.

Edo State is situated in South-South part of Nigeria, it is part of Niger Delta province. Niger Delta is perhaps the most important sedimentary basin in the country. It is made up of ecological zones such as sandy coastal ridge barriers, saline mangroves, seasonal swamp forest and lowland rainforest (Short and Stauble, 1967 and McCurry, 1976). The Benin Region is underlain by sedimentary formation of the South Sedimentary Basin. The geology is generally marked by top reddish earth, composed of ferruginized or literalized clay sand. The sediments spread across the southern fringes of the Anambra Basin and marking the upper facies off-flaps of the Niger Delta. Tattam (1943) used the name Coastal plain sands to describe the formation of red earth underlain by sands and clays that mark an ancient coastal plain environment now exposed in Calabar, Owerri, Onitsha and the Benin Region with the age Oligocene-Pleistocene. However Reyment (1965) reinstated the name Benin Formation to identify the reddish-brown-yellow generally white sands often with clayey and pebbly horizons with type-locality around Benin. The formation was further established by well logging of Etete 1, well drilled on-shore east of River Niger by Shell Petroleum Development Company (SPDC) Nigeria. The formation is about 1830m thick at the seashore but thins landwards. Geologically, the Benin Region comprises of the Benin Formation (Fig. 1.6) alluvium; drift/top soil and Azagba-Ogwashi (Asuba-Ogwashi) formation (Akujeze, 2004).

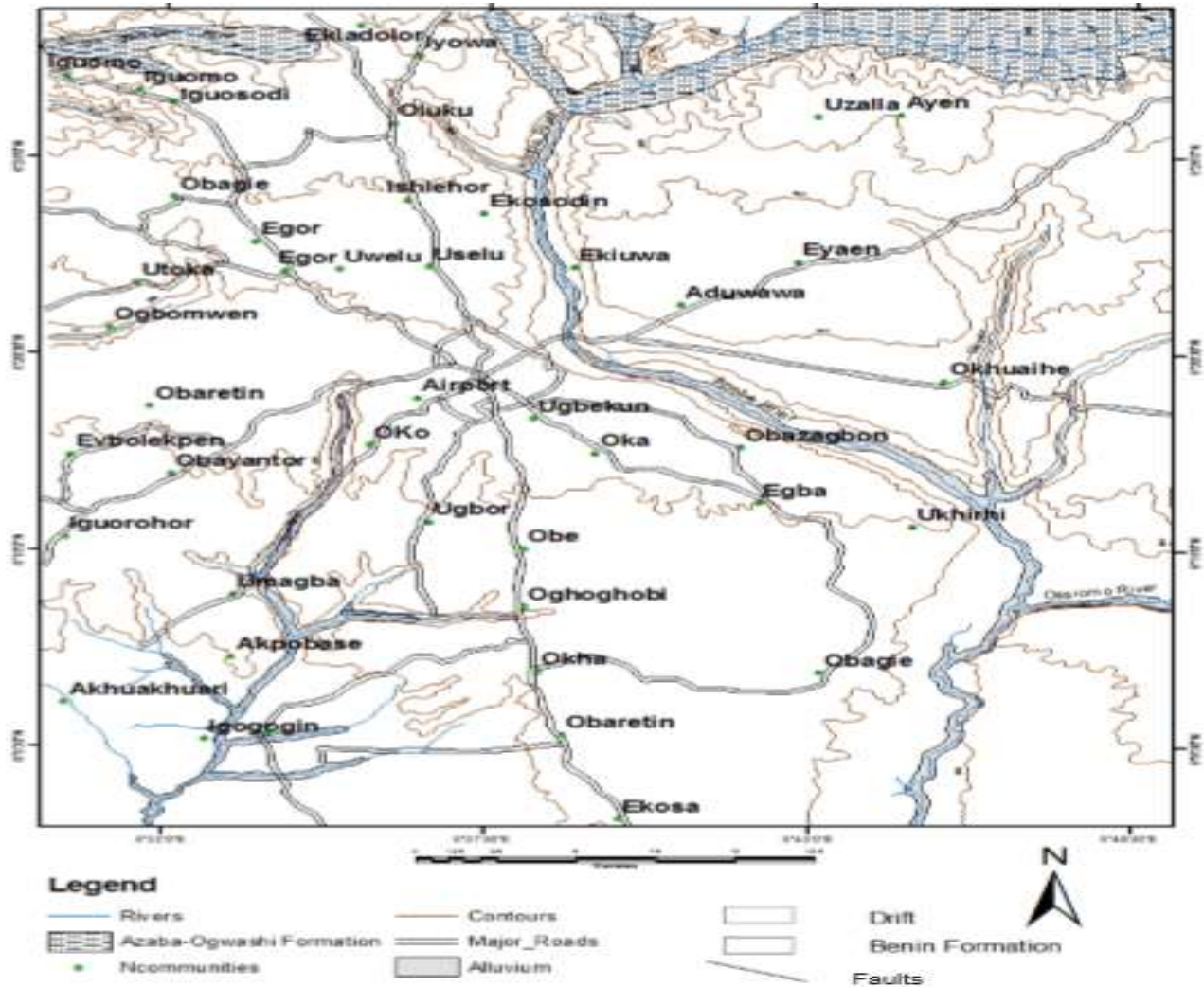


Fig. 1.6: Benin region geological formation (source: Akujieze, 2004).

1.4.3 The Benin Formation

It is assigned to the Oligocene-Pleistocene period in the continent of Africa and to the Oligocene-Pleistocene recent at the sub-oceanic (Short and Stauble 1967). The formation is characterized by top reddish to reddish brown lateritic massive fairly indurate clay and sand. This is often marked with reticulate mud racks. This caps the underlying more friable pinkish-yellowish white often gravelly-pebble sands clayey soils, sands and clay (Akujieze 2004). The sedimentary sequences are poorly bedded with discontinuous clay horizons at various depths. It is estimated to be about 800m thick under Benin City and about 1,830m near the sea shore sections of the formation. They

are exposed at various erosion sites, sand quarry sites, and road cuttings. The Benin formation covers 95% of the region.

1.4.4 Alluvium

These are found along Ikpoba and Ovia flood plains. They are made up of grayish-dirty white-yellowish-white sands, silts, clayey sands, gravels and even wood-plant materials (Akujeze, 2004). These have been washed down the river valley and deposited at the river banks. They are recent deposits.

1.4.5. Drift/Top Soil

Drifts are sediments still in the process of transportation or movement. They are made up of light brown-yellowish silt, mudflows and sands derived from the weathering of the parental Benin Formation. Drifts are washed down by fluvial agents especially the storms and floods dominating the wet season of the region. The drifts are not part of the solid geology. But they are mainly derived and reworked materials and loads dropped by moving floods. Drifts cover roadsides; fill up areas, concealing the underlying geology (Short and Stauble 1967).

1.4.6. Ogwashi-Asaba Formation

The Ogwashi-Asaba Formation consists of clays, sands and grits and seams of lignite alternating with gritty clays. It grades upwards into the Benin Formation. The Ogwashi-Asaba Formation is exposed in stream channels at the northern parts of the Benin Region, west of Ekiadolor-Iwu and 4 km east of Utekon and north of Azalla (Akujeze, 2004).

1.5 Electrical Properties of Rocks and Minerals

The electrical properties of rocks and minerals in the upper part of the Earth's crust depend primarily on the porosity, permeability, degree of water saturation and clay content. An increase in porosity typically leads to increase in water content and permeability, which reduces the electrical

resistivity of the subsurface materials. The presence of clay minerals in a water-bearing rock formation will increase the conductivity of the formation through ion-exchange process. Changes in this property, called resistivity of the layers in an inhomogeneous medium, results in variations between the applied current and the potential generated as measured on the surface. Measuring the resistivities of the unknown layers of the subsurface is very important in identifying the properties of such materials at the various layers (Herman, 2001). The resistivity of rocks is strongly influenced by groundwater, which act as an electrolyte. Resistivity is one of the most variable of physical properties. Porosity is the major control of the resistivity of rocks, and resistivity generally increases as porosity decreases (Kearey *et al.*, 2002). The salinity of the water in the pores is probably the most critical factor determining the resistivity. When porous rocks, particularly those with large concentrations of graphite or magnetite, lie above the water table at shallow depths, or when they occur at such great depths that all pore spaces are closed by ambient pressure, the conduction through them takes place within the mineral grain themselves. Under this condition the resistivity of the rock will depend on the resistivity of the grains. When the pores are saturated with fluids, it will be governed by the fluid resistivity as well. The conductivity of a sediment increases with the amount of groundwater it contains. This depends on the fraction of the rock that consist of the pore spaces and the fraction of this pore volume that is filled with the water. The resistivity measurement of unknown layers of the subsurface has the potential for being very useful in identifying the materials at the various layers, because it gives detailed information (Loke, 2004). Electrical methods are defined by their frequency of operation, the origin of the source signal and the manner by which the sources and receivers are coupled to the ground. Signal frequencies range from a few Hz in direct current (DC) resistivity measurements up to several GHz in ground-penetrating radar (GPR) surveys. Sources and receivers can be coupled to the ground through electrodes. The major progress in electrical resistivity measurement depends on the ability

to determine changes in the electrical path caused by these resistors and, ultimately, be able to determine their locations, depths and thicknesses. If the earth is homogeneous, the resistivity measured is called true resistivity, otherwise, the term apparent resistivity is used and this is the weighted average of the resistivities of the various formations (Osemeikhian, and Asokhia, 1994). The current-carrying medium is usually an aqueous solution of salts distributed through a complex structure of interconnected pores and fractures. Ions that conduct current in an electrolyte result from the dissociation of salts dissolved in water. Since each ion can only carry a finite quantity of charge, the more ions available in an electrolyte, the greater the charge that can be carried. An increase in temperature enhances the mobility of ions, which results in decreases of resistivity (Kearey *et al.*, 2002). Since temperature variations in the subsurface are generally small, this influence is usually negligible. The presence of clay minerals decreases the resistivity of water-bearing rock significantly through ion-exchange processes (Ward, 1990). In general, hard rocks are poor conductors of electricity, but geological processes can alter rock to reduce resistivity. Weathering, dissolution, faulting and shearing can increase the porosity and permeability of rock, and hence decrease resistivity. By comparison, compaction of sedimentary rock and metamorphism of all rock types may result in lower porosities and permeability. Resistivity is, therefore, a widely varying parameter, not only from lithology to lithology, but also within a particular formation. The range of resistivity values for common near-surface earth's materials varies widely from 0.1 - 10,000 Ω m and is given in (Fig. 1.7). Igneous and metamorphic rocks typically have high resistivities. Processes such as hardening by compaction or metamorphism, and precipitation of calcium carbonate or silica reduce the porosity and fluid permeability of the rock formation and hence reduces the conductivity. Sedimentary rocks, on the other hand, are generally more porous and permeable than igneous and metamorphic rocks. The resistivity, of sedimentary rocks is highly variable and usually low.

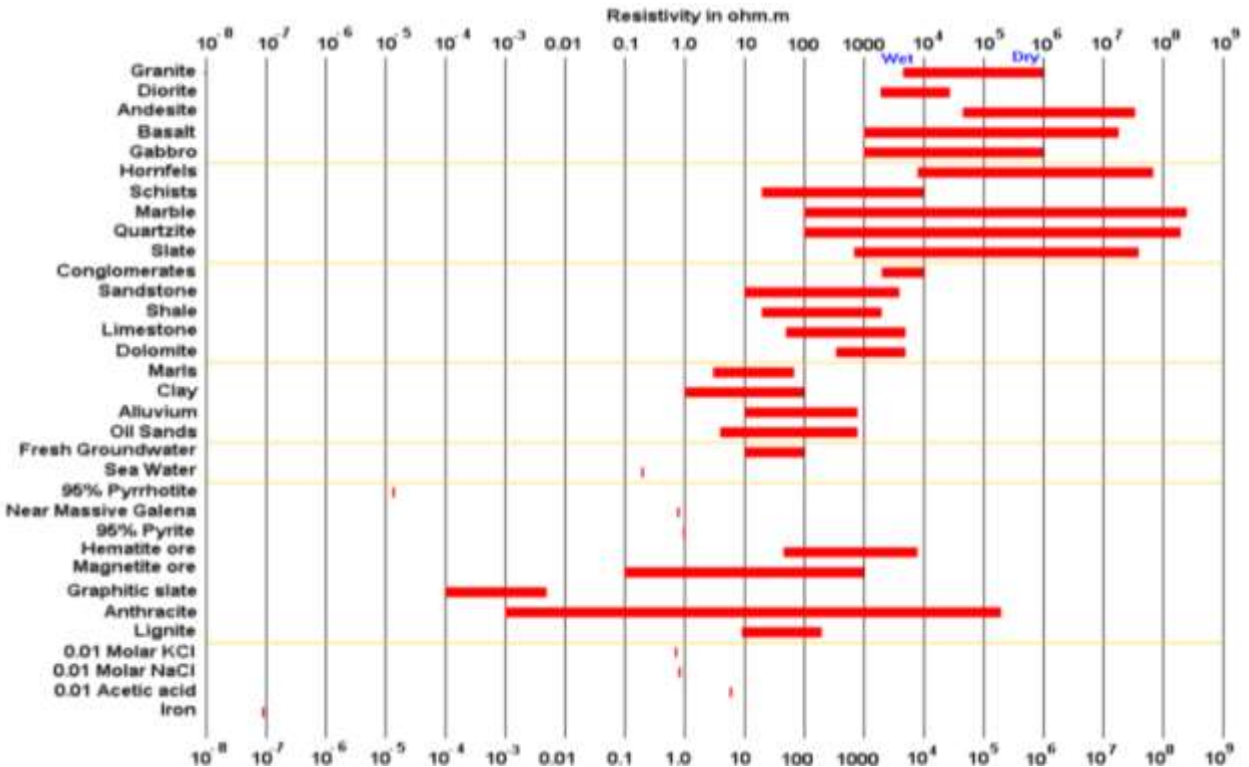


Fig. 1.7: Typical ranges of electrical resistivities/conductivities of earth materials (Loke, 2004).

However, if the pore spaces are not connected, as in basalt there would be no closed paths for the conduction of electric current through the rock. This would result in low permeability and high resistivity in the rock mass. Texture may also have a strong influence on resistivity. Pore space that contains electrolytes provides the means for current conduction through a rock. In general, sedimentary rocks conduct better than either igneous or metamorphic rocks. However, the resistivity range of any given rock type is wide and overlaps with other rock types. However, if the pores are not connected to each other (i.e., so-called unconnected or dead-end pore space), no closed path for current conduction can be formed, thus resulting in low permeability and high resistivity of the rock. A typical example of a high porosity rock with low conductivity due to its low permeability is basalt as shown in Figure 1.8f.

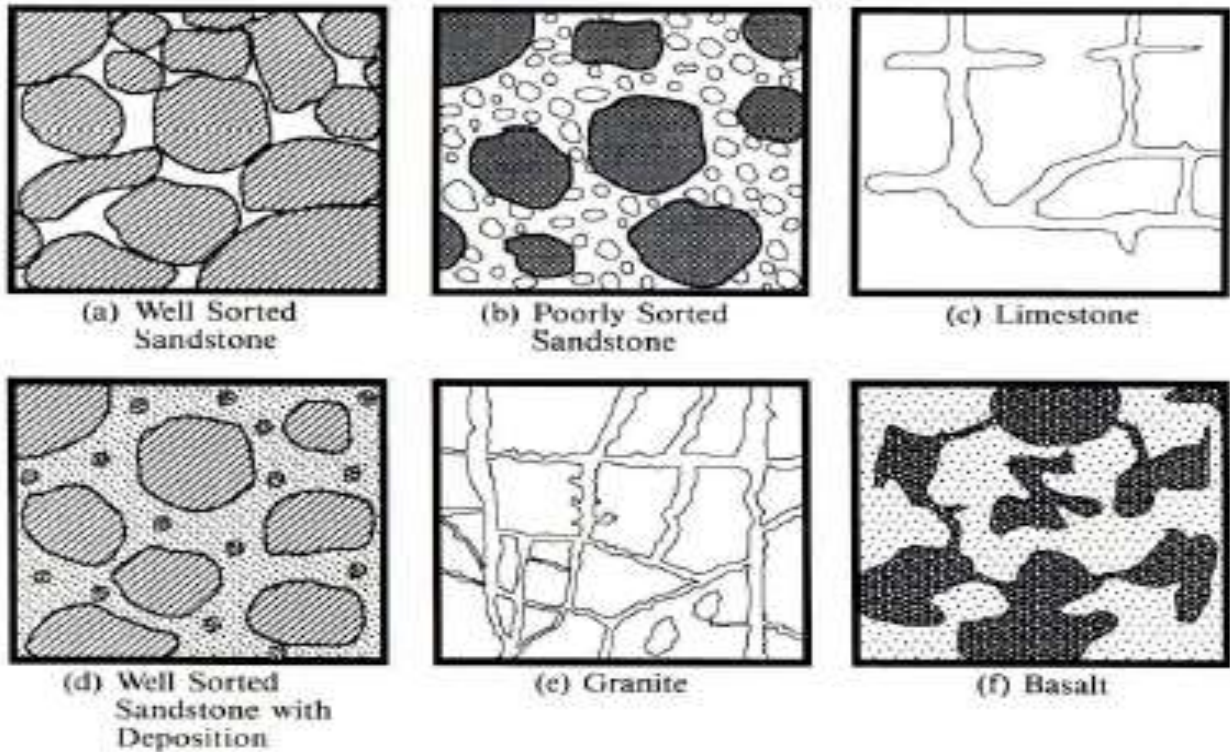


Fig. 1.8.: Various textures of rocks (Ward, 1990).

1.6 Statement of Research Problem

In Edo State, a few kilograms of municipal and domestic waste are produced per day, in each family. This waste is collected and transported from the town to municipal landfills where it is deposited without considering the environmental hazard. In the last decade, the increasing public concern with groundwater management problems due to waste disposal has generated significant hydrogeological and geochemical research in some part of the country to determine the state of our groundwater because water is essential for livelihood as well as socioeconomic development of any country. Many communities in Edo State rely on surface and groundwater for domestic, recreation and agricultural purposes and majority of these water sources are not treated to World Health Organisation Standard. In another vein, various groundwater exploration programs (1-D electrical resistivity profiling and sounding with four electrodes) that have been carried out in Benin City have not yielded the desired results in terms of success with regards to delineating the

lateral extent of contamination zones due to poor methodological approach and obsolete equipment which has contributed negatively to the failures of most groundwater projects and wrong siting of boreholes within Benin City. Moreover, lack of literature or document on the activities at the dumpsites coupled with the fact that the hydrogeological setting of Benin land is the least investigated, despite its closeness to the oil companies. Very little is known and documented to date as the hydrology of the area. In the past, the residents of Benin land depended on the slow-running rivers and hand-dug wells for their domestic water needs but today increased activities from companies and industrialization did not only increase the population of the area but drastically pollute the source of water supply and rendered it unfit for use. With the increasing awareness of guinea worm, diarrhea and other water borne diseases associated with untreated surface water the need to harness new groundwater sources becomes imperative in the country. Only few homes in Benin City could afford the treated water for consumption and other commercial purposes. This research is driven by the need for more efficient, environmental friendly and cost-effective integrated geophysical methods to ameliorate the environmental problems of dumpsite pollution within Benin City.

1.7 Aim and objectives of the study

The aim of this work is to employ integrated geophysical studies for environmental assessment of municipal dumpsites in Benin City, Edo State, Nigeria.

The objectives are to use integrated geophysical methods to:

1. delineate the near surface aquifers
2. locate weak zone for infiltrating surface water pathways and delineation of contaminant plumes
3. delineate the depth and lateral extent of groundwater contamination
4. Predict run off direction from the topographical contour map of the study area.

1.8 Scope and Limitation of the Study

This work covers three major government approved dumpsites in Benin City located in the midst of residential buildings. The research study is concerned mainly with the use of a more realistic, efficient and practical 2D data acquisition geometry for geoelectrical resistivity surveys in environmental investigations. The conventional Dipole-dipole electrode configuration is used to generate apparent resistivity data models and evaluate the subsurface within the study areas. The study is limited to interpreting subsurface features favourable for dumpsite contamination. The 3D geoelectrical resistivity images were obtained using parallel 2D lines (a set of 2D lines in one direction). The current electrode spacing was limited to a maximum spread of 168m for electrical resistivity tomography and 150 - 350m for the VLF electromagnetic survey. The VLF ABEM Wadi with frequency ranges from 17.5 - 27.5KHz and SuperSting R8/IP with 84 electrodes was used in this research to gather geophysical data. For the purpose of this research the SuperSting R8/IP was only limited to earth resistivity measurement and the sensor used was steel electrodes.

1.9 Significance of the Study

No research work has adequately addressed the present study objectives and applied integrated geophysical methods in the study area, though geophysical exploration projects have been carried out in Benin City using classical approach of resistivity surveys by researchers and students with a view of assessing the groundwater potential of the area. No meaningful research had been targeted toward environmental studies in the area. The results of the present study would therefore shed light, address and recommend appropriate measures to reduce endemic and epidemic disease derived from consumption of contaminated water and the adverse effects on individuals and all nations. The results of this study will also serve as a referenced document to future researchers and pave way for appropriate recommendations on areas where boreholes could be cited in Benin City to avoid abortive and contaminated boreholes.

CHAPTER TWO

LITERATURE REVIEW

2.1 Review of Related Literatures

Geophysical methods, have gained an increased popularity because of their ability to map hydrologic properties. Various authors have described the geology of the Niger-Delta: (Hospers 1965; Reyment 1965; Short and Stauble 1967; Maron, 1969; Avbovbo, 1970; Burke 1972; Oomkens 1974; Assez, 1976; Kogbe and Assez; 1979; and Akpokodje 1979).

Alkali, (1995) carried out resistivity measurements of the upper aquifer system around Lake Alau area and the result revealed only two water bearing horizons within the upper system of the Chad Basin.

Ezeigbo and Obiefuwa, (1995) identified three aquifer systems in the Ogbunike area and environs of Anambra State. These were the upper unconfined, the middle semi-confined and the lower confined aquifer system.

Etu-Effeotor, (1997) carried out a geophysical investigation for groundwater in part of eastern Niger-Delta and the result shows that the depth of the fresh-salt water interface ranged from 30.0 m to 42.0 m and 4.0 m to 30.0m with an average depth of 34.1m below the ground surface at Degema and Buguma respectively.

Meju, (2000) used electrical resistivity method in the delineation of landfills, the results obtained were quite encouraging. The main reason for the increasing interest in using geophysical methods in hydrogeological studies is that geophysics provides spatially distributed models of physical properties in regions that are difficult to sample using conventional hydrological sampling methods (Martinho *et al* 2006).

Oyedele, (2001) carried out a hydrogeophysical and hydrogeochemical analysis of groundwater quality in some parts of Lagos State, Nigeria and delineated two probable zones of intermediate and good quality fresh water at Victoria Island and Iwaya based on resistivity measurement.

Ufuah *et al.*, (2004) carried out water analysis along Ikpoba River in Edo State. The grab sampling techniques were used for sample collection. The result revealed that the turbidity, apparent colour and true colour were seasonal dependant but there were insignificant variations in the other parameters determined.

Triantafilis *et al.*, (2006) applied geophysical methods direct current (dc) resistivity techniques to demonstrate the inversion using a 1-dimensional inversion algorithm with lateral constraints of the apparent electrical conductivity measured in the horizontal coplanar and perpendicular coplanar arrays of a EM induction probe to develop a two dimensional model of the true electrical conductivity within a soil landscape southeast of Sydney in Australia. The research was to assess the public health risk and potential ecological impacts and the knowledge of the area and hydrogeological settings in which waste is disposed. The results from 2D models revealed that the soil is contaminated.

Pantelis *et al.*, (2007) conducted an integrated suite of environmental methods to characterize the hydrogeological, geological and tectonic regime of the largest waste disposal landfill of Crete Island, the Fodele municipal solid waste site, to determine the geometry of the landfill (depth and spatial extent of electrically conductive anomalies), to define the anisotropy caused by bedrock fabric fractures and to locate potential zones of electrically conductive contamination. A combination of geophysical methods and chemical analysis was implemented for the characterization and management of the landfill. Five different types of geophysical surveys were performed: 2D electrical resistance tomography (ERT), electromagnetic measurements using very low frequencies (VLF), electromagnetic conductivity (EM31), seismic refraction measurements

(SR), and ambient noise measurements. The above geophysical methods were used with the aim of studying the subsurface properties of a landfill and to define the exact geometrical characteristics of the site under investigation. The findings indicate the importance of using an integrated approach of geophysical techniques for acquiring the physical properties of the landfill. The employment of different techniques allows the resolution of possible discrepancies and the most accurate description of landfill characteristics.

Groundwater pollution in the vicinity of a landfill site in Nagpur, India was assessed with the help of resistivity imaging and GPR tools (Paras *et al.*, 2007). The resistivity imaging survey indicates high conductive anomalies in the topsoil as well as the underlying fractured rocks. Significant reflections from the GPR records are extracted with the help of maximum peak module and Hilbert transform module. These reflections can be attributed to presence of fractures, which are potential pathways for migration of the fluid. The geophysical findings are strengthened by the results of groundwater analysis from wells located close to the profile where resistivity and GPR survey have been carried out. The study has indicated the vulnerability of the unconfined aquifer underlying the predominantly clay layer.

Otobo *et al.*, (2007) investigated existing waste dump sites in Delta State without soil disturbance by using the vertical electrical sounding (VES). The soil overlying the aquifer at Ovwian-Aladja dump site has resistivity values ranging from 11.84 - 85.50 Ohm-m, thicknesses, 21.10-31.83m and at depths less than 1m, while at Warri it has resistivity values, 160 - 1074 Ohm-m, thicknesses, 1.53 - 7.87m, and at depths less than 1m. The soil overlying the aquifers in the dump sites have been identified and were found to be contaminated.

Elijah *et al.*, (2009) carried out 1D and 2D electrical resistivity methods to map aquifers in a complex geologic terrain of foursquare camp at Ajebo, South-western Nigeria to locate the sites for water supply and to adduce reason (s) for failure of most boreholes drilled there. Results from

twenty four (24) VES points show 3 – 4 geoelectric layers, which are weathered/fractured rocks of resistivity range from 68 – 394 Ω m with thickness range of 3.4 – 14.8m. Only two VES stations have aquifer thickness above 14m. However, results of eight (8) 2D resistivity imaging in the areas show about two points where productive boreholes could be sited. The results showed that the tomography/2D resistivity imaging gives a better lateral view of the subsurface layers than geoelectric section from 1D because of its ability to give a continuous record of subsurface image. Nasir *et al.*, (2010) carried out direct current electrical resistivity survey in Unguwan Dosa open dumpsite in Kaduna metropolis, North Western Nigeria. The dumpsite is the typical non-controlled waste facility that lack bottom liner. Eight vertical electrical soundings (VES) employing the Schlumberger electrode array were conducted with maximum electrode spacing of 100 m. Interpreted resistivities were obtained by iterative computer modeling of the apparent resistivity data. The VES data were plotted as pseudo and resistivity cross-sections in order to look at the spatial distribution of the contaminant plumes. The interpreted VES data measured inside the dumpsite showed contamination plumes as low zones with resistivity values ranging between 1 and 12.9 ohm-m extending from the surface down to the aquifer of shallow groundwater of less than 5m. The geologic sections revealed the various lithological compositions of various layers delineated. The generated pseudo and resistivity cross-sections showed leachate plumes extending below the water table, thus polluting the groundwater. A conclusion supported by the water quality analysis from existing hand dug wells which showed concentrations of organic/inorganic parameters exceeding permissible limits. The high concentration of detrimental heavy metals (lead, cadmium and chromium) was an indication of toxic or hazardous substances in the leachate. This is a major threat to human population, especially those within the area.

Electromagnetic (EM) techniques are used to map salt water intrusion in coastal aquifers (Adeoti *et al.*, 2010). If interpreted separately, these geophysical data sets only provide images of a certain

hydrologic property in space or time. However, the methods do not provide an explanation with regards to the physical processes underlying the distribution of the mapped hydrologic property, which is essential to make predictions for the hydrologic system under different management scenarios. For this purpose hydrologic models are needed. Numerous papers have been published about the inclusion of geophysical data for hydrogeological site characterization. The resistivity techniques have been successfully used in investigating groundwater potential in different geological settings.

Sahadat *et al.*, (2011) carried out enhanced leachate recirculation (ELR) landfills designed and operated for rapid waste stabilization, waste decomposition and increased rate of gas generation. The fundamental process improvement involved in the operation of ELR landfills is the addition of water and/or the recirculation of leachate into the landfill waste mass. The study of moisture movement within municipal solid waste due to leachate recirculation plays an important role in developing the design and optimizing the operation of a leachate recirculation system. The research examined the test results of moisture distribution and moisture movement within the landfill in Denton, Texas, USA. The study is performed using resistivity imaging. The City of Denton landfill uses horizontal recirculation pipes for the water addition and leachate recirculation. A series of resistivity imaging tests were performed at the City of Denton landfill. First set of tests was performed along the recirculation pipes to identify the vertical moisture movement through individual pipes during recirculation. The second set of tests was performed across the recirculation pipes to determine the zone of lateral moisture movement due to horizontal leachate recirculation system. The preliminary results show that the moisture movement can be mapped using resistivity imaging. Based on the test results, it can be observed that resistivity imaging techniques could be successfully employed to monitor the moisture movement within the solid waste due to leachate recirculation.

Ibitola *et al* (2011) examined the impact of solid waste disposal on the groundwater within the vadose and saturated zone of two dumpsites: Aba-Eku and Ajakannga in Ibadan Metropolis was investigated using Vertical Electrical Sounding (VES) to determine the depth and thickness of subsurface layers. Both qualitative and quantitative interpretations of the field data were carried out from Vertical Electrical Sounding (VES). The qualitative interpretation reveals points of anomalous resistivity along the traverses of 10m station separation. Partial curve matching and computer assisted iteration techniques were used for the interpretation of the VES data. The result from the VES data gives a qualitative lithology of topsoil and clayey soil which has a low resistivity zone < 100 Ohm-m, underlain by higher resistive basement. The combination of both interpretations obtained from geophysical survey and the digital elevation map was used for the establishment of the environmental and health hazards associated with groundwater movement within the subsurface (vadose and saturated zones) along the two dumpsites. Therefore, the open waste disposal sites in Aba-Eku and Ajakannga are summarised to produce negative impacts on the quality of ground water. The data obtained from the geophysical and topographical studies of these 2 dumpsites indicates danger to the underground water in the neighbouring communities.

Majumdar and Das, (2011) used geophysical method in estimation of the spatial correlation structure of hydraulic properties in a dumpsite, the results revealed the geological structures and hydraulic pressure within the study area.

Dijkstra, *et al.*, (2012) investigated changes in porosity in saturated silica sand using electrical resistivity probe for physical model testing. For non-conducting particles, electrical resistivity measurements in porous media actually measure the resistivity of the pore water, changes of which are directly related to porosity change. The sensor has been integrated in a measurement probe and a model pile to measure density changes continuously during penetration. The first implementation used in the geotechnical centrifuge shows the feasibility of the method, although the initial results

also show some systematic errors resulting from the construction of the probe and the measurement method itself. The method shows promising results when used for capturing the soil density change near a model pile which is fully surrounded by soil.

Dharmadhikari *et al.*, (2012) conducted an experimental setup used for detection of geopathic stress. It highlights the underground water as one of most important factor to generate geopathic stress. Such underground water locations and geopathic stress zone are interrelated. First time, detection of geopathic location has been done using dowsing and geo-resistivity meter method. It is found that, inside geopathic stress copper L rods gets deflected. Electrical resistivity decreases as water content increases. From the comparative study of resistivity technique and L rod dowsing, we can authenticate dowsing. The authenticity of dowsing will help us in the study of investigation of Geopathic stress. It will also help us to find water veins in the ground and hence provide a quicker method for detection of water. Presently, due to congested building arrangement the technique of resistivity meter is very lengthy and requires large area (as spacing of electrodes is equal to depth of investigations). But the dowsing by L rods is more suitable for these areas. Also it is a faster method and can be used in built-up structures where the resistivity technique cannot be used.

Alile *et al.*, (2012) carried out geophysical survey involving the use of resistivity sounding method to investigate the geoelectrical layers of groundwater resources in Obaretin, Iyanomon and Orhionmwonbor, in Ikpoba Okha Local Government Area of Edo State, Nigeria. Three vertical electrical sounding (VES) locations were carried out in the study area. The vertical electrical sounding was done using the Schlumberger electrode array and the linear filter method of interpretation was adopted. A correlation of the interpreted curves with the lithologic log from the borehole sections in the study area suggests that the major lithologic layers penetrated are laterite, clay, sand (sandstone) and sandy clay from basic depth interval as shown by the geoelectric section.

The sandstone layer which is the aquifer zone lies between the depth of 59.80m to 85.80m for VES 12, 63.16m to 89.36m in VES 28 and 69.36m to 95.37m for VES 14. Therefore, the depth to water table in the study area has a maximum drill depth within the range of 60m to 100m.

Olawofela *et al.*, (2012) carried out Electrical Impedance Tomography (EIT) which is a purely a medical imaging technique, for imaging and detecting underground contaminants in landfill sites in Abule Egba and Solous 1 dumpsites in Lagos, Nigeria. Conventional electrical imaging technique using Wenner configurations was also carried out on each of the sites in order to validate the EIT results. The conventional electrical resistivity data was inverted using software to obtain 2D resistivity structures. With the aid of the 3D impedance tomograms, two distinct contaminant plumes were mapped and identified within and around the landfills. These are highly conductive leachate contaminant plumes with conductivity values ranging from 1,000 to 5,000 S/m and highly resistive gaseous contaminants (with negative conductivity values on the tomograms) which are probably due to landfill gases as a result of the anaerobic decomposition of the landfill organic wastes. These contaminants are migrating in depths and distance away from the landfills into the aquifer. The study shows that the soil and groundwater system had been contaminated beyond the depth of 50 m in the study areas.

Andre *et al.*, (2012) carried out a geophysical survey in a contaminated site from a downstream municipal solid waste disposal site in Brazil using a 3D resistivity and induced polarization (IP) imaging technique. The purpose was to detect and delineate contamination plume produced by waste. The area was selected based on previous geophysical investigations, and chemical analyses were carried out in the site, indicating the presence of a contamination plume in the area. The resistivity model successfully imaged the waste presence, water table depth, and groundwater flow direction.

Ogungbe *et al.*, (2012) examined the contaminant impact of a municipal solid waste (MSW) landfill on groundwater at Solous III landfill site, Lagos, Nigeria with the aim of identifying the presence of any possible contaminants at the site. Two (2) profiles each were conducted at 15m locations on the site. The inversion of the data was accomplished using the electrical impedance and diffuse optical reconstruction software version 3.0 tool kits for MATLAB to obtain three-dimensional conductivity profiles called tomograms. From this result, it shows that there has not been much impact of leachate on the groundwater at Solous III landfill site.

Sunmonu *et al.*, (2012) carried out surface geophysical survey around Aarada refuse dumpsite, Ogbomosho, Oyo State, Nigeria to locate leachate plumes migration pathways using very low frequency electromagnetic and vertical electrical sounding techniques. Eight VLF-EM profiles of length 70 to 150m with 10m inter-station spacing and seven Vertical Electrical Soundings with current electrode separation varying from 150 to 200m were established. The analyzed VLF-EM data revealed the presence of conductive pollutants (leachate plumes) at the subsurface while the geoelectric sections generated from the processed VES data showed that the leachate plumes have actually migrated to a depth of 5.4m in the area which confirmed the VLF-EM results. The study reveals the importance of using an integrated approach of geophysical techniques for acquiring the physical properties of a waste disposal site. The employment of different techniques allows the resolution of possible discrepancies and reveals the most accurate description of a waste disposal site's characteristics.

George *et al.*, (2012) carried out a geophysical survey in Chalkidiki (Northern Greece), the objective of the geophysical survey was to study the general geological conditions of the area (stratigraphy and tectonism) and to focus on the hydrogeological behaviour of the geological formations in the area. The ultimate target was to point out the most promising locations for the successful construction of hydro wells. Since direct hydrogeological information was not available,

three different geophysical techniques were applied in order to follow a step by step approach to the exploration of the study area. Firstly, the Very Low Frequency (VLF) electromagnetic method was applied since the majority of the area was dominated by the formation of ophiolites and water flow was possibly expected only in fractured zones at a relatively small depth. Secondly, at the locations of the conductive zones detected by the VLF survey an additional Electrical Resistivity Tomography (ERT) sections at different scales were measured to provide more detailed information about the geometrical characteristics of the site. Finally, Self-Potential (SP) measurements along the same profiles were conducted in order to provide supplementary information concerning the nature of the conductive zones such as the possible relation with electrokinetic sources. The combined interpretation of the geophysical data proved very efficient for deciding the most promising locations for the construction of hydro wells.

Arlena., *et al* (2012) used geoelectrical measurements to detect groundwater pollution and to identify the conditions of soil and groundwater near the coal waste disposal “Panewniki” Halemba-Wirek Coal Mine. The first applied method was the VLF (Very Low Frequency) technique. The method utilised military signals, to perform the in-phase and the quadrature maps of the areas. Data were collected from four study areas located near the coal waste dump. Observed anomalies on both maps for each area showed places with different conductivity allowed to detect the contaminated and uncontaminated zones. The VLF survey indicated that the contamination occurs in the eastern part of study area and is characterized by positive values of both measured electrical fields (the in-phase and the quadrature components). After preliminary contaminated zones were recognized using VLF method, an electrical imaging method was applied. Two electrical imaging profiles were carried out near the waste dump. The measurements allowed to create the geoelectrical model of surrounding area and to investigate the leachate plume. The electrical

imaging showed that the greatest pollution occur in the area immediately adjacent to the coal waste which is confirmed by VLF survey.

Hussein (2013) used ERI technique at the University of Technology Indian site implementing the three common arrangements (Wenner, Wenner-Schlumberger and dipole-dipole) to characterize the subsurface. Different resolving powers were obtained for the used arrays. Wenner-Schlumberger array gives moderate number of possible measurements and has a median depth of investigation of about 10% larger than that for the Wenner array. It is moderately sensitive to both horizontal and vertical structures, thus it might be a good compromise between the Wenner and the dipole-dipole arrays. Good agreements were obtained between the stratigraphic columns of the site with the inversion models using the different arrays. The distribution of resistivity of the inversion models for the study site reflects the highly inhomogeneous subsurface soil with a wide variation of soil resistivity at different depths.

Yalo *et al.*, (2013) used electromagnetism (EM34) and electrical resistivity tomography (ERT) to evaluate the infiltration of leachate in Benin because the presence of dumpsite of rubbish can cause pollution of the groundwater. Indeed, the leachate resulting from the seepage of rain water into rubbish can infiltrate and pollute the water table. The electromagnetic map circumscribed the lateral limits of the leachate diffusion and the electromagnetic surveys showed that it infiltrated with a depth of 20m. The two cross sections of electrical resistivity tomography of NS and SW-NE direction made it possible to map the plume of leachate. These results show that the contact water table - leachate is rather discontinuous. The results indicated that leachate infiltration occurs with variable depths and is not everywhere in contact with the water table. This discontinuous pollution has been observed in the water quality of the wells. The analyses of water samples of the wells showed a great variation of heavy metal pollution in rather close wells. The 2D electric resistivity

tomography sections showed the in-depth leachate plume and made it possible to deduce that the contact between the leachate plume and the top of the water table is rather discontinuous.

Ariyo *et al.*, (2013) used electrical resistivity method to investigate the effect of leechate contamination of groundwater at Sotubo solid waste dumpsite. Both Vertical Electrical Sounding (VES) and Constant Separation Traverse (CST) technique were carried out using Schlumberger and Wenner electrode configuration, the estimated apparent resistivities were interpreted using partial curve matching technique and computer iteration. The inferred lithology includes topsoil, sandy layer, limestone and sandy-clay with resistivity of 90, 421.5, 907.8, 143.0 Ωm and thickness of 1, 3.8, 29.0 m and infinity, respectively. The pseudosection revealed the leachate had a thickness of 19.8 to 25.0 m with ρ of 0.17 to 32.5 Ωm in the NW part of profile 1. In contrast, apparent resistivity of the leachate is less than 5.95 Ωm in profile 2. The leachate has infiltrated potential aquifers such as the sandstone layer. Aquiferous layer exceeding the depth of the contaminated zone can be drilled with screened borehole in order to avert groundwater pollution. Sotubo dumpsite is a non-engineered landfill. It neither has a bottom liner nor leechate collection and treatment system. The leachate generated finds its way into underground water system.

John *et al.*, (2013) combined several near surface geophysical investigation techniques with high resolution remote sensing image interpretation in order to define the groundwater flow paths and whether they can be affected by future seismic events. The research was to define the water pathways in order to investigate and understand the exact mechanism of the spring by mapping the exposed discontinuity network with classic field mapping and remote sensing image interpretation and define their underground continuity with the contribution of near surface geophysical techniques. Five Very Low Frequency (VLF) profiles were conducted at different directions around the spring aiming to detect possible conductive zones in the conglomeratic formations that the study area consists of. Moreover, two Electrical Resistivity Tomography (ERT) sections of a

total length of 140m were carried out parallel to the VLF profiles for cross-checking and verifying the geophysical information. Both of the geophysical techniques applied for this study proved to be ideal for indicating conductive zones.

Ozezin *et al* (2017) carried out an assessment of the effects of waste dumpsite using electromagnetic and electrical resistivity methods in dump located along Police Barrack Road, Ekpoma in Esan West Local Government Area of Edo State. Very Low Frequency - Electromagnetic (VLF-EM) field data were obtained in three traverses measuring 70 m, 40 m and 45 m at profiles 01, 02 and 04 respectively. The VLF-EM data were analyzed using qualitative interpretation of the curves and analysed using Karous-Hjelt Software to delineate the conductive and non-conductive zones in the study area. Four Vertical Electrical Sounding (VES) stations were utilized, using Schlumberger configuration. Data obtained from the VES technique were processed using IP2win software. The VES curves obtained revealed simple subsurface geology with characteristic H and A curve types with low resistivities in the range of 37.21 Ωm to 44.9 Ωm indicative of leachate contamination. The VLF technique revealed lithology with high amplitudes in the region of 35 m and 40 to 45 m, 21 to 30 m and 17 to 24 m also indicative of contamination arising from leachate wastes and underground pollution in the dumpsites. Results from the analysis of data also reveal leachate generated by surface water percolating through the waste has polluted and contaminated the top soil.

2.2 Geophysics Background

The rapid advances in microprocessors and associated numerical modeling solutions had made the use of geophysics for both groundwater resource mapping and for water quality evaluations experience tremendous increase over the years due to the heavy reliance on groundwater not only as a primary drinking water source but also for both agricultural and industrial use. Significant

technological advancement has been made in the field of geosciences over the years in the area of groundwater contamination studies. This is possible through the measurement of the vertical and horizontal changes in the apparent soil electrical conductivity. Geophysical applications in groundwater studies include:

- (i) mapping aquitards or confining units
- (ii) mapping the depth and thickness of aquifers
- (iii) locating preferential fluid migration paths such as fractures and fault zones
- (iv) mapping contamination to the groundwater such as leachate plumes from solid waste and saltwater intrusion.

Electrical methods have proved particularly applicable to groundwater studies as many of the geological formation properties that are critical to hydrogeology such as the porosity and permeability of rocks can be correlated with electrical conductivity signatures. In groundwater resource mapping it is not the groundwater itself that is the target of the geophysics rather it is the geological structures in which the water exist. The use of geophysics for groundwater studies has been stimulated in part by a desire to reduce the incidence of abortive boreholes and also a desire to reduce cost. Today the geophysicist also provides useful parameters for hydrogeological modeling of both new groundwater supplies and for the evaluation of existing groundwater contamination. Geophysics is only one tool that can be applied in groundwater investigation and its success must rely on the careful interpretation and integration of the results with the other geologic and hydrogeology data for the site. For groundwater investigation, the most significant parameters that have been used for describing an aquifer system are ones that relate to the porosity and permeability of the aquifer and the surrounding aquitards. Electrical conductivity or its inverse resistivity is the proportionality factor relating the electrical current that flows in a medium to the applied electric field. It is the ability of an electrical charge to move through a material. It is being

correlated with porosity through the work of Archie (1942). The successful use of every geophysical method is dependent not only on the careful design of the survey but also on the consideration of a number of geological and cultural factors together with the geophysical data.

These factors are:

- (i) Nature of target: The target geophysical signature must be different from that of the background geology or hydrogeology.
- (ii) Depth of buried target: The depth of burial of the feature of interest is important as different techniques have different investigation ranges. The depth range is technique dependent; however, there is always a trade off between penetration depth and resolution of the technique with respect to the feature of interest.

2.3 Diffuse electromagnetic (EM) methods

A variety of electromagnetic tools, such as frequency domain electromagnetic (e.g. ground conductivity EM 31) transient electromagnetic, radio magnetotelluric, and very low frequency resistivity have been developed for the investigation of the subsurface (McNeill, 1990). The very early time electromagnetic (VETEM) method is a new technology specially designed for shallow applications (Smith *et al.*, 2000). The electromagnetic methods are currently amongst the most popular and multifaceted type of geophysical techniques. This is mainly as a result of their high acquisition speed. Inductive coupling allows data to be collected without the need to have physical contact between the electromagnetic equipment and the ground. Originally the EM induction method was developed for reconnaissance exploration survey of conductive base metal underlying relatively thin and resistive overburden of the Precambrian Shield in Scandinavia and Canada (Telford *et al.*, 1990). The most important shallow application of electromagnetic method has been associated with hydrological studies. There have been numerous reports in which aquifer and

aquitard have been mapped for the quantification of groundwater resources, quality control of drinking ground water, and monitoring of groundwater intrusion (Wynn *et al.*, 2000). The radio magnetotelluric technique has been employed successfully, for example on the surface of lake to determine groundwater contamination. Closely associated with groundwater studies are investigations of landfills, industrial regions, and the sites of accidental spills of pollutants. The use of frequency-domain electromagnetic systems for mapping the lateral extent of anomalous conductive zones is widespread because of their rapid recording, processing and interpretation characteristics (Wisén *et al.*, 1999). Senos *et al.*, (1994) combined 2-D inversion results of more than 500 radio magnetotelluric soundings recorded on a closely spaced grid to yield a detailed pseudo 3-D image of an investigated landfill. So far characterizing the content of a land fill by electromagnetic has been limited to determining the location and electromagnetic responses of buried conductors. The electromagnetic phenomena are all controlled by Maxwell equations. One of the most fundamental phenomena is that a varying electric field will again create another varying magnetic field. This phenomenon determines the propagation of electromagnetic fields which is referred to as electromagnetic radiation.

2.4 Ground Penetrating Radar

Georadar techniques are based on similar principles like the magnetic methods, except that electromagnetic waves of frequency ranging from 10MHz to 2000MHz travel through the media. They supplement the seismic methods by providing very detailed information on the very shallow subsurface (Powers *et al.*, 1999). The similarities between the georadar and seismic techniques have inspired many researchers to apply seismic reflection recording, processing, and imaging techniques to georadar data. Examples have included multi-fold data acquisition, spatial filtering, stacking and migration (Beres *et al.*, 2000). However, Lehmann and Green, (2000) have pointed

out that conventional seismic migration algorithms are not suitable for regions characterised by moderate to high topographic relief. In Germany georadar surveys have been used for 20 years to detect salt deposits. Engineering applications have involved monitoring road deterioration and potential weakness of an ice runway, slope stability analysis, detecting karstic voids in a tunnel construction area, and characterizing buried tanks and pipes (Arcone, 1998). Georadar methods have been useful for non intrusive 2D and 3D studies of quaternary sediments that a critical components of the groundwater regime. Georadar method is also gaining increased acceptance as an archaeological investigation tool (Green, 1999). Nevertheless, large metallic objects, such as drums, may be detected. Knowledge about aquifers, subsurface barriers, and possible pathways in the sediments surrounding waste material is critical for estimating potential risks of groundwater contamination.

2.5 Very Low Frequency Electromagnetic Survey

The primary electromagnetic field travels from the transmitter coil to the receiver coil via paths both above and below the surface. Where the subsurface is homogeneous there is no difference between the fields propagated above the surface and through the ground other than a slight reduction in amplitude of the latter with respect to the former. However, in the presence of a conducting body the magnetic component of the electromagnetic field penetrating the ground induces alternating currents, or eddy currents, to flow in the conductor (Fig. 2.1).

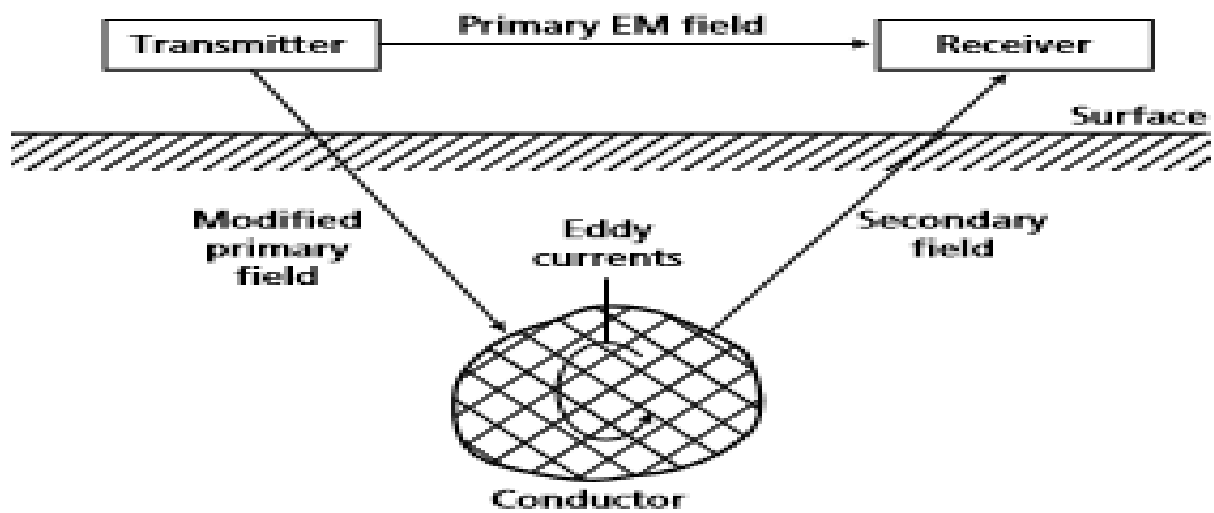


Fig. 2.1: General principle of electromagnetic surveying (Kearey *et al.*, 2002)

The eddy currents generate their own secondary electromagnetic field which travels to the receiver. The receiver then responds to the resultant of the arriving primary and secondary fields so that the response differs in both phase and amplitude from the response to the primary field alone. These differences between the transmitted and received electromagnetic fields reveal the presence of the conductor and provide information on its geometry and electrical properties. These transmitters are meant for long distance marine communications and situated on the coastal areas worldwide. They operate in the lower band (15 – 30 kHz) of communication frequency. These signals from the transmitters travel a long distance and are utilized for geophysical measurements. Since the primary field is horizontal, VLF method is ideal for the investigation of vertical and dipping conducting structures in the subsurface. It is emphasized that, in principle, VLF method uses the highest frequency compared to other electromagnetic methods. The name “very low frequency” comes from the transmitter used for long distance marine communication. Indeed, 15 – 30 kHz is very low with regard to other communication frequencies used in radio, television and mobile communications. The VLF method advantages are, the equipment is small and light, being

conveniently operated by one person, and that there is no need to install a transmitter. Very Low Frequency Electromagnetic (VLF-EM) method is used for electrical conductors surveying without contact with the ground, it is suitable for ground surveying in a wide area and has been widely used to map the geology of the subsurface for the past forty years. The technique makes use of signal radiation from military radio transmitters. The signals from these stations are effectively used for a variety of applications such as ground water detection, soil engineering and mineral exploration. The ABEM Wadi VLF instrument that utilizes only a magnetic field component was used for this study.

2.5.1 Basic Theory of Electromagnetic field propagation in the Earth

Electromagnetic methods use the response of the ground to the propagation of incident alternating electromagnetic waves which are made up of two orthogonal vector components, an electric intensity (E) and magnetizing force (M) (Fig. 2.2).

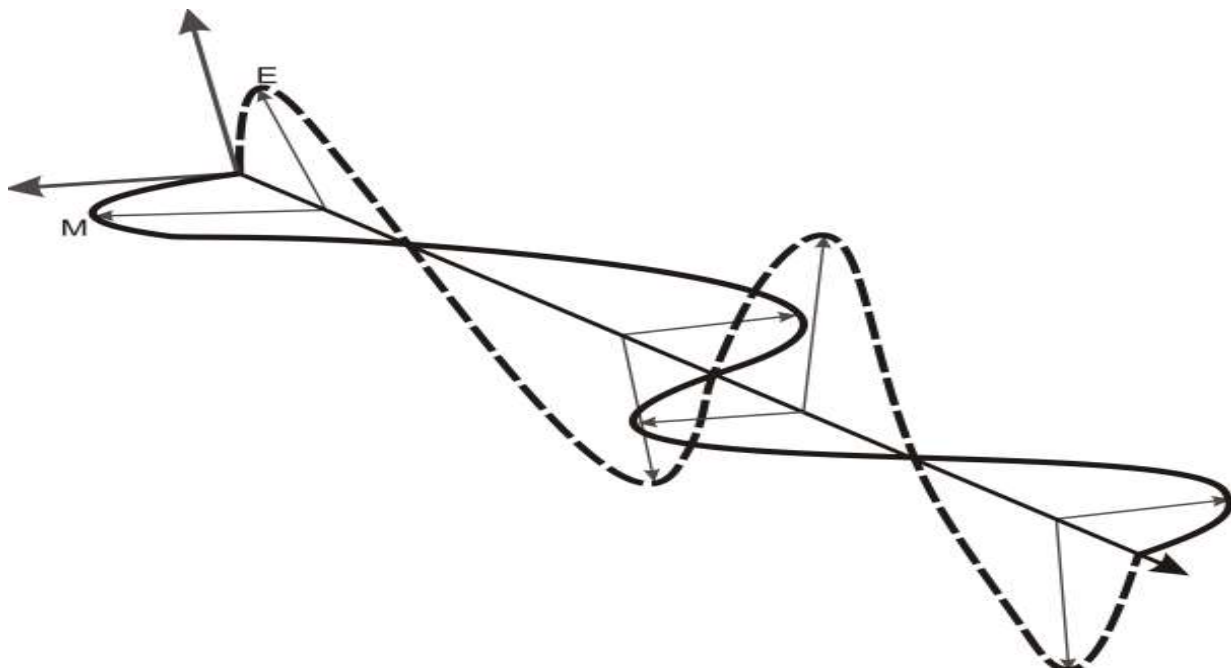


Figure 2.2: Basic elements of an electromagnetic wave, showing the two principal electric (E) and magnetic (M) components.

To understand how Electromagnetic signals propagate in the Earth, we will begin with Maxwell's equations. Maxwell's great contribution to the understanding of Electromagnetic phenomena was to show that all the measurements and laws of field behaviour could be derived from a few compact mathematical expressions. Starting with these equations, let us consider an electromagnetic wave that is travelling through a region characterized by conductivity (σ), magnetic permeability (μ) and dielectric permittivity (ϵ). The local electric charge density is $Q(x, y, z)$. The electric (E) and magnetic fields (B) vary in space and time as $E(x, y, z, t)$ and $B(x, y, z, t)$ and are described by Maxwell's equations 2.1 to 2.4.

$$\nabla \wedge B = \mu J + \mu\epsilon \frac{\partial E}{\partial t} \quad 2.1$$

$$\nabla \wedge E = -\frac{\partial B}{\partial t} \quad 2.2$$

$$\nabla \cdot E = \frac{Q}{\epsilon_0} \quad 2.3$$

$$\nabla \cdot B = 0 \quad 2.4$$

The ultimate goal is to eliminate B and obtain an equation for E

The constitutive relation gives us $J = \sigma E$ with Amperes Law becoming

$$\nabla \wedge B = \mu\sigma E + \mu\epsilon \frac{\partial E}{\partial t} \quad 2.5$$

Note that the first term on the right hand side represents conduction current. While the second represents displacement current. Taking the curl of Faradays Law (equation 2.2) give us

$$\nabla \wedge (\nabla \wedge E) = -\frac{\partial}{\partial t} (\nabla \wedge B) \quad 2.6$$

Substituting (2.5) into (2.6) and using the vector identity

$$\nabla \wedge (\nabla \wedge E) = \nabla (\nabla \cdot E) - \nabla^2 E \quad 2.7$$

We then have

$$\nabla (\nabla \cdot E) - \nabla^2 E = -\frac{\partial}{\partial t} (\mu\sigma E + \mu\epsilon \frac{\partial E}{\partial t}) \quad 2.8$$

Now if it is assumed that the Earth properties (conductivity, permeability and permittivity) do not vary with time, then we can write.

$$\nabla(\nabla \cdot E) - \nabla^2 E = -\mu\sigma \frac{\partial E}{\partial t} - \mu\epsilon \frac{\partial^2 E}{\partial t^2} \quad 2.9$$

Coulombs Law states that: The electric force between two point charges, q_1 and q_2 separated by a distance r is directly proportional to the product of the charges and inversely proportional to the square of the distance between the charges. i.e $E = \frac{F}{q}$ and $q = \frac{F}{E}$

$$\nabla \cdot E = \frac{Q}{\epsilon} \quad 2.10$$

Assumption 1: Assume there are no free electric charges ($Q = 0$). Note that this will not be true if electric current crosses boundaries between regions of differing resistivity. This requires that:

$$\nabla \cdot E = 0 \quad 2.11$$

Which simplifies (2.9) to give

$$\nabla^2 E = \mu\sigma \frac{\partial E}{\partial t} + \mu\epsilon \frac{\partial^2 E}{\partial t^2} \quad 2.12$$

We now have a second order differential equation for $E(x, y, z, t)$ where the time-variation can be completely general. This represents the time-domain.

Limiting cases

1. If the conduction current term is much larger than the displacement current term, the (2.12) simplifies to a diffusion equation

$$\nabla^2 E = \mu\sigma \frac{\partial E}{\partial t} \quad 2.13$$

2. However if the displacement current term is much larger than the conduction current term, them (2.12) simplifies to a wave equation.

$$\nabla^2 E = \mu\epsilon \frac{\partial^2 E}{\partial t^2} \quad 2.14$$

Comparison with the standard wave equation shows that the wave velocity is

$$C = \frac{1}{\sqrt{\mu\varepsilon}} \quad 2.15$$

Which for free space values of μ and ε gives $c = 3 \times 10^8$ m/s, showing that this is a radio wave moving at the speed of light. There is therefore need to determine which of these limiting case will apply for electromagnetic signals travelling in the Earth.

Assumption 2: Analysis is simplified if the magnetic field is transformed into the frequency domain that is, we assume that the electric and magnetic fields have a harmonic time variation at angular frequency ω . The angular frequency (ω) and frequency (f) are related as $\omega = 2\pi f$. This allows variables to be separated as $E(x, y, z, t) = E_0(x, y, z)e^{-i\omega t}$ 2.16

Where $i = \sqrt{-1}$. Substitution of (2.14) into (2.10) give

$$\nabla^2 E_0 = -i\omega\mu\sigma E_0 + \omega^2\mu\varepsilon E_0 \quad 2.17$$

Note that the first term on the right hand side represents conduction current, while the second represents displacement current. To understand which term will dominate, consider some numerical values for two common types of geophysical exploration. The ratio of displacement current to conduction current can be written as $R = \omega\varepsilon/\sigma$. For the exploration method that uses a low frequency electromagnetic signal at $f = 1$ Hz in a region where $\sigma = 0.01$ S/m, so assuming a free space value of dielectric permittivity, this gives $R = 5.56 \times 10^{-9}$ showing that conduction current is dominant and the signal will propagate by diffusion.

Considering for the high frequency electromagnetic signal for example 1GHz signal travels in glacial ice with $\sigma = 10^{-5}$ S/m giving $R = 5561$. Displacement current is dominant and the signal travels as an electromagnetic wave.

Assumption 3: This shows that for all practical electromagnetic applications in the Earth, displacement current can be ignored. Thus ignoring the displacement, we then consider a

simplified geometry of an electromagnetic signal travelling vertically in the Earth. When the displacement current is ignored, we can write:

$$\nabla^2 E_0 = -i\omega\mu\sigma E_0 \quad 2.18$$

This can be expressed in component form (less concisely) as

$$\frac{\partial^2 E_x}{\partial x^2} + \frac{\partial^2 E_x}{\partial y^2} + \frac{\partial^2 E_x}{\partial z^2} + i\omega\mu\sigma E_x = 0 \quad 2.19a$$

$$\frac{\partial^2 E_y}{\partial x^2} + \frac{\partial^2 E_y}{\partial y^2} + \frac{\partial^2 E_y}{\partial z^2} + i\omega\mu\sigma E_y = 0 \quad 2.19b$$

$$\frac{\partial^2 E_z}{\partial x^2} + \frac{\partial^2 E_z}{\partial y^2} + \frac{\partial^2 E_z}{\partial z^2} + i\omega\mu\sigma E_z = 0 \quad 2.19c$$

where $E_0 = \begin{cases} E_x \\ E_y \\ E_z \end{cases}$

Assumption 4: if it is assumed that the electric field polarized in the x-direction, then we can write

$$E_0 = \begin{cases} E_x \\ 0 \\ 0 \end{cases} \text{ and equation (2.19b) and (2.19c) can be ignored. Thus we need to solve the second-order}$$

partial differential equation:

$$\frac{\partial^2 E_x}{\partial x^2} + \frac{\partial^2 E_x}{\partial y^2} + \frac{\partial^2 E_x}{\partial z^2} + i\omega\mu\sigma E_x = 0 \quad 2.20$$

Assumption 5: Now if the wave is assumed to be planar, then it will not vary in the x and y

directions, which can be expressed as $\frac{\partial}{\partial x} = 0$ and $\frac{\partial}{\partial y} = 0$. This further simplifies (2.20) to an

ordinary differential equation

$$\frac{\partial^2 E_x}{\partial z^2} + i\omega\mu\sigma E_x = 0 \quad 2.21$$

We can seek a trial solution of the form

$$E_x(z) = Ae^{kz} \quad 2.22$$

Where A and k are constants to be determined. Substitution into (2.21) gives

$$k^2 A + i\omega\mu\sigma A = 0 \quad 2.23$$

which gives

$$K = \sqrt{-i\omega\mu\sigma} \quad 2.24$$

Since there are two possible solutions,

$$K = \pm(1 - i)\sqrt{\frac{\omega\mu\sigma}{2}} \quad 2.25$$

we need to write a general form of the solution as:

$$E_x(z) = A_1 e^{(1-i)\sqrt{\frac{\omega\mu\sigma}{2}}z} + A_2 e^{-(1-i)\sqrt{\frac{\omega\mu\sigma}{2}}z} \quad 2.26$$

which can be expanded as

$$E_x(z) = A_1 e^{\sqrt{\frac{\omega\mu\sigma}{2}}z} e^{-i\sqrt{\frac{\omega\mu\sigma}{2}}z} + A_2 e^{-\sqrt{\frac{\omega\mu\sigma}{2}}z} e^{i\sqrt{\frac{\omega\mu\sigma}{2}}z} \quad 2.27$$

Note that each term consists of exponential function and an oscillatory function. We need to determine A_1 and A_2 by applying appropriate boundary conditions.

Boundary condition 1

This solution must remain bounded as $z \rightarrow \infty$. This is the only possible if $A_1 = 0$.

Boundary condition 2

Can specify that at $z = 0$, $E_x(0) = E_x^s$, which requires $A_2 = E_x^s$.

Thus the solution can be written as:

$$E_x(z) = E_x^s e^{-\sqrt{\frac{\omega\mu\sigma}{2}}z} e^{i\sqrt{\frac{\omega\mu\sigma}{2}}z} \quad 2.28$$

Considering the real part, we can write:

$$E_x(z) = E_x^s e^{-\sqrt{\frac{\omega\mu\sigma}{2}}z} \cos\left(\sqrt{\frac{\omega\mu\sigma}{2}}z\right) \quad 2.29$$

Consider the modulus of the electric field

$$|E_x(z)| = |E_x^s| e^{-\sqrt{\frac{\omega\mu\sigma}{2}}z} \quad 2.30$$

This decays monotonically as z increases. The depth at which $|E_x(z)|$ has decreased from the value at $z = 0$ by a factor of $1/e$ is defined as the skin depth (δ)

$$\frac{|E_x(z=\delta)|}{|E_x^s|} = \frac{1}{e} = e^{-\sqrt{\frac{\omega\mu\sigma}{2}}\delta} \quad 2.31$$

which requires

$$\sqrt{\frac{\omega\mu\sigma}{2}}\delta = 1 \quad 2.32$$

$$\text{This can be arranged to give } \delta = \sqrt{\frac{2}{\omega\mu\sigma}} \quad 2.33$$

Substituting for $\mu = \mu_0 = 4\pi 10^{-7}$ gives an expression for the skin depth in metres as

$$\delta = \frac{503}{\sqrt{\sigma f}} \quad 2.34$$

Thus the skin depth is given as

$$\delta = \frac{503}{\sqrt{\sigma f}}$$

2.5.2 Electrical Resistivity Method

The use of geophysical techniques for earth resistivity measurement and groundwater resource management have increased dramatically over the years, due to the rapid advances in microprocessors and associated numerical modelling solutions (Ewusi, 2006). Electrical resistivity measurement helps to determine subsurface changes in the earth resistivity. The large contrast in resistivity between ore bodies and their host rocks is exploited in electrical resistivity prospecting, especially for minerals that occur as good conductors. Electrical resistivity measurement is also an important geophysical technique in environmental applications (Forté, 2011). The standard

arrangement in the field measurement for the electrical conductivity measurement is shown in Fig.

2.3.

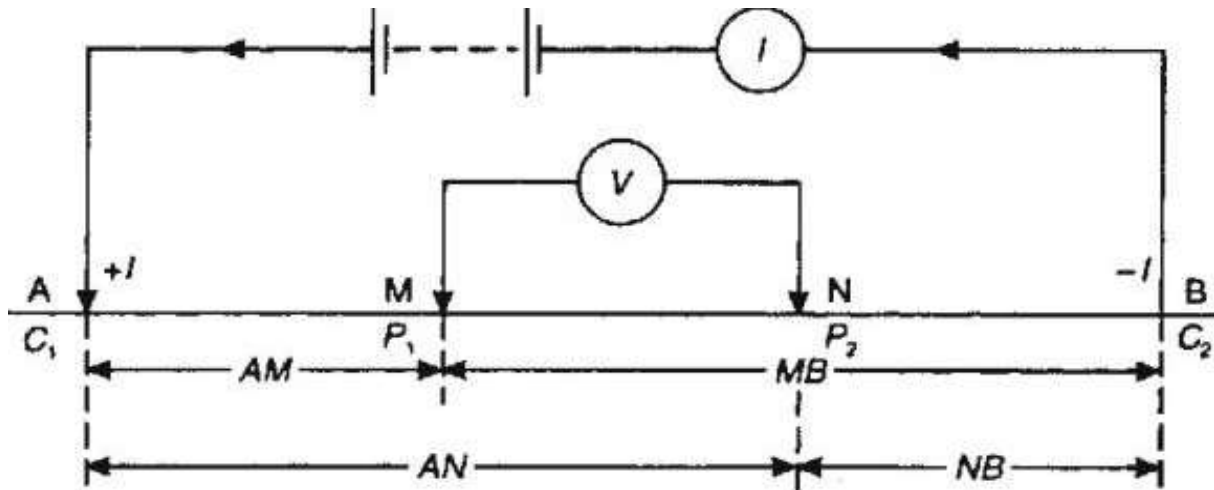


Fig. 2.3 Generalized four electrode configuration used in resistivity measurement (Kearey *et al.*, 2002)

Direct current is introduced into the ground through a pair of electrodes at position A and B. While the potential across is measured with the electrodes M and N. Electrical methods have broad application to geoenvironmental problems. They may be used to identify leachate plume, directly applicable to hydrologic investigations, and can be used to identify structures and lithologies. The resistivity method is used in the study of horizontal and vertical discontinuities in the electrical properties of the ground, and also in the detection of three-dimensional bodies of anomalous electrical conductivity. Thus moving the array without changing the distance between the electrodes (electrode spacing) moves the region of investigation. The size of the region of investigation, and therefore the depth, is directly related to the size of the array. The size of the array is controlled by the electrode spacing. Thus increasing the current electrode spacing without changing the center point of the array increases the size, and coincidentally the depth, of the region of investigation as shown in Fig. 2.4.

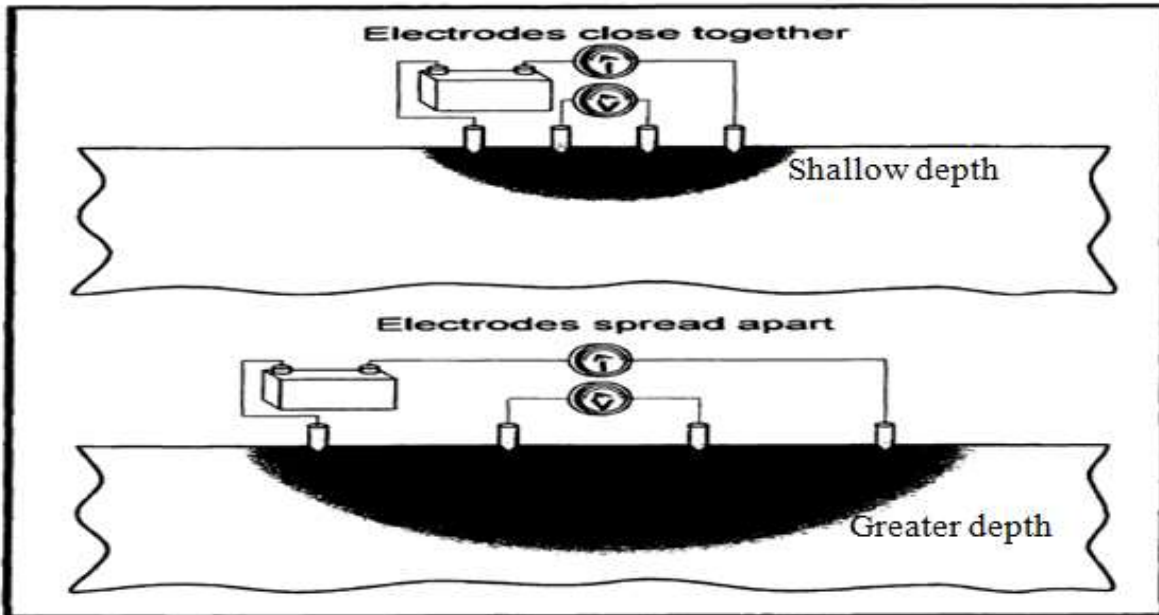


Fig. 2.4 Changing the distance between the electrodes in an electrode array (Baines, 2001)

2.5.3 Basic Theory of Electrical Resistivity Method

Applied geophysics has been very useful for over a decade, particularly for shallow and near-surface investigations. Electrical methods of geophysical investigations are based on the resistivity (or its inverse, conductivity) contrasts of subsurface materials. Electrical resistivity measured in Ohm-meters (Ωm) and represented by the Greek letter ρ (rho), is a bulk physical property of materials that describes how difficult it is to pass an electrical current through a block of the material with a given length and cross-sectional area (Kearey *et al.*, 2002). Consider an electrically uniform cube of side length L through which a current (I) is passing. The material within the cube resists the conduction of electricity through it, resulting in a potential drop (V) between opposite faces. The resistance (R) is proportional to the length (L) of the resistive material and inversely proportional to the cross-sectional area (A), the constant of proportionality is the 'true' resistivity (symbol: ρ). According to Ohm's Law the ratio of the potential drop to the applied current (V/I) also defines the resistance (R) of the cube and these two expressions can be combined to form the product of a resistance (Ω) and a distance (area/length; meters); hence the units of resistivity are

ohm-meters (Ωm). The inverse of resistivity ($1/\rho$) is conductivity (σ) which has units of Siemens/meter (S/m) which are equivalent to mhos/meter ($\Omega^{-1} \text{m}^{-1}$). It is well known that resistance, R in Ohms (Ω), of a wire is directly proportional to its length L and is inversely proportional to its cross-sectional area A .

That is

$$R \propto L/A \quad 2.35$$

$$R = \rho L/A \quad 2.36$$

where ρ = the constant of proportionality, is the electrical resistivity which is a characteristics of the material and is independent of its shape or size. From Ohm's law, the resistance is given by: $R =$

$$\Delta V/I \quad 2.37$$

Where ΔV is the potential difference across the resistance, R , and I is the electric current through the resistance. Putting equation (2.36) into equation (2.37) and rearranging it gives:

$$\rho = A/L \cdot \Delta V/I \quad 2.38$$

Equation (2.36) may be used to determine the resistivity ρ of a homogeneous and isotropic material in the form of regular geometric shapes, such as rectangles and cylinders. If the cross-sectional area and length of an element within the semi-infinite material are shrunk to infinitesimal size then the resistivity ρ may be defined as:

$$\rho = \frac{\lim_{L \rightarrow 0} (\Delta V/L)}{\lim_{A \rightarrow 0} (I/A)} \quad 2.39$$

$$\rho = E_L/J \quad 2.40$$

where E_L is the electric field and J is the current density. In terms of electromagnetic field quantities, for an electric field E (volts/m) with current density J (amps/m²) and resistivity, ρ (Ωm).

The vector form of Ohm's law is:

$$\rho = E/J \quad 2.41$$

$$J = \sigma \nabla V \quad 2.42$$

where

V = electric potential in volts and σ = conductivity measured in $(\Omega\text{m})^{-1}$. For a whole space, the total current I , flow away from one electrode to another across the sphere of an area $4\pi r^2$. Ohm's law for one electrode then becomes:

$$j = \frac{I}{4\pi r^2} = \frac{-1}{\rho} \cdot \frac{dv}{dr} \quad 2.43$$

$$\frac{I}{4\pi r^2} \int dr = \frac{-1}{\rho} \int dv \quad 2.44$$

$$\frac{I}{4\pi} \int r^{-2} dr = \frac{-1}{\rho} \int dv \quad 2.45$$

$$\frac{-I}{4\pi r^1} = \frac{-1}{\rho} V_{(r)} \quad 2.46$$

$$V_{(r)} = \frac{\rho I}{4\pi r} \quad 2.47$$

For a half-space, the total current (I), flows across the sphere with area $\frac{1}{2}(4\pi r^2)$.

$$V_{(r)} = \frac{\rho I}{2\pi r} \quad 2.48$$

I = total current flowing from one current electrode to the other through the ground.

However, the potential and current electrodes are usually arranged in a collinear pattern as shown in Fig. 2.3.

The distances between the electrodes are given by AM , BM , AN , and BN . The potentials at M and N can be calculated using equation (2.48).

$$V_M = \frac{\rho I}{2\pi} \left[\frac{1}{r_{AM}} - \frac{1}{r_{BM}} \right] \quad 2.49$$

V_N can also be written as

$$V_N = \frac{\rho I}{2\pi} \left[\frac{1}{r_{AN}} - \frac{1}{r_{BN}} \right] \quad 2.50$$

The voltage drop, ΔV between two electrodes, M and N is.

$$\Delta V = V_M - V_N \quad 2.51$$

Putting equations (2.49) and (2.50) into (2.51) gives

$$\Delta V = \frac{\rho I}{2\pi} \left[\frac{1}{r_{AM}} - \frac{1}{r_{BM}} - \left(\frac{1}{r_{AN}} - \frac{1}{r_{BN}} \right) \right] \quad 2.52$$

$$\Delta V = \frac{\rho I}{2\pi} \left[\frac{1}{r_{AM}} - \frac{1}{r_{BM}} - \frac{1}{r_{AN}} + \frac{1}{r_{BN}} \right] \quad 2.53$$

$$\Delta V = \frac{\rho I}{2\pi} \left[\frac{1}{r_{AM}} + \frac{1}{r_{BN}} - \frac{1}{r_{BM}} - \frac{1}{r_{AN}} \right] \quad 2.54$$

By solving for ρ in equation 2.54, the apparent resistivity ρ_a of the subsurface becomes.

$$\rho_a = 2\pi \frac{\Delta V}{I} \left[\frac{1}{r_{AM}} + \frac{1}{r_{BN}} - \frac{1}{r_{BM}} - \frac{1}{r_{AN}} \right]^{-1} \quad 2.55$$

$$\text{where } k = 2\pi \left[\frac{1}{r_{AM}} + \frac{1}{r_{BN}} - \frac{1}{r_{BM}} - \frac{1}{r_{AN}} \right]^{-1} \quad 2.56$$

Equation (2.55) is the fundamental equation in electrical resistivity prospecting. The factor

$\frac{2\pi}{\frac{1}{r_{AM}} + \frac{1}{r_{BN}} - \frac{1}{r_{BM}} - \frac{1}{r_{AN}}}$ is called the “geometric factor” denoted by letter K. Therefore,

$$\rho_a = K \frac{\Delta V}{I} \quad 2.57$$

$$\therefore \rho_a = R \times K \quad 2.58$$

If the measurement of ρ is made over a semi infinite space of homogeneous and isotropic material, then the value of ρ computed from equation (2.55) will be the true resistivity. However, if ground is inhomogeneous or anisotropic medium, the resistivity measured from equation (2.57) is called apparent resistivity ρ_a .

$$\rho_a = RK, \text{ where } R = \delta V/I. \quad 2.59$$

2.5.4 Electrical Resistivity Survey Techniques

In the resistivity method, electric current is introduced into the ground through a pair of electrodes called the current electrodes, and the resultant potential difference from the current flowing are measured at the surface through another pair of electrodes called the potential electrodes which may or may not be located within the current electrodes. Deviations from the pattern of potential difference expected from the homogeneous ground provide information on the electrical properties of subsurface. The most common techniques used in hydrogeological and environmental surveys are as follows:

- i. Vertical electrical sounding or electric drilling.
- ii. Electrical resistivity profiling (constant separation traversing).
- iii. Two-dimensional (2D) electrical resistivity imaging.
- iv. Three-dimensional (3D) electrical resistivity imaging.

Vertical electrical sounding is used for investigating variation of resistivity with depth and horizontal electrical profiling is used for assessing lateral variations. The basic difference between these two aspects of measurements is that in profiling, measurements are taken at various stations on the traverse. Another improvement in the electrical methods is the 2-D and 3-D electrical imaging methods. These methods take care of the resistivity changes in both the vertical direction as well as the horizontal direction along the survey line (Loke, 2000).

2.5.5 Vertical Electrical Sounding (VES)

The technique measures the variation in apparent resistivity of the earth with depth beneath a given location. In Vertical Electrical Sounding (VES) the centre point of the array remains fixed (fixed potential electrodes) but the current electrode separation is progressively increased (Kearey *et al.*,

2002). It is known as depth probing. This technique is carried out in such a way that the electrode spacing is gradually increased to yield information from greater depth, at a specific location, based on the fact that deeper current penetration is governed by wider current electrode separation as presented in (Figure 2.4). Although most electrode configurations can be used for VES, the Schlumberger arrangement offers important logistic advantages (only two electrodes have to be moved at a time). Interpretations of VES data are based on the assumption that the area under investigation is underlain by a finite number of horizontal layers. Primitive analysis involves comparing the sounding curve shape (logarithmic apparent resistivity versus logarithmic half-distance of current electrodes) with model curves of typical resistivity structures. The technique is extensively used in geotechnical survey to determine overburden thickness and hydrogeology to define horizontal zones of porous strata.

2.5.6 Electrical Resistivity Profiling

This technique measures the lateral variations of apparent resistivity in the ground using an electrode arrangement with fixed spacing and progressively moved along a profile. This method is employed in mineral prospecting to locate faults or shear zones and to detect localized bodies of anomalous conductivity. The current and potential electrodes are maintained at a fixed separation. After taking a particular set of readings the whole configuration is shifted progressively along a profile (Loke, 2001). Data obtained from profiling are mainly interpreted qualitatively. The Wenner configuration is best suited for this approach due to the equidistant spacing between the electrodes. When the movement is perpendicular to the strike, the profile is termed as inline but when parallel to the strike, it is referred to as broadside and this is used in the mapping of line or structures such as faults, cavity, metal drum, basement depression and buried stream channel. The Wenner and dipole-dipole arrangements are often used in this technique that can be employed to

define aquifer limits or to map a distinct variation in groundwater salinity. The method could also be called lateral profiling.

2.5.7 Two-Dimensional (2D) Electrical Resistivity Imaging

Two-dimensional resistivity measurements provide a two-dimensional picture of the subsurface. The two-dimensional (2-D) electrical survey can be defined as the collection of a number of profiles along the same direction with continuously increasing inner-electrode spacing or as a series of successive electrical soundings along a line (Martinho *et al.*, 2006). Two-dimensional resistivity measurements provide a two-dimensional vertical picture of the sounding medium. The current and potential electrodes are maintained at a regular fixed distance from each other and are progressively moved along a line on the earth surface. At each step, one measurement is recorded. The set of all these measurements at this first inter-electrode spacing gives a profile of resistivity values. The inter-electrode spacing is increased by a factor $n = 2$ and a second measurement line is carried out. This process of increasing the factor n is repeated until the desired spacing between electrodes is reached. An increase in the distance between two electrode pairs gives the apparent resistivity at greater depths. The measured apparent resistivity is a volume-averaged value affected by all the geologic layers through which the current flows and an inversion program converts the array of apparent resistivity data into a model of the geology that would yield the observed distribution of apparent resistivity values (Zhou *et al.*, 2000). Also, the product of the data inversion process is a 2-dimensional image (a tomograph) showing a distribution of true (modelled) resistivity values. However, current distribution in the subsurface depends on resistivity contrasts of the different media and the depth of investigation deduced from the electrode spacing is called the “pseudo-depth”. The data are then arranged in a 2D pseudo-section plot that gives a simultaneous display of both horizontal and vertical variations in resistivity (Samouelian *et al.*, 2007). A two-dimensional

geoelectric section may be made up of a series of one-dimensional soundings combined together to form a two-dimensional section (Loke, 2000). Two-dimensional images of the subsurface apparent resistivity variation are called pseudo-sections and data plotted in cross-section is a simplistic representation of actual complex current flow paths. The 2-dimensional electrical imaging method increases electrode separation as well as makes measurements at multiple locations along the horizontal axis and provides data for two dimensional interpretation of subsurface (Allen, 2004). An arrangement used to build up a pseudo-section in a 2-dimensional surface electrical tomography is as shown in Fig. 2.5.

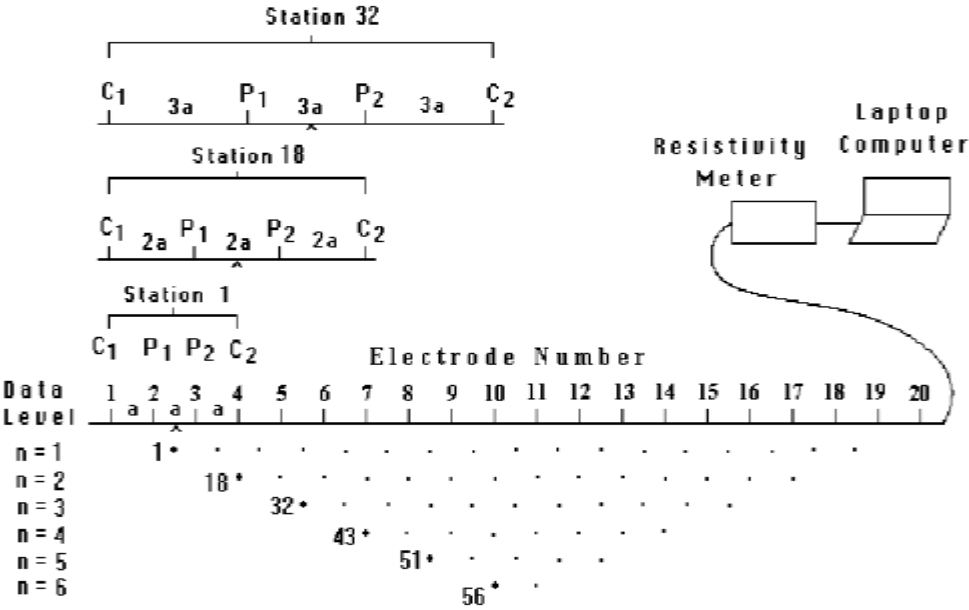


Fig. 2.5: Construction of pseudo-section for Wenner resistivity data (Loke, 2001)

According to Loke, (2000) geo-electrical section obtained from the two-dimensional inversion of each of the profiles investigated can be combined in a three-dimensional volume in software. Finally, electrical resistivity imaging is a straightforward extension of the traditional electrical resistivity survey.

2.5.8 Three-Dimensional (3D) Electrical Resistivity Imaging

In 3D electrical resistivity surveys, electrodes are commonly arranged in square or rectangular grids with constant electrode spacing in both the x- and y-directions (Fig. 2.6). The geological structures and spatial distribution of the subsurface physical properties are inherently 3D in nature. The 3D gives a better image of the subsurface in environmental and engineering investigations where the geology is highly heterogeneous and subtle. Images resulting from 2D resistivity surveys often contain spurious features due to 3D effects and violation of the 2D assumption. This usually leads to misinterpretation of the observed anomalies in terms of magnitude and location (Bentley and Gharibi, 2004). Hence a 3D survey with a 3D interpretation model in which the resistivity is allowed to vary in all directions should, in theory, give the most accurate and reliable results especially in subtle heterogeneous subsurface. The large amount of data observed in 3D electrical resistivity imaging requires automated data processing and inversion to obtain a 3D model resistivity values. Numerical modelling and inversions techniques based on finite difference and finite element methods are commonly used. The principles are generally the same with those used in 2D imaging but the computational power required in 3D imaging is much higher (Dahlin and Zhou, 2002). The resolution of surface electrical resistivity surveys decreases with depth and very long layouts are needed for large depth penetration. The presence of a conductive layer at the surface can significantly reduce the depth of penetration. The existing surface configurations or computer modelling techniques have not been able to overcome this fundamental physical limitation.

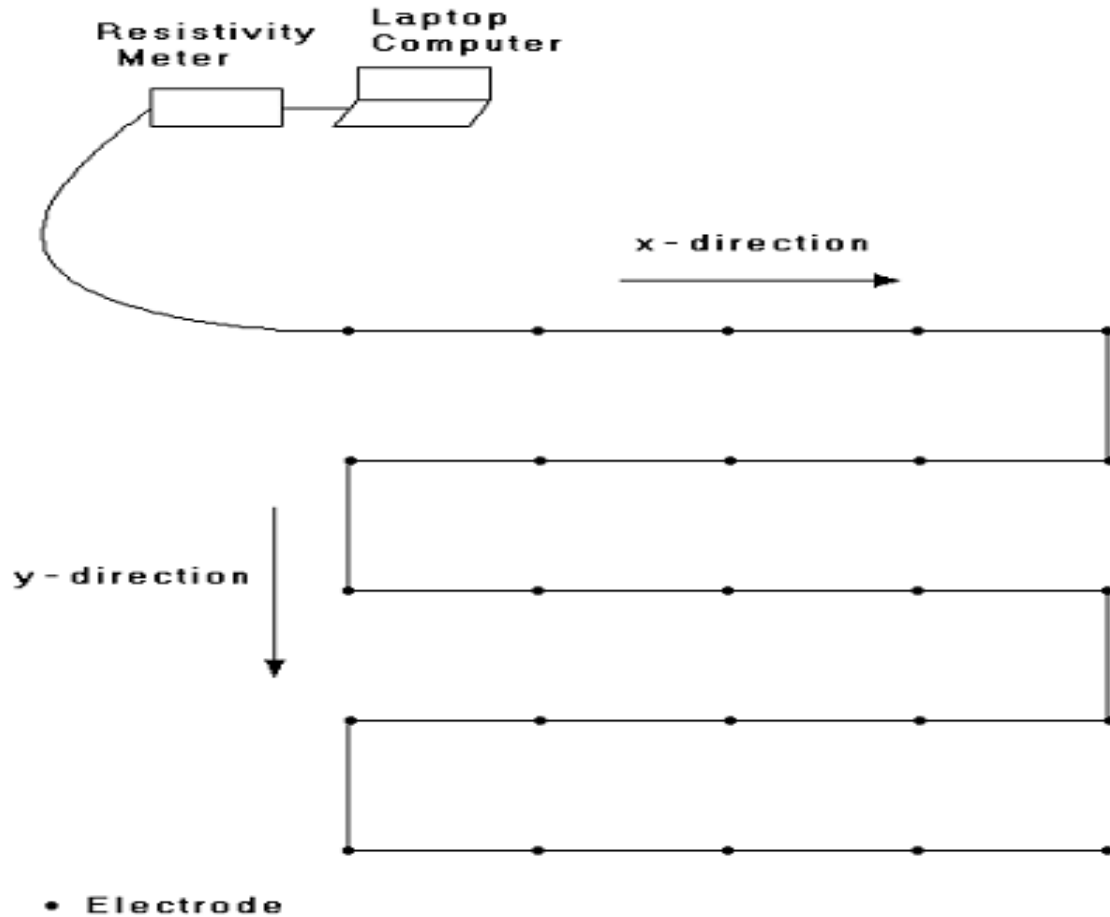


Fig. 2.6: Arrangement of electrodes for 3D survey (Loke, 1999)

2.6 Types of Array

All the arrays of electrodes used to obtain the apparent resistivity are variants of the four-electrode scheme. All the arrays are basically superposition of the fundamental equation for the potential from a current source with appropriate sign for the current. The formulas for apparent resistivity are a product of the impedance $\frac{V}{I}$ (Ohms) and a geometric factor with the units of length (meters).

To investigate the resistivity distribution with depth, called a sounding, the arrays are expanded about a center point. In the more general case the apparent resistivities are plotted as a function of array spacing and lateral position using plotting conventions that have become accepted for each

type of array. The choice of array to be used depends on the objective of the research. Example of some arrays is as follows:

- Dipole-dipole
- Wenner
- Schlumberger
- Pole-pole
- Pole-dipole

For the purpose of this project, the Dipole-dipole array would be employed. The last four arrays will only be mentioned for the sake of completeness.

2.6.1 Dipole-Dipole Array

The dipole-dipole array is very sensitive to horizontal changes in resistivity, but relatively insensitive to the vertical changes in the resistivity and it is useful in mapping vertical structures such as dykes and cavities but relatively poor in mapping horizontal structures such as sills or sedimentary layers (Ewusi, 2006). The dipole-dipole array is logistically the most convenient in the field, especially for large spacing. In the dipole-dipole array, the potential electrodes are situated outside the current electrodes. Each pair has a constant separation and it is such that if the separation between individual pairs is 'a', the separation between the separate pairs becomes 'na'. The convention for the dipole-dipole array in Fig. 2.7 is that current and voltage electrode spacing is the same, a, and the spacing between them is an integer multiple of a. Therefore $\rho_a = \pi n(n +$

$$1)(n + 2)a \frac{\Delta v}{I}$$

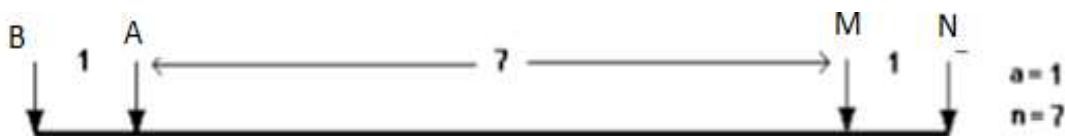


Fig. 2.7 The Dipole-dipole electrode configuration

2.6.2 Wenner Array

This array is relatively sensitive to vertical changes in the subsurface resistivity below the center of the array and less sensitive to horizontal changes in the surface resistivity (Loke, 2000). The Wenner array is now seen to be a simple variant of the pole-dipole in which the distant pole at infinity is brought in and all the electrodes are given the same spacing, a , as seen in the following configuration (Fig. 2.8). In Wenner array, vertical resolution of the various resistivities of the subsurface layers is achieved by increasing the common distance between the electrodes while maintaining the location of the center point of the array. Wenner current and potential electrodes are placed at equal distance from each other. For Wenner array, $\rho_a = 2\pi a \frac{\Delta v}{I}$

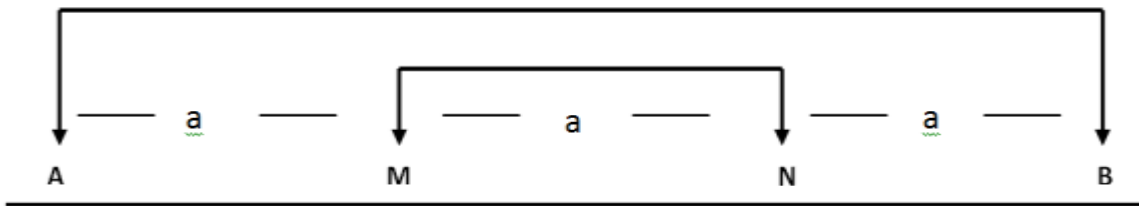


Fig. 2.8 The electrode array for Wenner configuration

2.6.3 Schlumberger Array

One of the first arrays used in the 1920's and still popular today is the Schlumberger array (Fig. 2.9). It is another variant of the pole-dipole, again with the second current electrode placed symmetrically opposite the first. The voltage difference is consequently doubled and so the apparent resistivity is the same as that for the general pole-dipole with a factor of 1/2 in the geometric factor. In a Schlumberger sounding the potential electrodes are usually kept small and fixed while only the s spacing is changed (Loke, 2001). Further, it is conventional to consider the spacing to be the distance from the center of the array to the outermost electrodes, i.e. $AB/2$. In the Schlumberger array, the current electrodes, separated by AB are symmetrical about the potential

electrodes, MN. The current electrodes are then expanded and the geometric factor assumes the

$$\text{form. } \rho_a = \frac{\pi \left(\frac{s^2 - a^2}{4} \right) \Delta v}{a I}$$

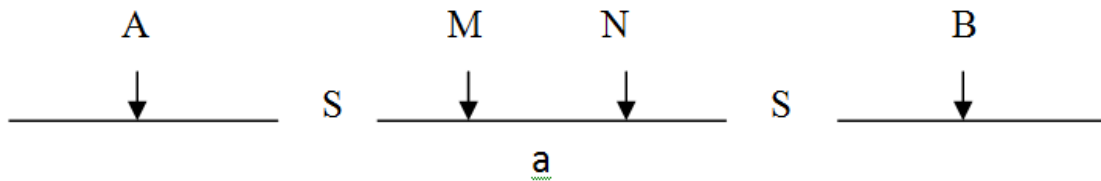


Fig. 2.9 The Schlumberger electrode configuration

2.6.4 Pole-Pole Array

The simplest array is one in which one of the current electrodes and one of the potential electrodes are placed so far away that they can be considered at infinity. This array can actually be achieved for surveys of small overall dimension when it is possible to put the distant electrodes some practical distance away. For a survey in an area of a few square meters “infinity” can be on the order of a hundred meters. The Fig. 2.10 represents a pole-pole array.

$$\rho_a = 2\pi n \frac{\Delta v}{I}$$



Fig. 2.10 The Pole-pole electrode configuration

2.6.5 Pole-Dipole Array

If only one of the current electrodes is placed at “infinity” the configuration and the apparent resistivity are as shown in Fig. 2.11. This array is used frequently in resistivity surveying and the spacing are usually described, and taken, in integer multiples of the voltage electrode spacing. The standard nomenclature is to call the potential electrode spacing a , pole-dipole sounding data is

plotted as apparent resistivity versus, a . The pole-pole, pole-dipole and dipole-dipole arrays are normally used in profiling mode to map lateral as well as depth variations in resistivity. The resulting “maps” of apparent resistivity are contoured at constant (usually logarithmic) intervals. The contoured sections are called “pseudo sections” because they look somewhat like resistivity cross-sections of the ground but they are not, they are simply a graphical representation of the data. The vertical scale is not depth but some function of the array spacing.

$$\rho_a = 2\pi r(n + 1)a \frac{\Delta v}{I}$$

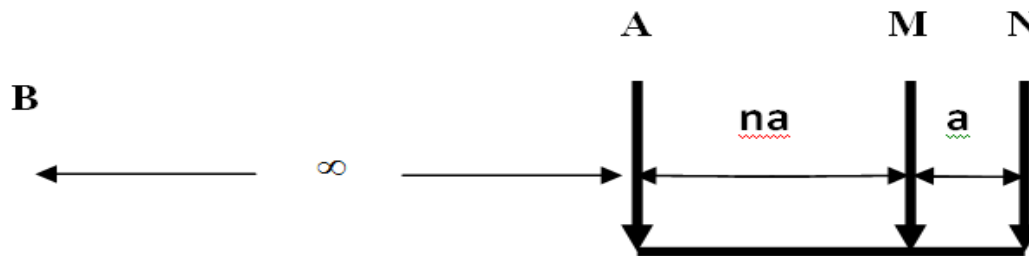


Fig. 2.11 The Pole-dipole electrode configuration

CHAPTER THREE

MATERIALS AND METHOD

3.1 Field Measurement

Preliminary work in the area took the form of reconnaissance survey using global positioning system (GPS) device and VLF-EM method. The three study sites investigated were used previously for road fill, the sites were excavated to depths of about 10m. Two methods of geophysical investigation were used for this research: Very Low Frequency-Electromagnetic method (VLF - EM) and electrical resistivity tomography method. For the design of the geophysical survey, several factors were taken into account, such as the area under investigation and the existing geological and hydrogeological information. The rough terrain and the requirements of increased investigation depths mainly in the region also played an important role in designing this survey. The geophysical survey was conducted in two phases. An initial reconnaissance survey delineated the regions of geological and hydrogeological interest. Based on the reconnaissance survey results, we conducted a high resolution survey using electrical resistivity tomography method, in order to image the subsurface features in the investigated area.

3.2 Geophysical survey using resistivity and VLF-EM

Nine resistivity survey profiles, three each on every site were laid out on the three dumpsites each of 168m with the exception of Capitol that had 84m length. Resistivity data were collected with Dipole-dipole array. The lines were laid parallel to each other at 25m - 30m line spacing. The ERT profiles (ERT 1, ERT 2 and ERT 3) respectively as shown in Fig. 3.1 - 3.3. For ERT data acquisition, SUPERSTING R8/IP was used with 2m electrode spacing at Ikhueniro and Oluku, while 1m electrode spacing was used at Capitol. The model resistivity images were displayed up to 39.4m and 19.7m depth respectively. The VLF-EM is straight forward to use and thirty survey

profiles (PL1 - PL10) were laid out each on the three dumpsites and each of length 300m (Fig. 3.4 - 3.6). From the VLF-EM data collated anomaly maps (Fig. 3.4, 3.5 and 3.6) of the survey areas were plotted using Surfer 13 software. This was aimed at studying the geology and selecting geophysical transverses approximately normal to the strike of the VLF-EM anomaly. The anomaly map of the study area aided laying the ERT profiles along the VLF-EM profiles.

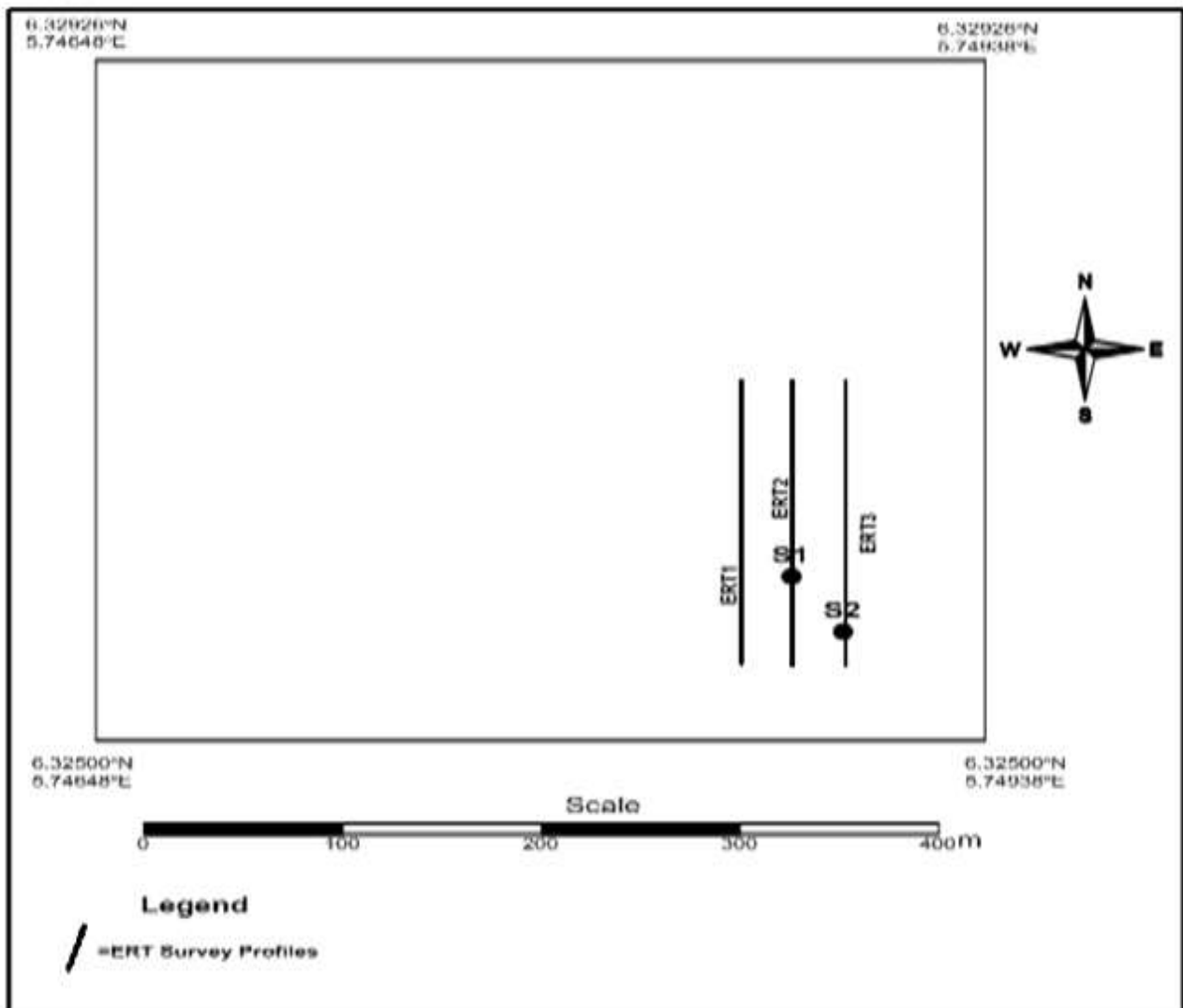


Fig. 3.1: ERT profiles at Ikheuniro

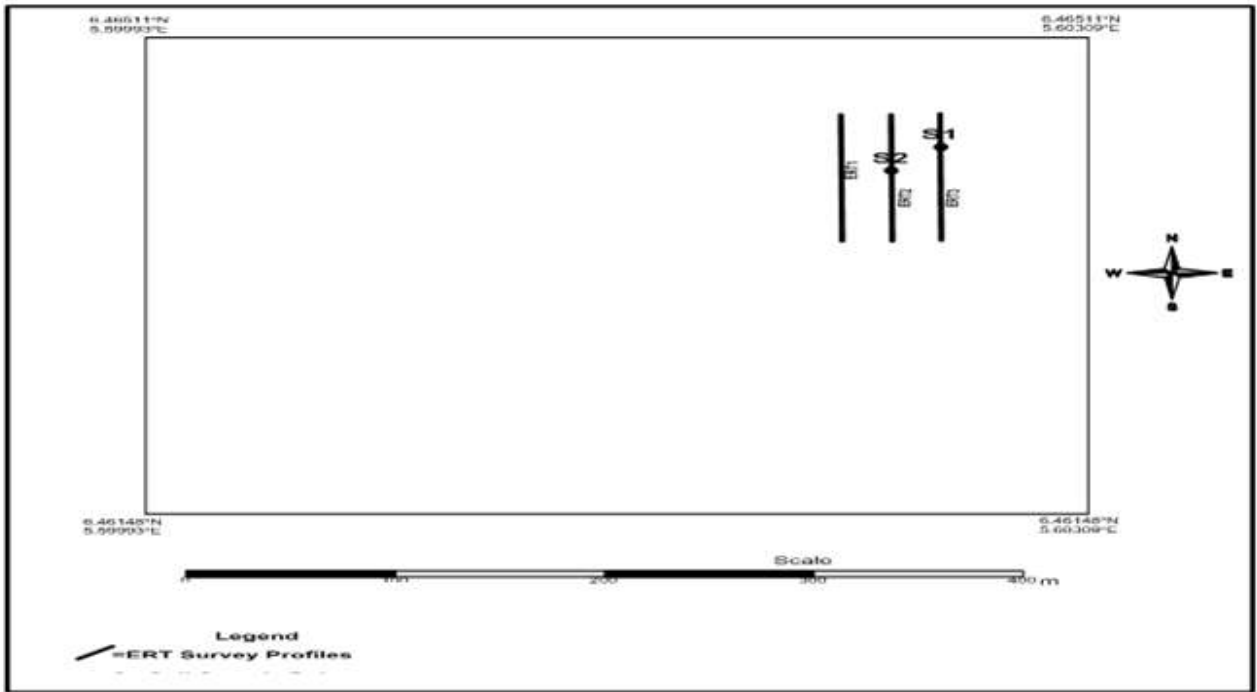


Fig. 3.2: ERT profiles at Capitol

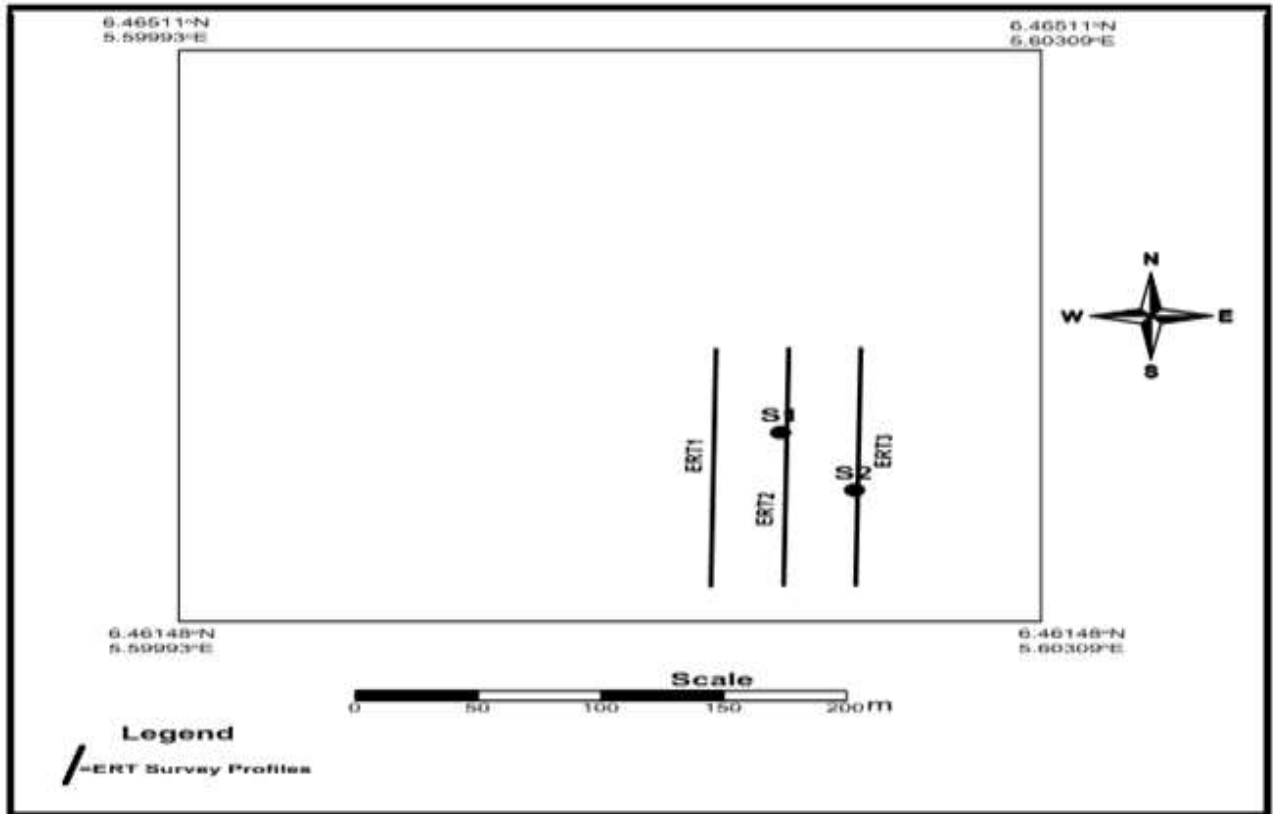


Fig. 3.3: ERT profiles at Oluku

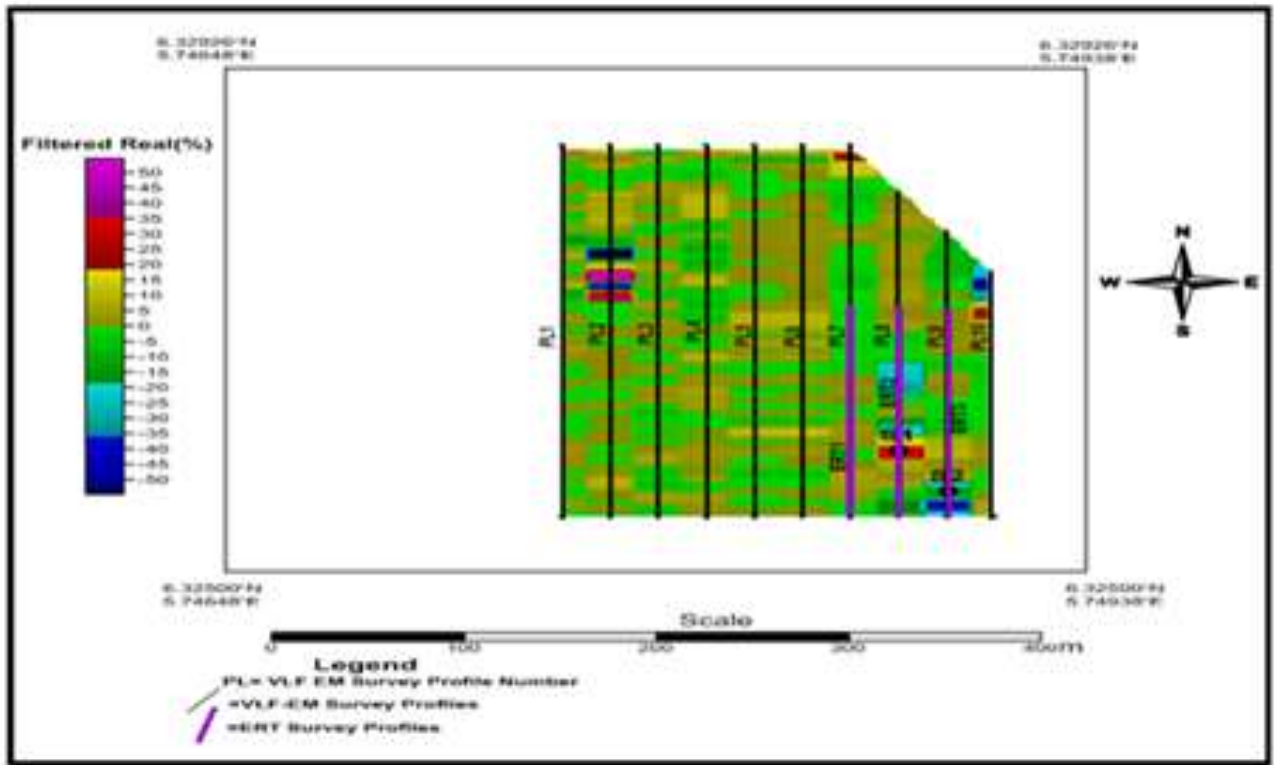


Fig. 3.4: ERT survey tracks superimposed on the VLF anomaly map at Ikhueniro dumpsite

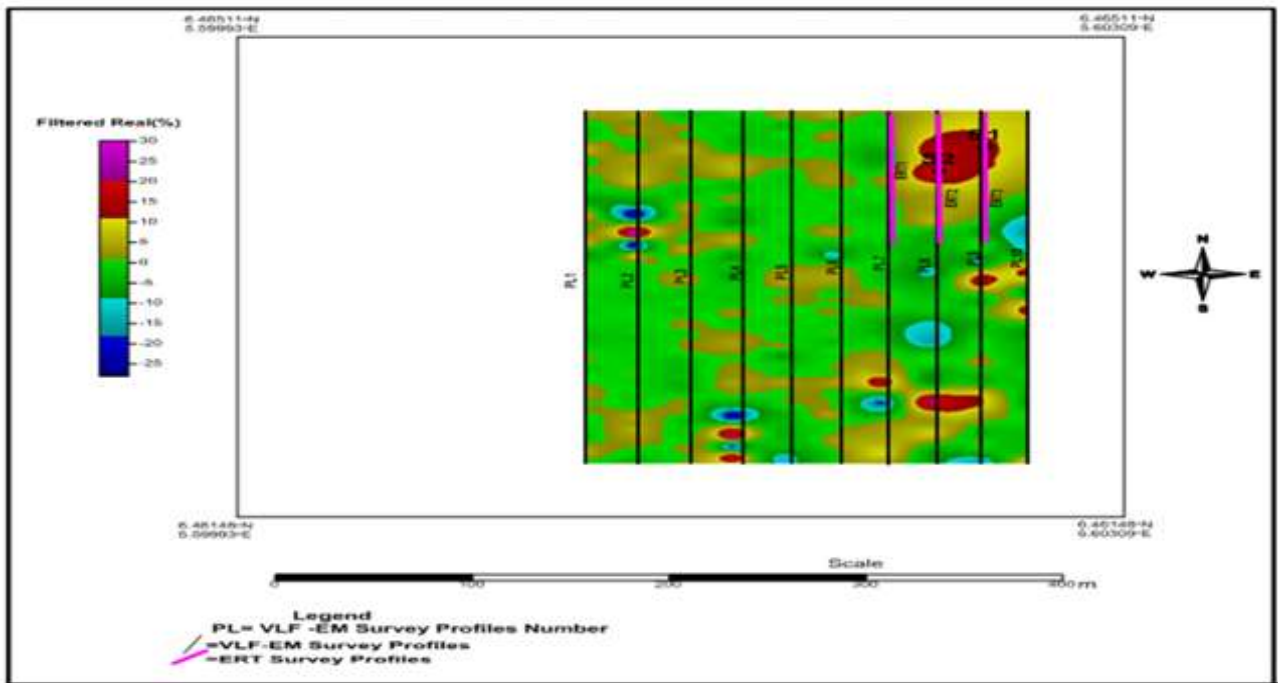


Fig. 3.5: ERT survey tracks superimposed on the VLF anomaly map at Capitol dumpsite

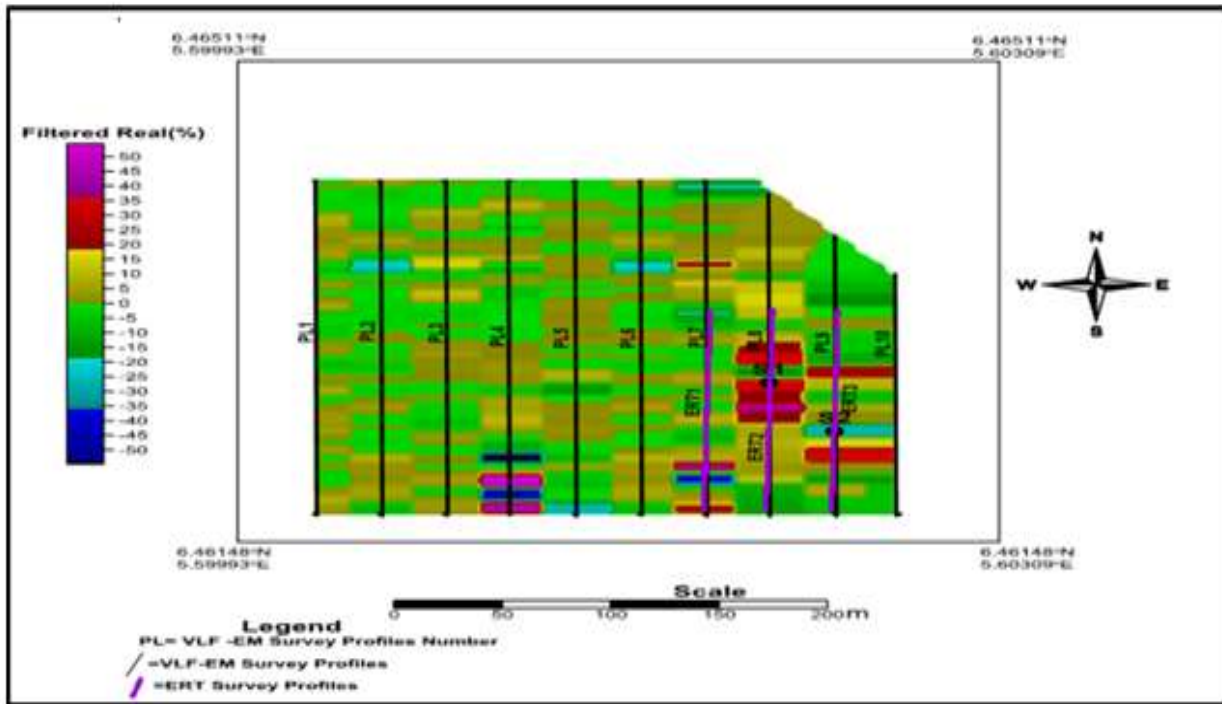


Fig. 3.6: ERT survey tracks superimposed on the VLF anomaly map at Oluku dumpsite

3.3 Instrumentation

The Resistivity Imaging Tomography data were recorded using the SUPERSTING R8/IP as shown in Fig. 3.7. The complete system consists of the Sting instrument console, the Swift interface box (the electronic switching unit), Sting to Swift communication cable, Sting to Swift ABMN cable, Swift-cables with addresses 1 - 14 (cable no.1), 15 - 28 (cable no.2), 29 - 42 (cable no.3), 43 - 56 (cable no.4), 57 - 70 (cable no.5) and 71 - 84 (cable no.6), with 84 stainless steel electrodes. While the electromagnetic (EM) response was measured using the ABEM Wadi as shown in Fig. 3.8.



Fig. 3.7: The SuperSting and swift devices to collect 3D resistivity data



Fig. 3.8: ABEM Wadi and Accessories used for the VLF Electromagnetic Survey

3.3.1 Three-Dimensional Digital Elevation and Terrain Model of the Study Area

This has to do with spatial distribution of data or features such as well location, total depth of the well and depth to the water level in 3-D perspectives. The 3-D digital elevation models of the areas were achieved by using GPS device or receivers to collect longitude, latitude and elevation data of surface topography. Suffer 13 software was used to plot the digital elevation model of the study area. The surface elevation model using GPS assisted in determining surface run-off direction in the survey sites. The 3-D model is useful in groundwater modeling and for environmental studies.

3.4 Field Measurement Using VLF-EM Data Collection

The VLF measurements were carried out with ABEM Wadi operating at a frequency of 17.5kHz - 27.5 kHz with an average spacing of 5m - 10m in all the dumpsites on the 7th of March, 2014. Ten VLF profiles were taken at each of the dumpsites for the purpose of this study. The VLF profiles gives information of the conductive and non conductive zone. High amplitudes indicated areas of conductive zones and low amplitudes indicated areas of non conductive zones. The VLF-EM instrument measures the electrical properties of subsurface materials. It displays the filtered real anomaly on the screen, and this anomaly can be roughly interpreted on site. The profile lengths were from 150m to 350m in all the dumpsites. For each profile, filtered real and filtered imaginary values were plotted against their corresponding station positions. The VLF-EM profiles were quantitatively analyzed. The quantitative analysis enabled the identification of profiles where positive amplitude of filtered real cross over the inflection points of the filtered imaginary as points of anomaly for possible identification of fractures or conductive body. The Fraser filter or Karous and Hjelt software (Karous and Hjelt, 1983) transform the field data into peaks enhancing the signals strength of the conductive body.

3.4.1 Electrical Resistivity Tomography (2-D) Data Collection

The equipment used for electrical resistivity measurement was SuperSting R8/IP. It can be used in four basic modes, namely the Manual, Automatic, User and personal computer (PC) modes. More information on these can be obtained from the Sting R8/IP User's Manual (2010). In this survey, the User mode was used. This allows the user to program any automatic array command file in a computer and download the command file into the Sting. The Sting/Swift can then be used in the field to record data, without having to carry the fragile computer to the field. Six command files were created to record dipole-dipole data at 1m electrode separation at Capitol and 2m electrode

separation at Ikhueni and Oluku. The six command files were designed to measure different parts of the profile line. The first spread begins with cable 1 followed by cable 2 and cable 6 with electrodes 1 - 14, 15 - 28 and 71 - 84 respectively. Measurement commences at electrodes 1, 2, 3, and 4 using its corresponding command file. The spacing is then doubled with active electrodes becoming 1, 3, 5, and 7. In the field, the data collection always starts with placing the stainless steel electrode stakes into the ground at intervals of 2m along selected lines. The swift cables are then laid out on the ground and a spring/rubber band is used to tie the “smart” electrode to its electrode stake, making sure that there is an electrical contact between them. The switching on and off of the “smart” electrodes are controlled automatically by the electronics in the swift box. The details of the traverse from which data is to be collected are entered into the Sting and made ready for data collection. A contact resistance test is run to check for poorly connected electrodes or abnormally high contact resistance reading. The actual measurement was carried out after the contact resistance test output gave good results, otherwise, the causative electrode(s) were checked and properly connected. The start and end locations of survey lines were mapped with a Global Positioning System (GPS). After a successful collection of data from a particular spread, the measured apparent resistivity data was downloaded to a Laptop. Negative data are automatically removed during this process. In all, nine (9) profile lines were surveyed, including three “instrument test” profiles. Majority of the survey time was used in the packing, carrying and laying out measurements of cables, ‘hammering-in’ of the metallic stakes, tying of the electrodes to the stakes. The main factors that determined daily progress included the battery’s power supply, the weather condition (rain and thunderstorms) and terrain accessibility (obstructions).

3.4.2 3D Slice Electrical Resistivity Data collection

The 2D mesh was composed by parallel profile lines from 2D survey on every dumpsite. Dipole–dipole array was used with 2m electrode spacing. All data were assembled into a single data set and submitted to 3D inversion routine. Data were processed with commercial Voxler 3 software which transformed the parallel 2D data set to 3D images.

3.4.3 Data Acquisition in Ikhueniro Dumpsite

The field investigation commenced with a reconnaissance survey using VLF electromagnetic method in order to determine the conductive zones within the dumpsites. The transverse lines were oriented in the N-S direction for VLF-EM (PL1 - PL10) in the dumpsite to delineate the conductive zones. The electrical resistivity tomography survey commenced after determining the conductive zones and anomaly map with the VLF-EM equipment. Three profiles lines were laid for the investigation as shown in (Fig.3.1). The three profiles namely ERT1, ERT2 and ERT3 which were oriented in the N-S direction were laid parallel to each other on the dumpsite. The electrodes were spread 2m apart making the profile length 168m because of available space at the location. Fig. 3.9 shows the satellite image map of Ikhueniro dumpsite.

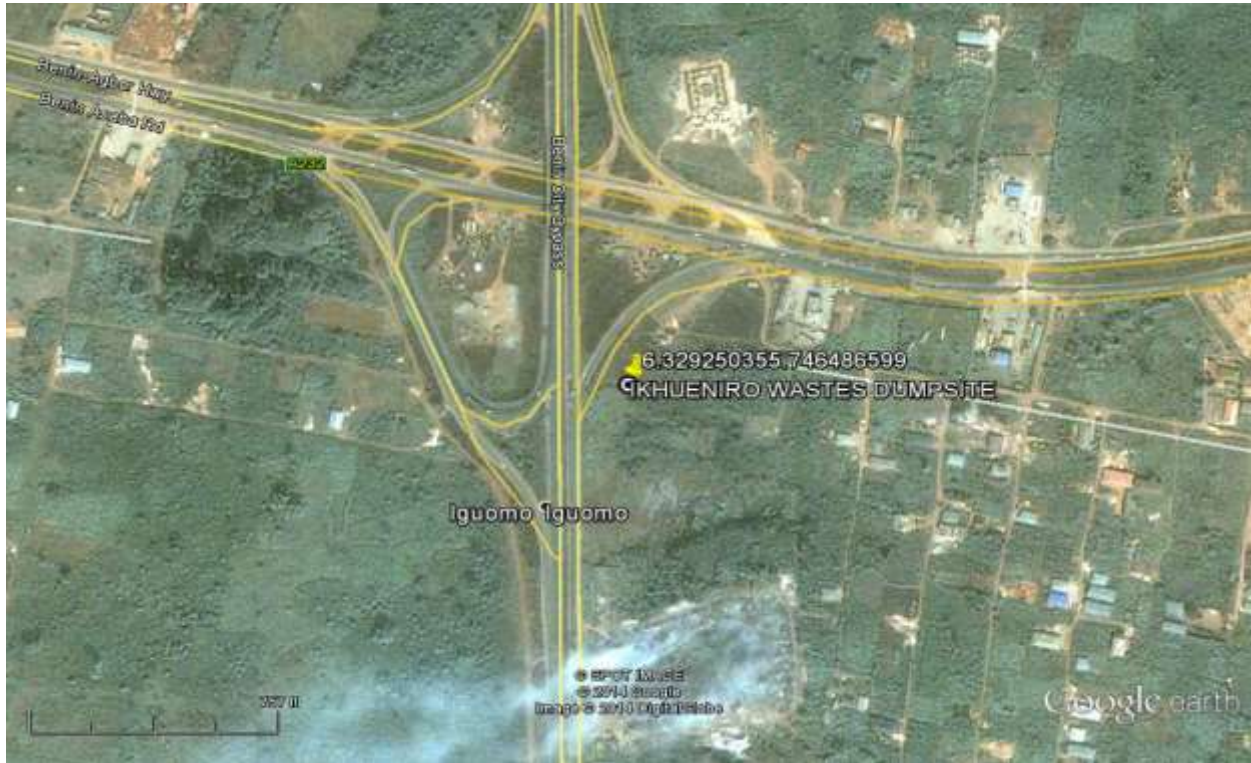


Fig. 3.9: Satellite Imagery map of Ikhueniro Dumpsite (www.google earth, 2014)

3.4.4 Data Acquisition in Capitol Dumpsite

The field investigation commenced with a reconnaissance survey using VLF electromagnetic method in order to determine the conductive zones within the dumpsites. The transverse lines were oriented in the N-S direction for VLF-EM (PL1 - PL10) in the dumpsite to delineate the conductive zones. The electrical resistivity tomography survey commenced after determining the conductive zones with the VLF equipment. Three profile lines were laid for the investigation as shown in (Fig. 3.2). The three profiles namely ERT1, ERT2 and ERT3 which were oriented in the N-S direction were laid parallel to each other on the dump. The electrodes were spread 1m apart making the profile length 84m because of available space at the location. The satellite image of Capitol dumpsite is shown in Fig. 3.10.

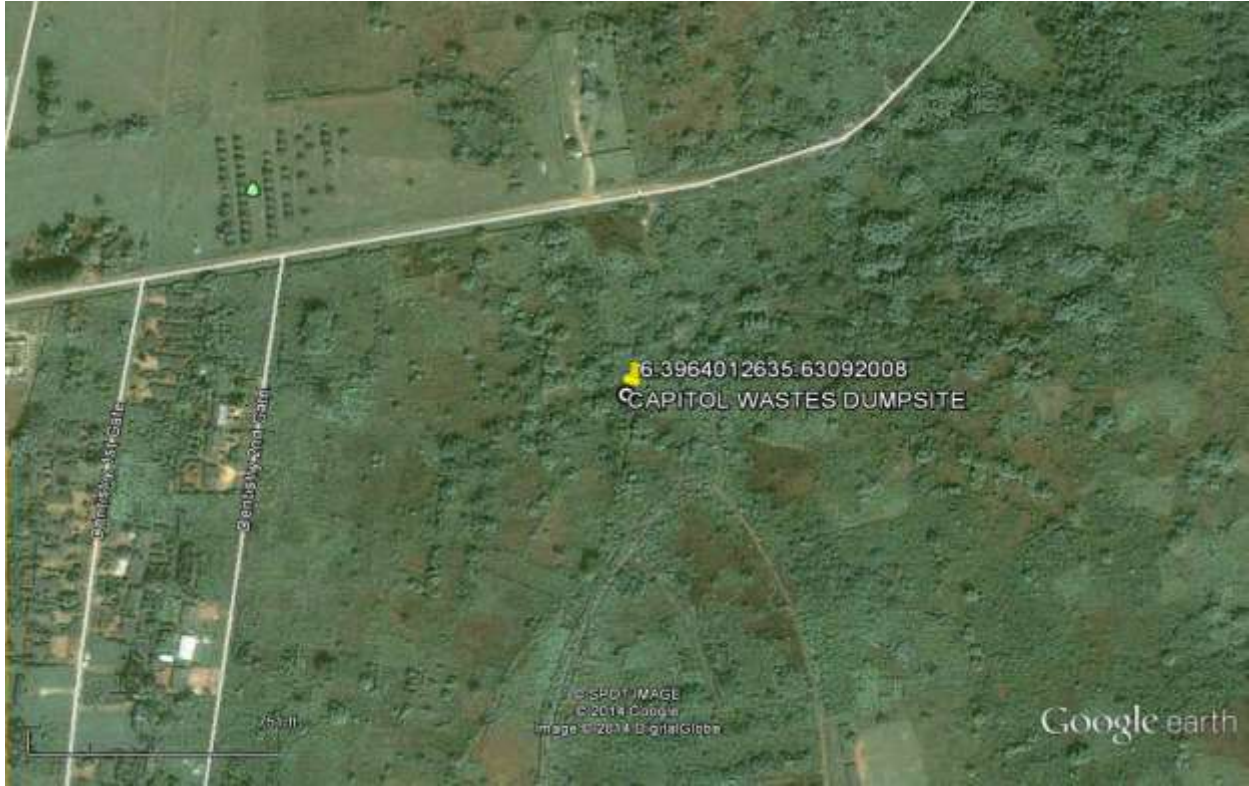


Fig. 3.10: Satellite Imagery Map of Capitol Dumpsite (www.google earth, 2014)

3.4.5 Data Acquisition in Oluku Dumpsite

The field investigation commenced with a reconnaissance survey using VLF electromagnetic method in order to determine the conductive zones within the dumpsite. The transverse lines were oriented in the N-S direction for VLF-EM (PL1 - PL10) in the dumpsite to delineate the conductive zones. The electrical resistivity tomography survey commenced after determining the conductive zones with the VLF equipment. Three profiles lines were laid for the investigation as shown in (Fig. 3.3). The three profiles namely ERT1, ERT2 and ERT3 which were oriented in the N-S direction were laid parallel to each other on the dump. The electrodes were spread 2m apart making the profile length 168m because of available space at the location. The satellite image of Oluku dumpsite is shown in Fig. 3.11.

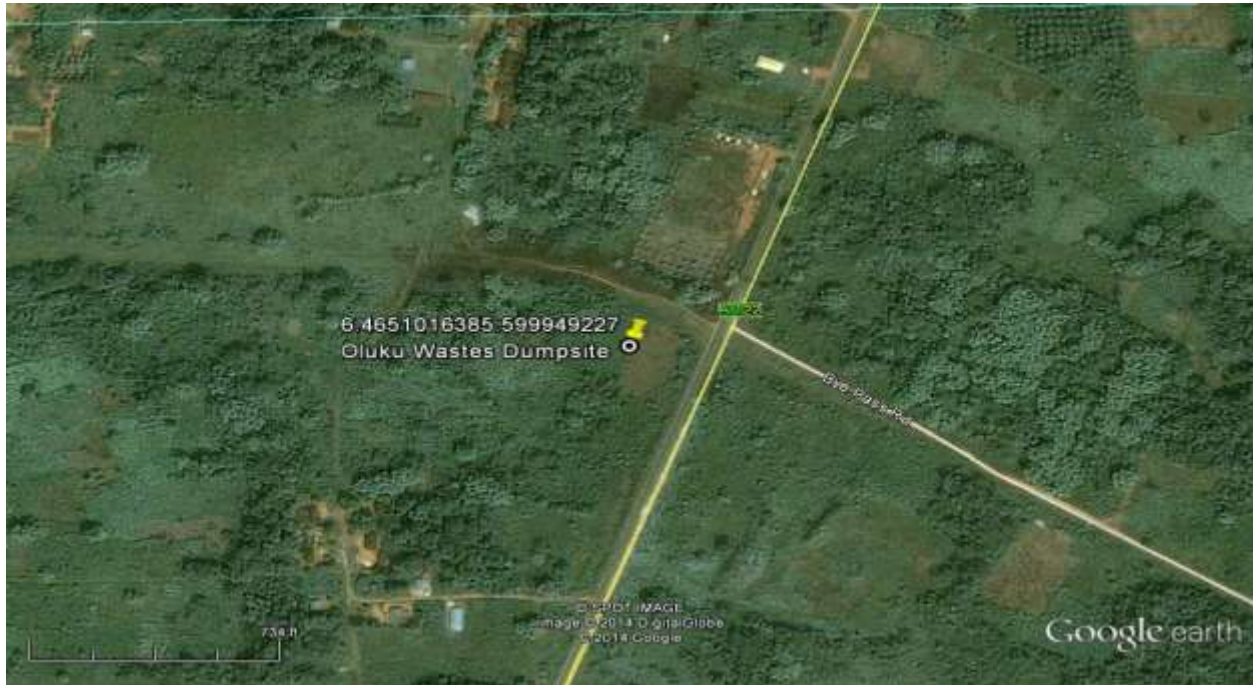


Fig. 3.11: Satellite Imagery Map of Oluku Dumpsite (www.google earth, 2014)

3.5 Processing of VLF Electromagnetic Data

The electromagnetic (EM) response was measured using the ABEM Wadi VLF-EM instrument. The instrument measures the electrical properties of subsurface materials. It displays the filtered real anomaly on the screen, and this anomaly can be roughly interpreted on site. For each profile, filtered real and filtered imaginary values were plotted against their corresponding station positions. The EM profiles were quantitatively analyzed. The VLF-EM sections were plotted with Karous-Hjelt filter (KHFFILT) program. This process yields pseudo-section of relative current density variation with depth. A higher value of relative current density corresponds to conductive subsurface structures.

3.5.1 Processing of Electrical Resistivity Data

The SuperSting data were downloaded to a computer where bad data, particularly negative values are removed in the process of filtering. These raw Sting data files were converted with the Earth

Imager software into the appropriate format readable by the inversion software. The individual input files for all the resistivity imaging survey lines were generated and made ready for inversion into 2D “true resistivity” image in the program. The routine practice is to open a file for a particular traverse results, and view the apparent resistivity data values in form of profiles and to eliminate or remove any inherent bad data points. The main reason for this step is to manually remove bad data points (i.e. obviously too large or too small compared to the neighbouring data points). Though, careful procedures were adopted in the field, during the data collection, nevertheless, bad data could come from sources such as, the failure of the relays at one of the electrodes and poor electrode-ground contact due to dry soil. If bad data points occur, then they must be removed, else they can influence the final output model. After editing the input data, inversion of the data set was then carried out with least squares inversion routine. A model was accepted at the iteration beyond which the root mean square (RMS) error does not change significantly. This usually occurred between the 5th and 8th iteration. The final output file displayed after inversion was the inverse model resistivity section.

3.5.2 2D Resistivity Imaging

The Earth Imager software package was employed in the processing of the Resistivity Imaging Data. Earth Imager software is a computer program designed to invert the “apparent resistivity” data obtained from electrical imaging surveys into a two-dimensional (2D) “true resistivity” model of the subsurface in an automatic and robust manner with minimal input from the user. Therefore the program basically determines a resistivity model that approximates the measured data within the limits of data error. The program first subdivides the subsurface into a number of rectangular blocks, the arrangement of which is loosely tied to the distribution of the measured data points in the pseudo section but it can also be manipulated. It then determines the resistivity of the

rectangular blocks that will produce an apparent resistivity pseudo section that agrees with the actual measurements. It is worth stating that for the same data set, there would be a range of equivalent models whose calculated apparent resistivity values would agree with the measured values to the same degree. Thus the program takes off by not only trying to minimize the difference between the measured and the calculated apparent resistivity values, but the inversion method also attempts to reduce other quantities that will produce certain undesired characteristics in the resulting model. The Earth Imager software uses a forward modelling subroutine (smoothness-constrained method) to calculate apparent resistivity values and a non-linear least-squares optimization technique for the inversion routine. As indicated earlier, the optimization method tries to reduce the difference between the calculated and the measured apparent resistivity values by adjusting the resistivity of the model blocks.

3.5.3 3D Resistivity Imaging Slice

The 3D images slices were derived from the 2D data sets by combining the profiles on every dumpsite. Dipole–dipole array was used to acquire the 2D data with 2m electrode spacing. All 2D data sets on each dumpsite were assembled into a single data set and submitted to 3D inversion routine to produce 3D image for every location. The data were processed with commercial Voxler 3 software. The software transformed parallel 2D data set to 3D set, by using smoothness-constrained least-square method.

3.6 Lithological and Geophysical Control

The lithological and geophysical information used as control in this research include:

1. The borehole log data within the study location (Edo State Ministry of Water Resources, 2012).
2. Result of resistivity data, inverted 2D image in the study area and environment Alile *et al.*, (2012), Iyoha *et al.*, (2013) and Ozegin *et al* (2017).
3. Nature of superficial deposits published by some researchers (Maron, 1969; Assez, 1976; Akpokodje, 1979; Kogbe and Assez, 1979).
4. Published resistivity values of rocks types and contaminants (Ward, 1990)

Table 3.1: The ranges of resistivity values representing the probable type of material based on previous researchers.

<u>Resistivity value (Ωm)</u>	<u>Probable types of material</u>	<u>References</u>
1 – 20	Contaminated soil/groundwater	Meju, 2000
10 – 100	Fresh soil/groundwater	Keller and Frischknecht, 1970
150 – 400	Aluminum, Clay, sandstone, shale and limestone	Loke, 2000 and 2004
400 – 2000	Potential hydrocarbon contamination	Atekwana <i>et al.</i> , 1998
More than 2000	Vadose zone and hard rock or loose fill material	Atekwana, <i>et al.</i> , 1998

CHAPTER FOUR

RESULTS AND DISCUSSION

4.1 VLF and Resistivity survey results

This section comprises four subsections which includes the VLF results and interpretation, the 2D resistivity profile interpretation, 3D plan view of resistivity interpretation and the combination of all geophysical results.

4.2 2D Resistivity Tomography

The nine resistivity profile displayed similar results. The resistivity values ranges between $1\Omega\text{m}$ - $10,000\Omega\text{m}$. An interpretation is made by dividing the values into five, $2000\Omega\text{m}$ and more than $2000\Omega\text{m}$. Based on the five ranges of resistivity values, the lower range (less than $20\Omega\text{m}$) mostly distributed near the surface of resistivity profile (more than 39m depth) is mostly due to manmade contaminated layer which is the most interesting range because it represent a major contamination zone by leachate.

4.3 Three-Dimensional Digital Elevation Model Result of the Study Area

The 3-D digital elevation models of Ikhueniro, Capitol and Oluku landfills were achieved by using GPS device or receivers to collect longitude, latitude and elevation data of surface topography. From the digital elevation model it was deduced that the 3 landfill sites are located at higher elevation as represented by digital elevation values of 84m as higher elevation and 81m as lower elevation at Ikhueniro dumpsite. From the digital elevation model the surface run off direction at Ikhueniro is toward the North and Northwestern part of the region as indicated with an arrow as shown in Fig. 4.1.

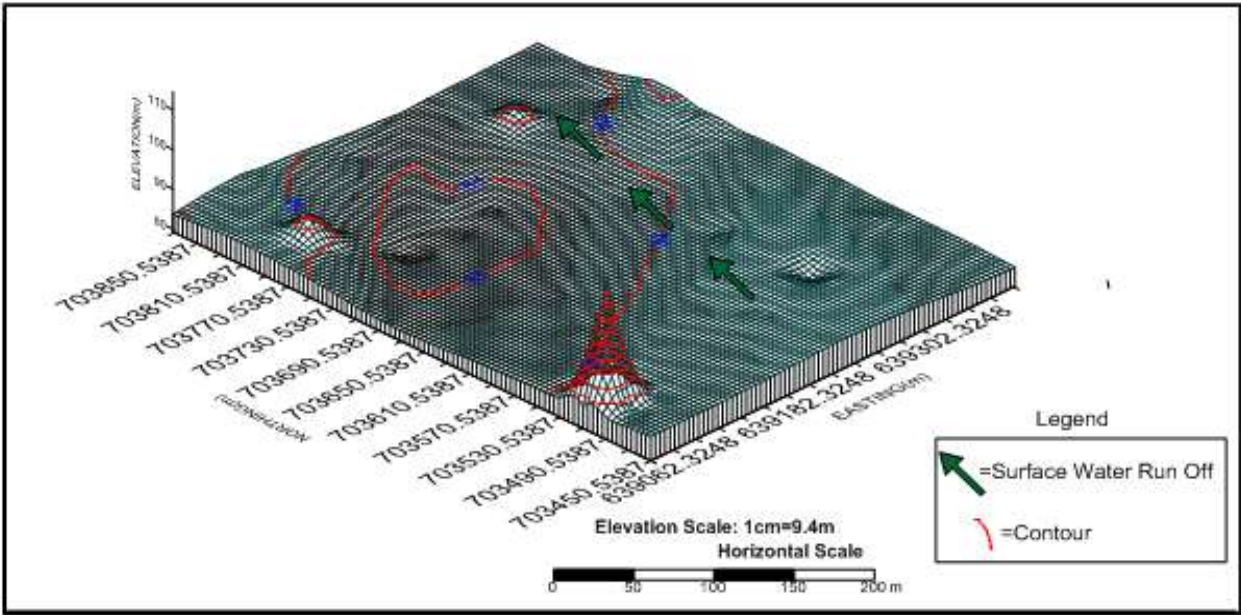


Fig. 4.1: Elevation model of Ikhueniro landfill site, showing the direction of surface water run off. The digital elevation values of 113m as higher elevation and 103m as lower elevation at Capitol dumpsite. At Capitol the surface run off direction is toward the North and Northeastern part of the region as shown in Fig. 4.2.

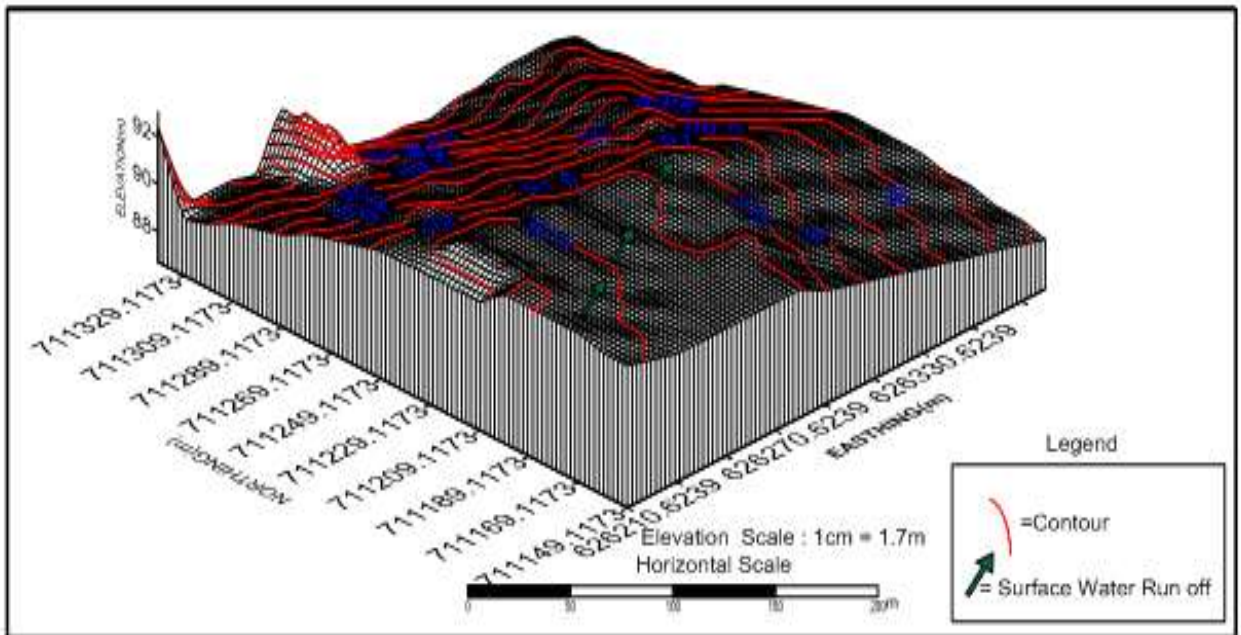


Fig. 4.2: Elevation model of Capitol landfill site, showing the direction of surface water run off

The values 113m correspond to higher elevation and 108m as lower elevation at Oluku dumpsite. Therefore at Oluku dumpsite the surface run off direction is toward the South and Northwestern region as shown in Fig. 4.3.

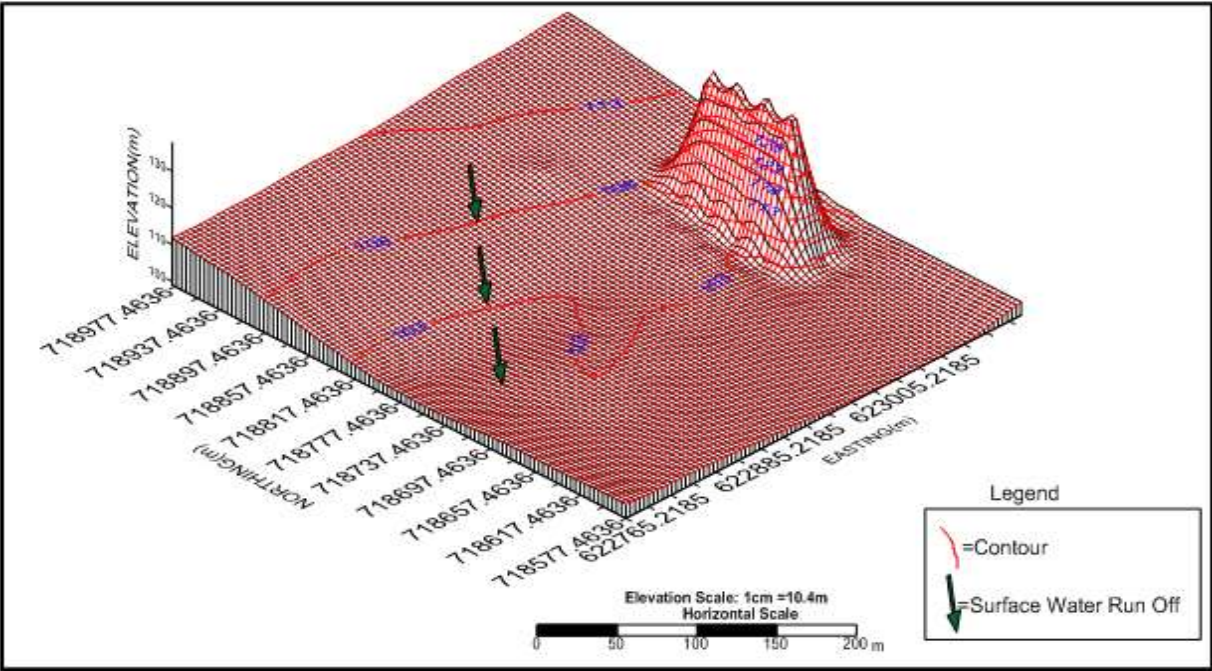


Fig. 4.3: Elevation model of Oluku landfill site, showing the direction of surface water run off

The surface elevation model assisted in determining surface run-off direction in the survey sites. As a result of this nature of landfill site topography, surface run off of water produced during rainfall and flooding may erode leachate from dumpsite into the groundwater reservoir down slope, therefore contaminating the water table and wells dug within the zone, and with time may percolate into the saturated zone. The 3-D model is very good for groundwater modeling which is an important tool for the groundwater hydrologists. 3-D model are used to express points basically on the groundwater flow system in the basement and sedimentary environment. The surface water flow direction in the sedimentary area can be influenced by elevation.

4.3.1 Borehole Lithology

The two borehole lithology logs within the study locations (Ikhueni, Oluku and Capitol environs) are shown in Table. 4.1.

Table 4.1: Lithology logs of Ikhueni and Oluku/Capitol environs

Soil type	Ikhueni environ depth (feet)	Oluku/Capitol depth (feet)
laterite soil	1-10	1-70
Brown sand	90	125
Coarse sand	100	150
Clay	210	316 - 332

The geophysical investigation results of the electrical resistivity method in the study areas agreed with the possibility of having a successful borehole in the area. The subsurface geological materials in the study area are mainly laterite soil, sandstone and clay as shown in Fig. 4.4, which was equally revealed by the ERT results. There was therefore a good correlation between ERT results and actual drilling results in the study area.

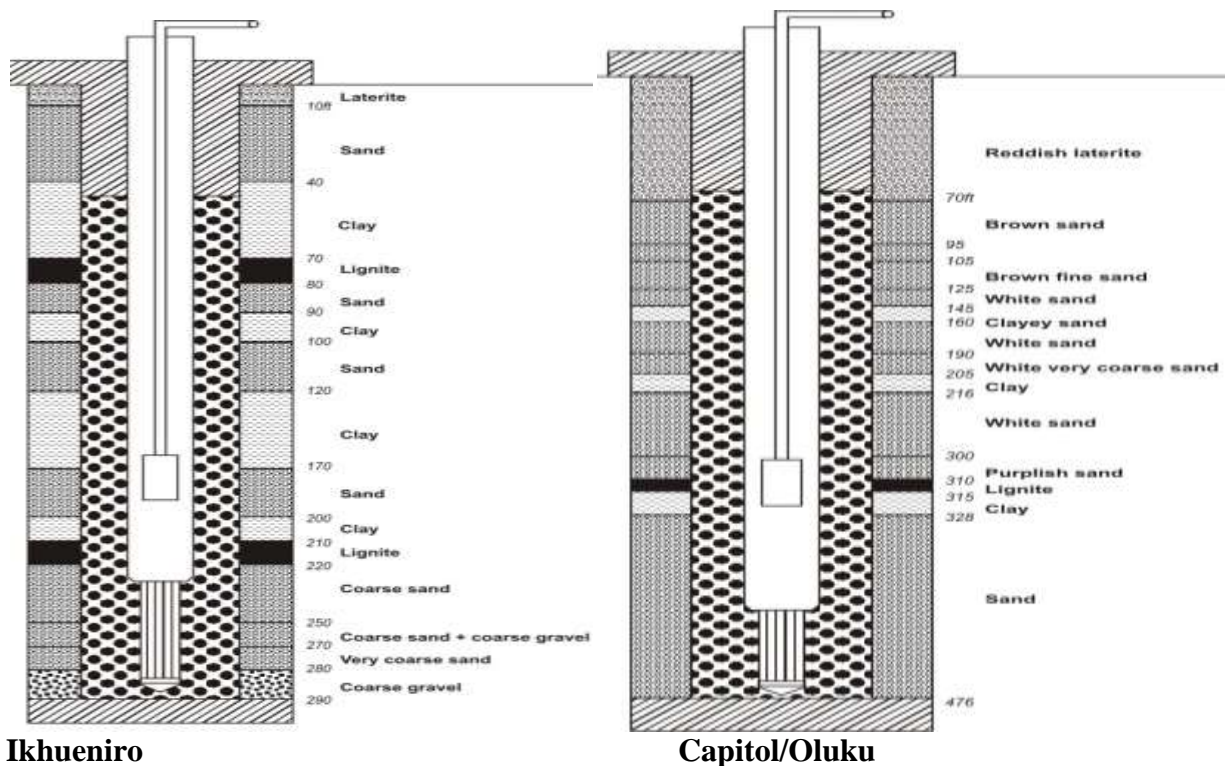


Fig. 4.4: Borehole Lithology at Ikhueni, Capitol and Oluku (Edo State Ministry of Water Resources, 2012)

4.4 Deductions and Discussion of the VLF-EM Results

4.4.1 The Karous-Hjelt filtered pseudo-sections of Ikhueniro Dumpsite

The VLF-EM profiles in this study were processed using the Karous-Hjelt filter. Figs. 4.5a - 4.14b shows the computed relative current densities for ten VLF-EM profiles carried out at Ikhueniro dumpsite. The areas of high current density correspond to positive values (red colour) in the image map. All the VLF-EM profiles (PL1 - PL10) were oriented along N-S direction of the landfill. Profile 1 (Figs. 4.5a - 4.5b) show high current density values at sites located around 1m - 20m, 40m - 80m, 210m - 230m, 240m - 260m and 280m - 300m respectively, this indicates the presence of conductive zone. In Profile 2 (Figs. 4.6a - 4.6b) the current density values were observed at distance of 20m - 40m, 200m - 240m and 300m - 310m respectively, this indicates the presence of conductive zone. In Profile Three (Figs. 4.7a - 4.7b) the current density values were observed along this profile between the distance of 10m - 30m, 40m - 70m, 100m - 150m, 180m - 210m, 230m - 250m and 320m - 340m respectively, this indicates the presence of conductive zone. In Profile four (Figs. 4.8a - 4.8b) the current density values were observed along the distance of 10m - 40m, 100m - 180m, 210m - 240m and 260m - 320m respectively, which indicate a possible presence of weak zone. In Profile five (Figs. 4.9a - 4.9b) the current density values were observed along this profile between the distance of 20m - 30m, 50m - 90m, 120m - 200m and 230m - 350m respectively, this indicates the presence of conductive zone. In Profile 6 (Figs. 4.10a - 4.10b) the current density values were observed along this profile between the distance of 20m - 30m, 80m - 100m, 160m - 200m and 330m - 350m respectively, which indicate presence of conductive zone. In Profile 7 (Figs. 4.11a - 4.11b) the current density values were observed along this profile between the distance of 10m - 50m, 60m - 140m, 250m - 300m and 320m - 350m respectively, this indicates the presence of conductive zone. In Profile 8 (Figs. 4.12a - 4.12b) the current density values were observed along this profile between the distance of 50m - 70m and 100m - 110m respectively, this indicates the presence of conductive zone. In Profile 9 (Figs. 4.13a - 4.13b) the current density values were observed along this profile between the distance of 1m - 10m, 30m - 50m, 60m - 80m and 120m - 140m respectively, this indicates the presence of conductive zone. In Profile 10 (Figs. 4.14a - 4.14b) the current density values were observed along this profile between the distance of

1m - 20m, 50m - 70m and 150m – 200m respectively, this indicates the presence of conductive zone. These conductive zones may be caused by leachate plumes, artificial or geological conductors.

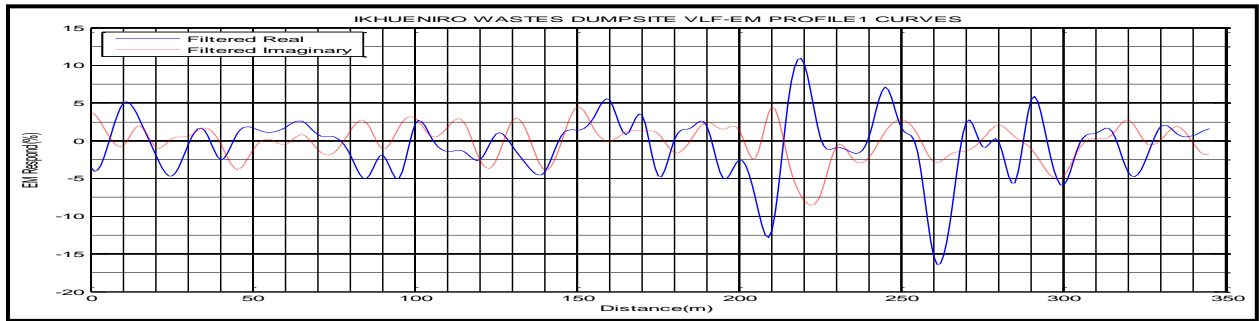


Fig. 4.5a: Ikhueniro VLF-EM Curve (filtered real and filtered imaginary) of Profile (PL1)

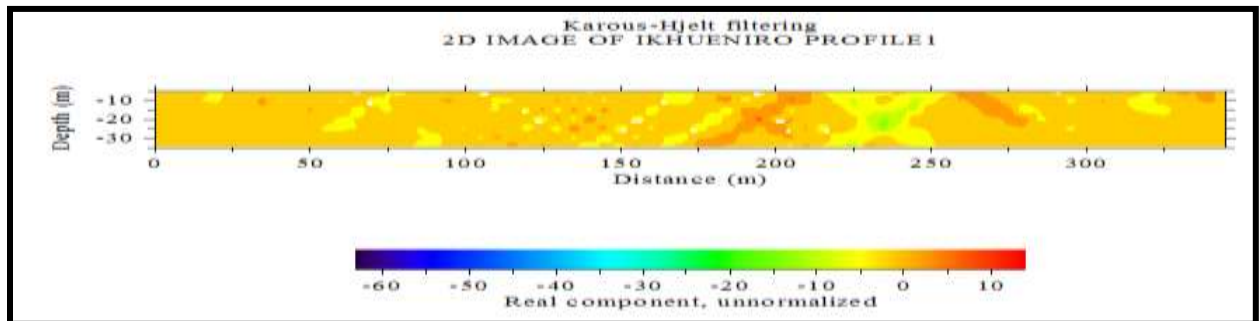


Fig. 4.5b: Ikhueniro VLF-EM Image of Profile (PL1)

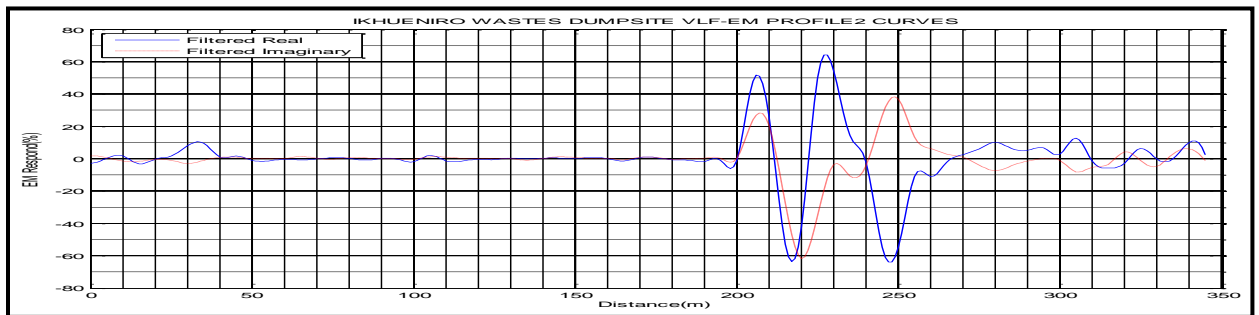


Fig. 4.6a: Ikhueniro VLF-EM Image (filtered real and filtered imaginary) of Profile (PL2)

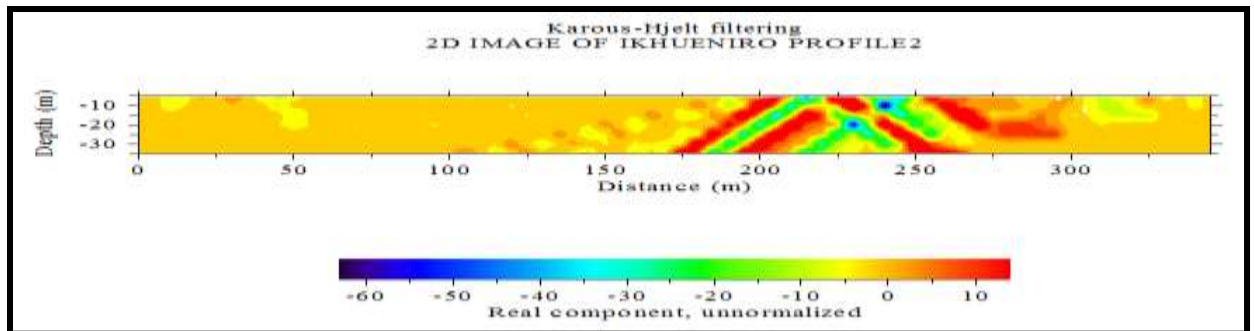


Fig. 4.6b: Ikhueniro VLF-EM Image of Profile (PL2)

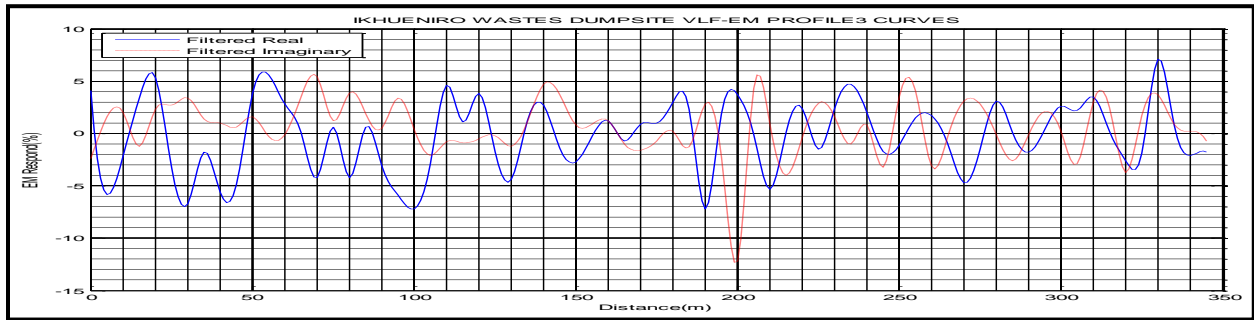


Fig. 4.7a: Ikhueniro VLF-EM Curve (filtered real and filtered imaginary) of Profile (PL3)

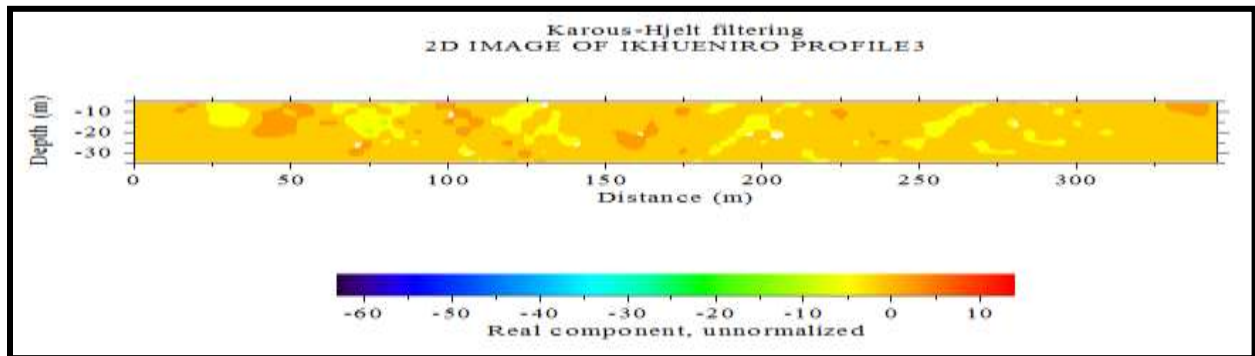


Fig. 4.7b: Ikhueniro VLF-EM Image of Profile 3 (PL3)

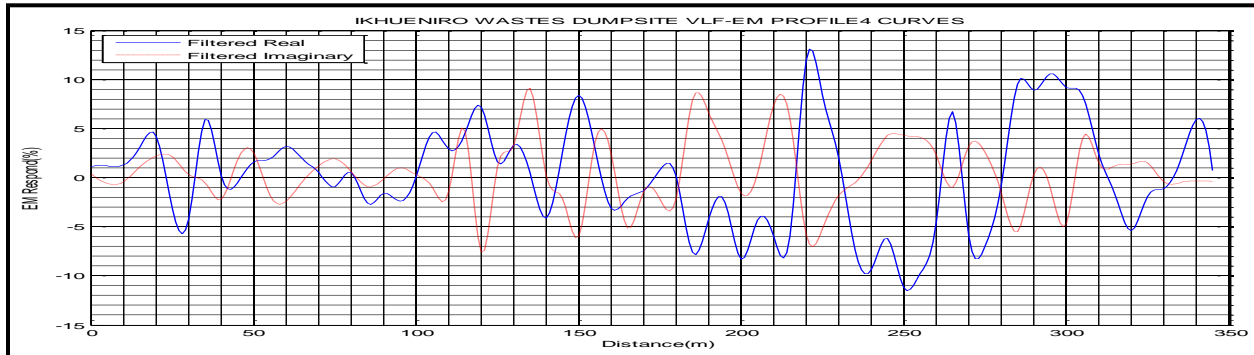


Fig. 4.8a: Ikhueniro VLF-EM Curve (filtered real and filtered imaginary) of Profile (PL4)

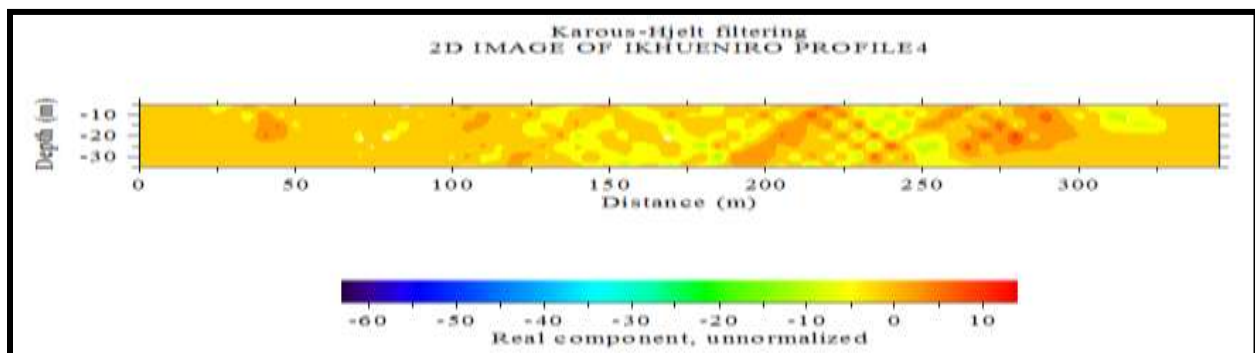


Fig. 4.8b: Ikhueniro VLF-EM Image of Profile (PL4)

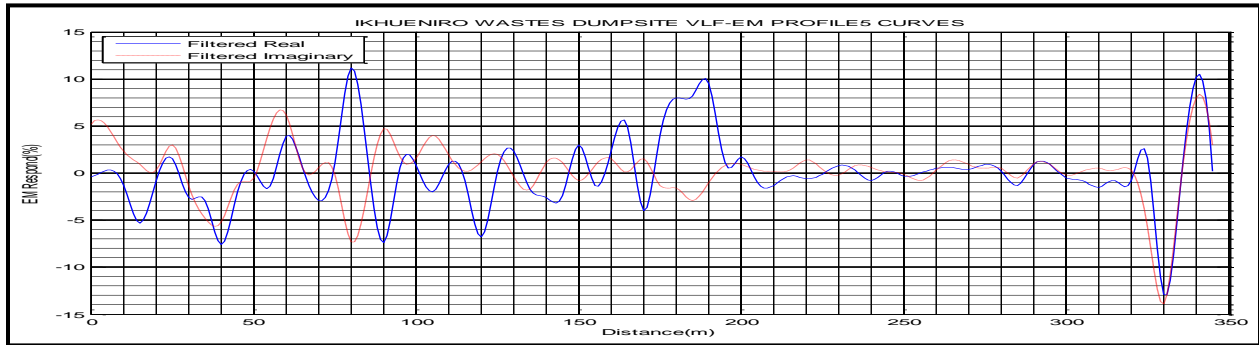


Fig. 4.9a: Ikhueniro VLF-EM Curve (filtered real and filtered imaginary) of Profile (PL5)

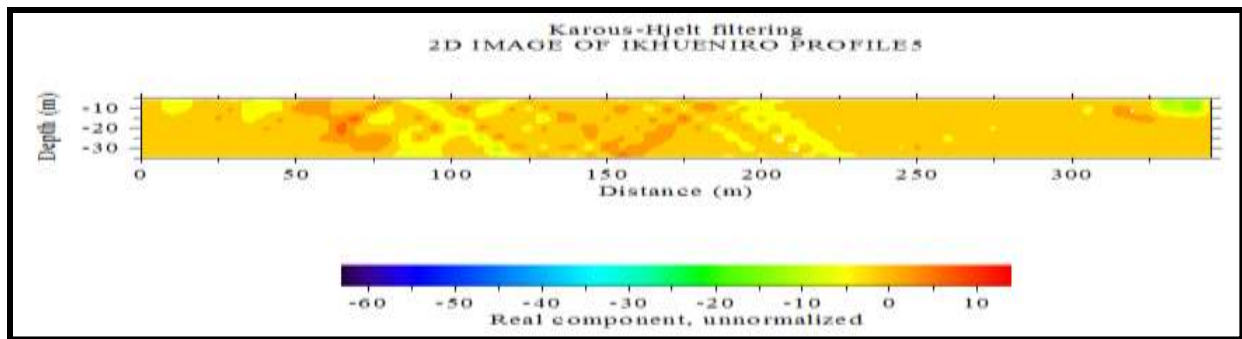


Fig. 4.9b: Ikhueniro VLF-EM Image of Profile (PL5)

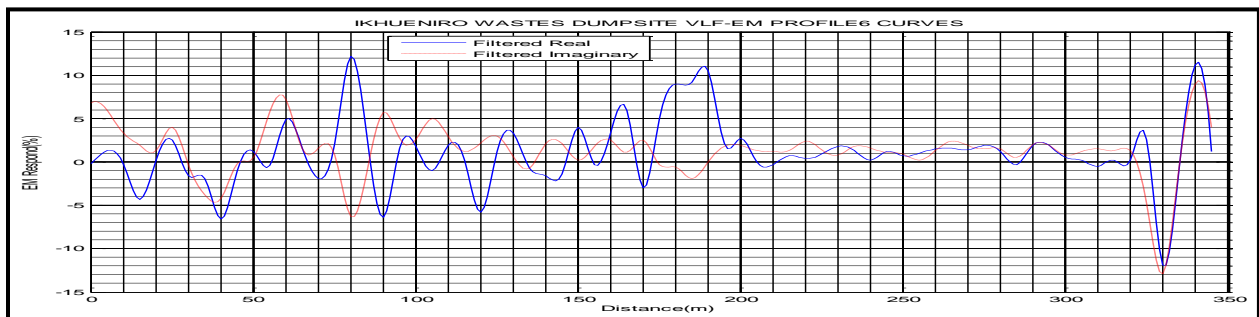


Fig. 4.10a: Ikhueniro VLF-EM Curve (filtered real and filtered imaginary) of Profile (PL6)

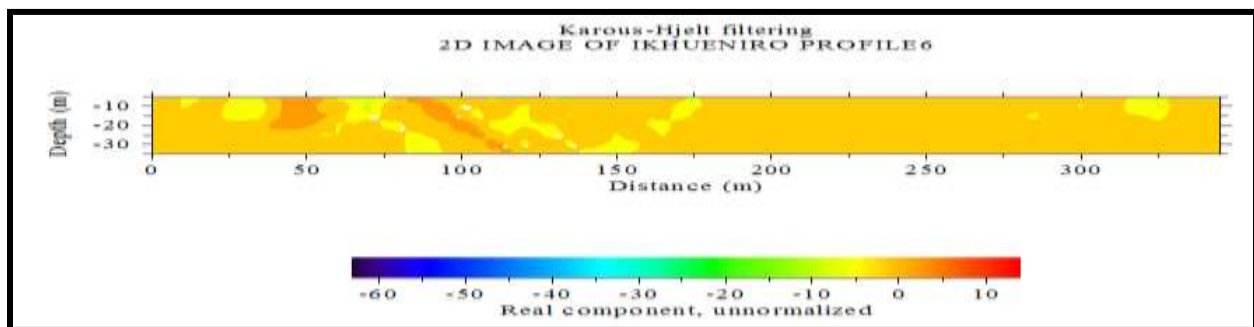


Fig. 4.10b: Ikhueniro VLF-EM Image of Profile (PL6)

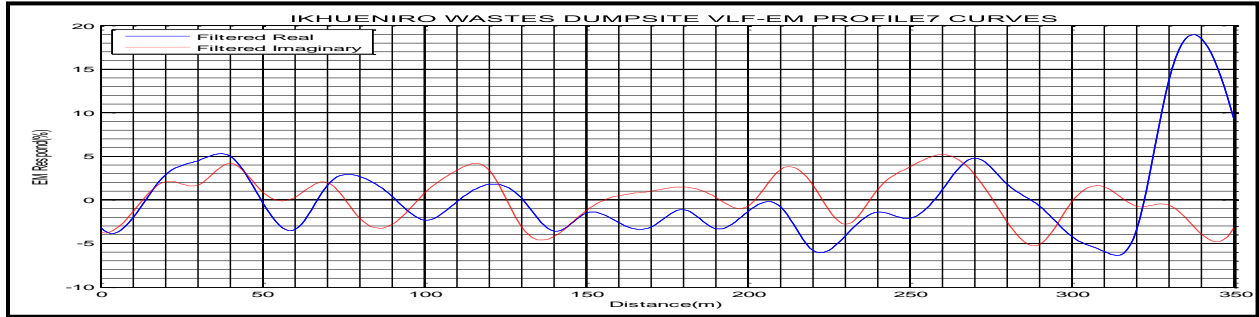


Fig. 4.11a: Ikhueniro VLF-EM Curve (filtered real and filtered imaginary) of Profile (PL7)

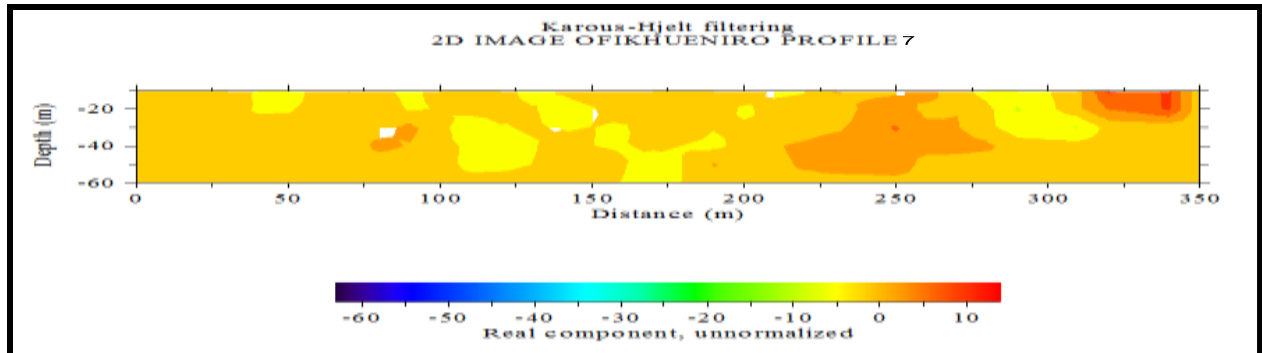


Fig. 4.11b: Ikhueniro VLF-EM Image of Profile (PL7)

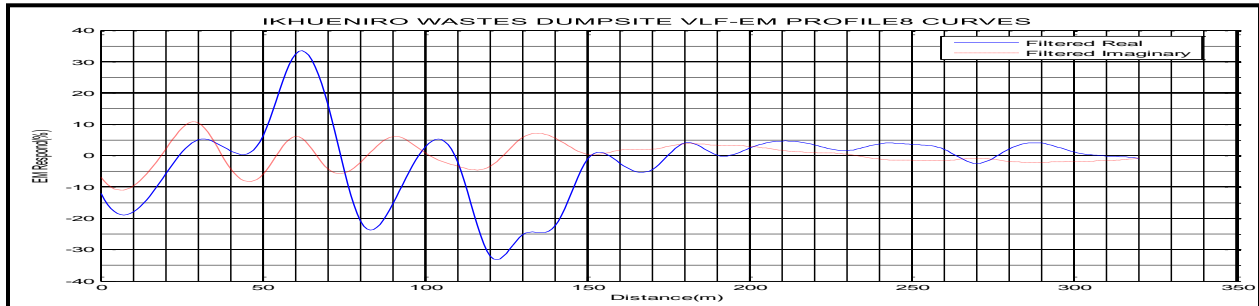


Fig. 4.12a: Ikhueniro VLF-EM Curve (filtered real and filtered imaginary) of Profile (PL8)

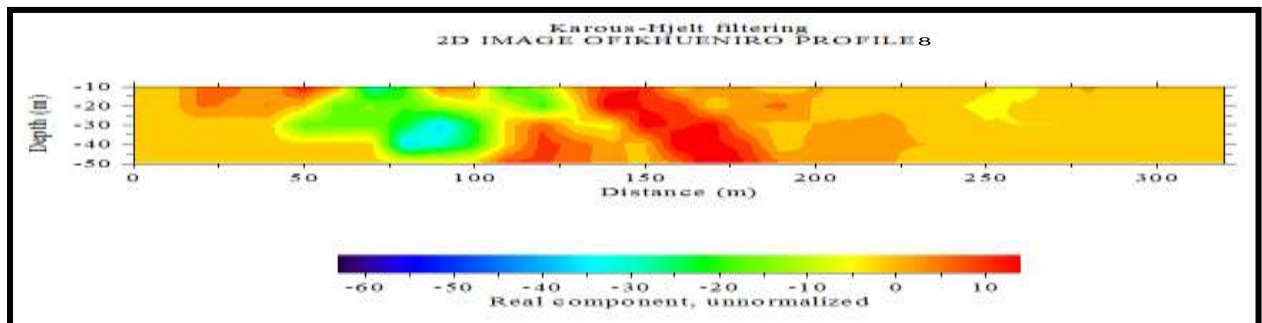


Fig. 4.12b: Ikhueniro VLF-EM Image of Profile (PL8)



Fig. 4.13a: Ikhueniro VLF-EM Curve (filtered real and filtered imaginary) of Profile (PL9)

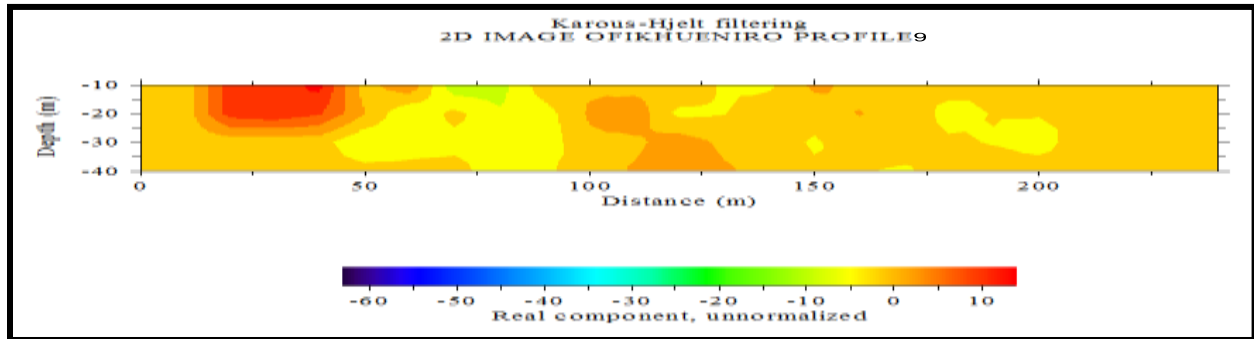


Fig. 4.13b: Ikhueniro VLF-EM Image of Profile (PL9)

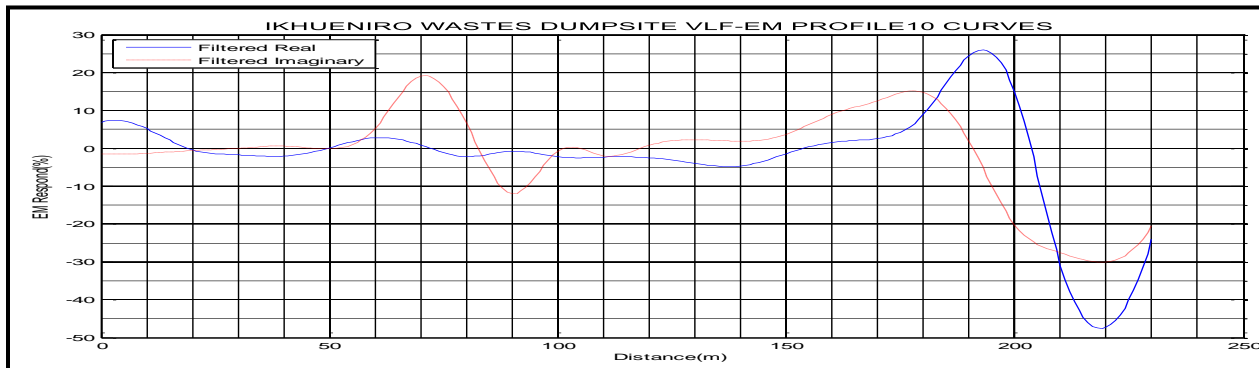


Fig. 4.14: Ikhueniro VLF-EM Image (filtered real and filtered imaginary) of Profile (PL10)

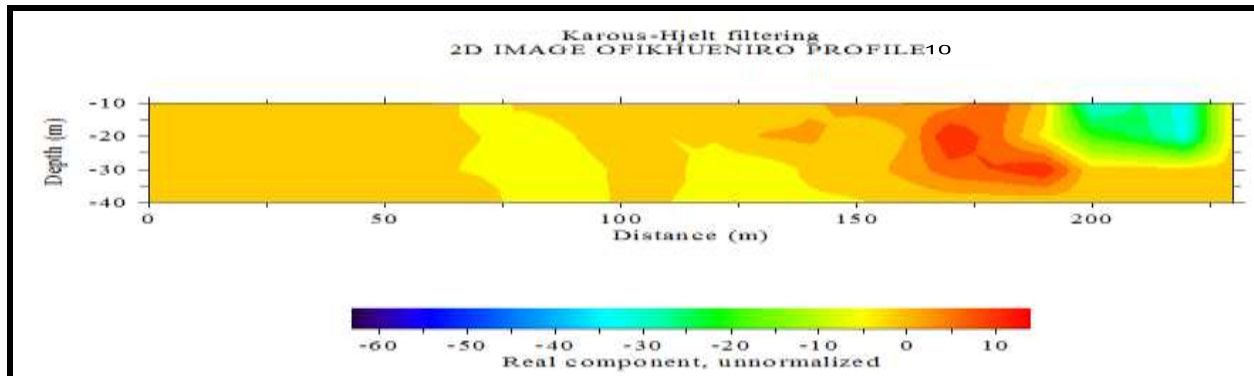


Fig. 4.14b: Ikhueniro VLF-EM Image of Profile (PL10)

The Fraser filter or Karous and Hjelt software transform the data into peaks enhancing the signals of the conductive structures. Figs. 4.5a - 5.14b shows the Karous and Hjelt filtered data (real and imaginary components). The in-phase profiles show positive peaks of different intensities and sharpness, suggesting the presence of shallow and deep conductors. The presences of shallow and deep conductors are determined by the dip, size and nature of the conductor. These conductive zones may be due to leachate plumes

4.4.2 The Karous–Hjelt filtered pseudo-sections of Capitol Dumpsite

The VLF-EM profiles in this study were processed using the Karous–Hjelt filter Figs. 4.15a – 4.24b and show the computed relative current densities for ten VLF-EM profiles carried out at Capitol dumpsite. All the VLF-EM profiles (PL1 - 10) were oriented along N-S direction of the landfill. The areas of high current density correspond to positive values (red colour). In Profile 1 (Figs. 4.15a - 4.15b) the current density values were observed along this profile between the distance of 1m - 20m, 45m - 96m and 100m – 120m respectively, this indicates the presence of conductive zone. In Profile 2 (Figs. 4.16a - 4.16b) the current density values were observed along this profile between the distance of 1m - 10m, 35m - 60m, 70m - 90m and 100m - 115m respectively, this indicates the presence of conductive zone. In Profile 3 (Figs. 4.17a - 4.17b) the current density values were observed along this profile between the distance of 15m - 30m, 40m - 60m, 85m - 95m and 128m - 136m respectively, this indicates the presence of conductive zone. In Profile 4 (Figs. 4.18a - 4.18b) the current density values were observed along this profile between the distance of 16m - 28m, 40m - 58m and 124m – 138m respectively, this indicates the presence of conductive zone. In Profile 5 (Figs. 4.19a - 4.19b) the current density values were observed along this profile between the distance of 1m - 20m, 48m - 60m, 64m - 80m and 100m – 120m respectively, this indicates the presence of conductive zone. In Profile 6 (Figs. 4.20a - 4.20b) the current density values were observed along this profile between the distance of 1m - 20m, 48m - 60m, 64m - 92m, 100m - 120m and 128m - 140m respectively, this indicates the presence of conductive zone. In Profile 7 (Figs. 4.21a - 4.21b) the current density values were observed along this profile between the distance of 18m - 40m and 68m -

100m respectively, this indicates the presence of conductive zone. In Profile 8 (Figs. 4.22a - 4.22b) the current density values were observed along this profile between the distance of 20m - 28m and 118m - 132m respectively, this indicates the presence of conductive zone. In Profile 9 (Figs. 4.23a - 4.23b) the current density values were observed along this profile between the distance of 18m - 28m, 32m - 40m and 72m - 100m respectively, this indicates the presence of weak zone. In Profile 10 (Figs. 4.24a - 4.24b) the current density values were observed along this profile between the distance of 1m - 28m, 44m - 60m, 80m - 96m and 100m - 112m respectively, this indicates the presence of conductive zone.

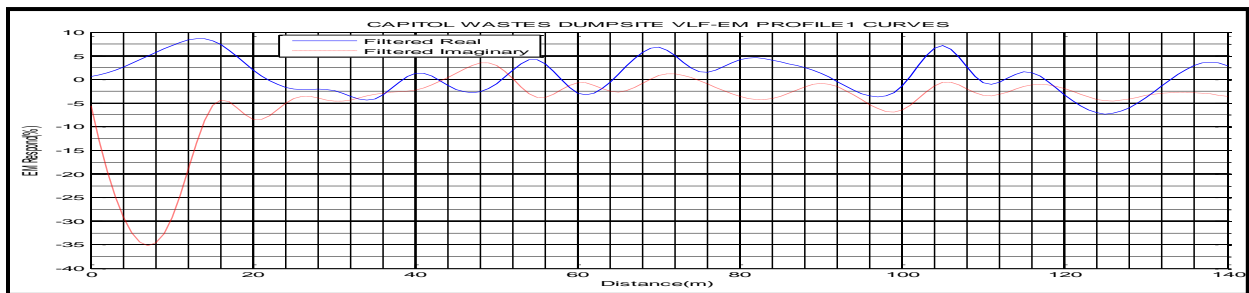


Fig. 4.15a: Capitol VLF-EM Curve (filtered real and filtered imaginary) of Profile (PL1)

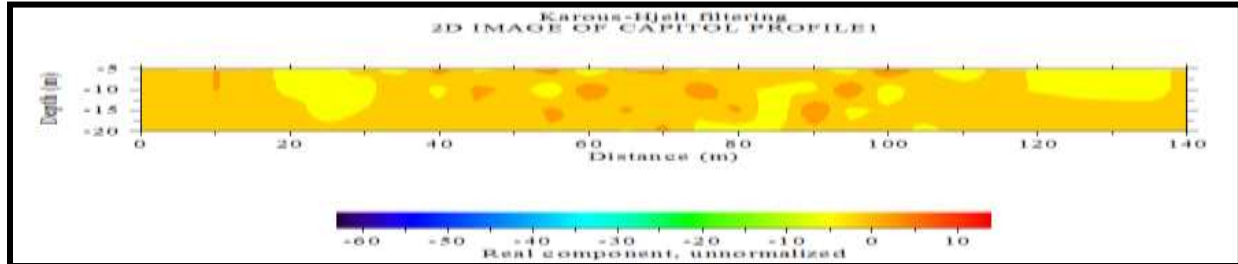


Fig. 4.15b: Capitol VLF-EM Image of Profile (PL1)

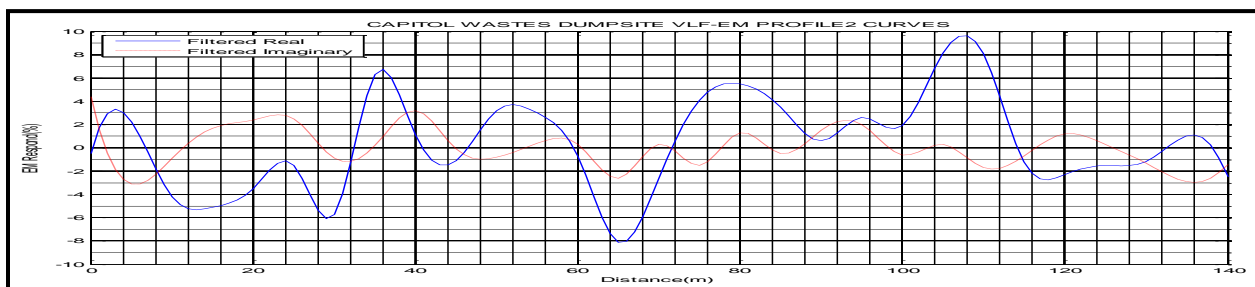


Fig. 4.16a: Capitol VLF-EM Curve (filtered real and filtered imaginary) of Profile (PL2)

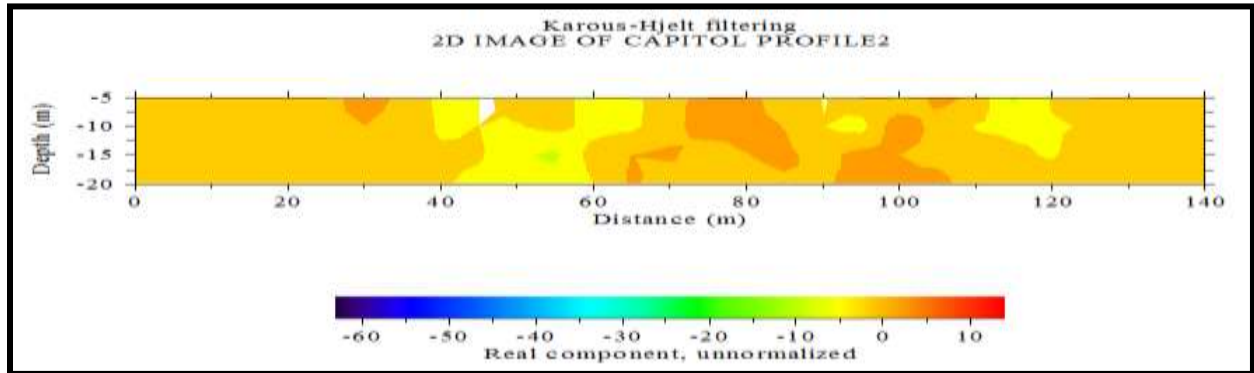


Fig. 4.16b: Capitol VLF-EM Image of Profile (PL2)

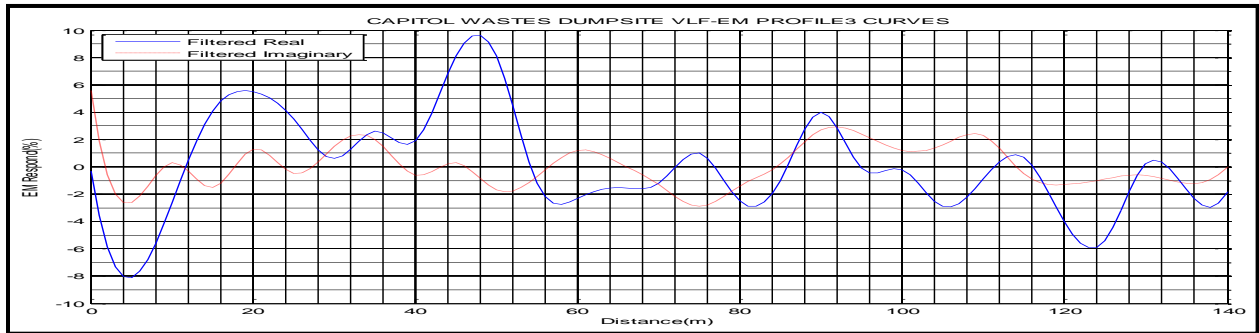


Fig. 4.17a: Capitol VLF-EM Curve (filtered real and filtered imaginary) of Profile (PL3)

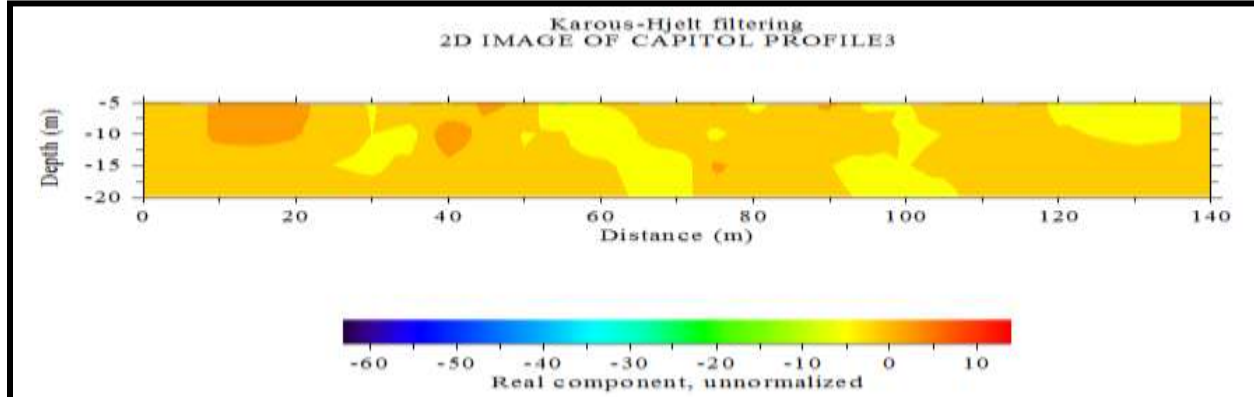


Fig. 4.17b: Capitol VLF-EM Image of Profile (PL3)

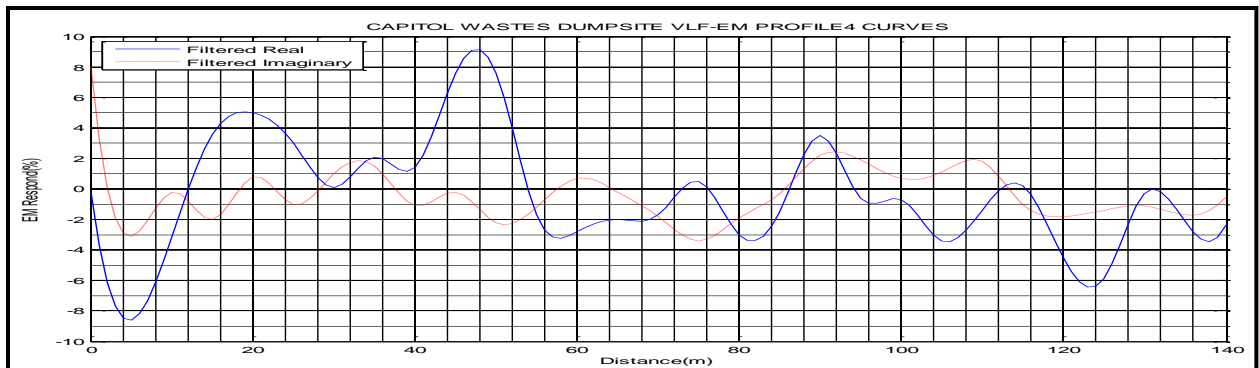


Fig. 4.18a: Capitol VLF-EM Curve (filtered real and filtered imaginary) of Profile (PL4)

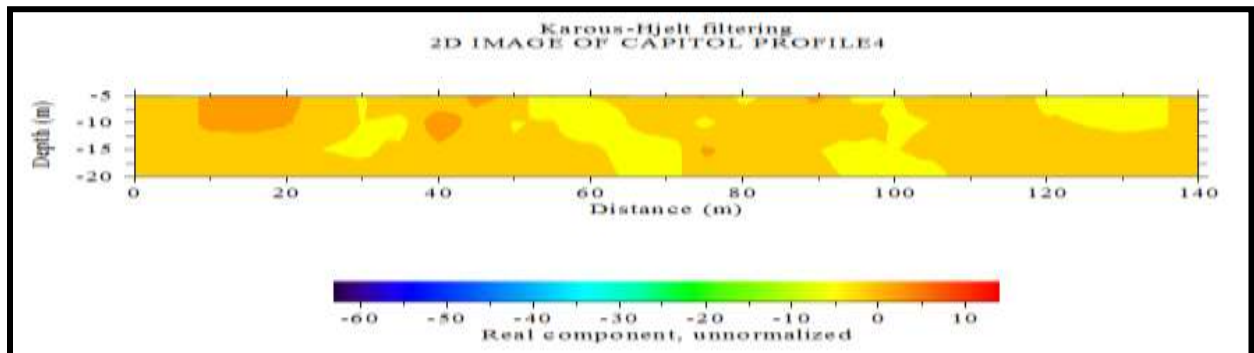


Fig. 4.18b: Capitol VLF-EM Image of Profile (PL4)

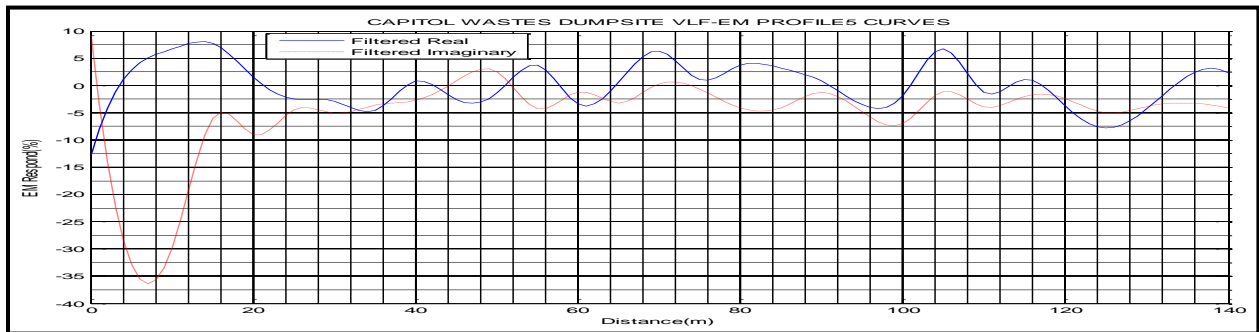


Fig. 4.19a: Capitol VLF-EM Curve (filtered real and filtered imaginary) of Profile (PL5)

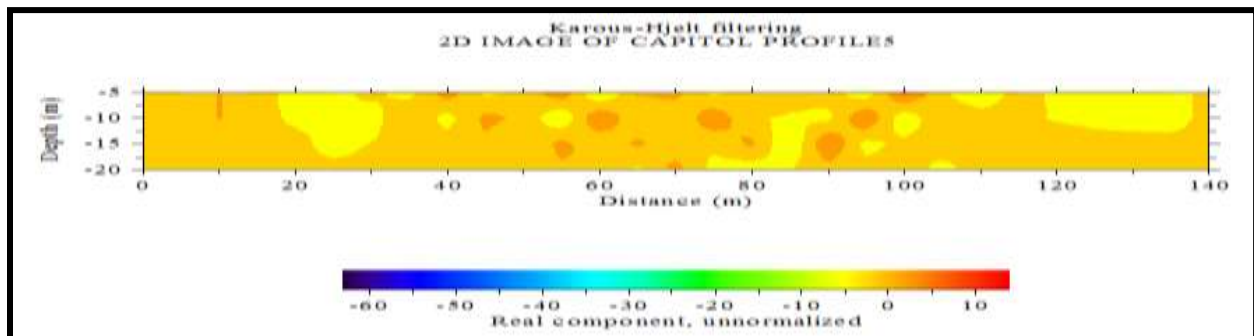


Fig. 4.19b: Capitol VLF-EM Image of Profile (PL5)

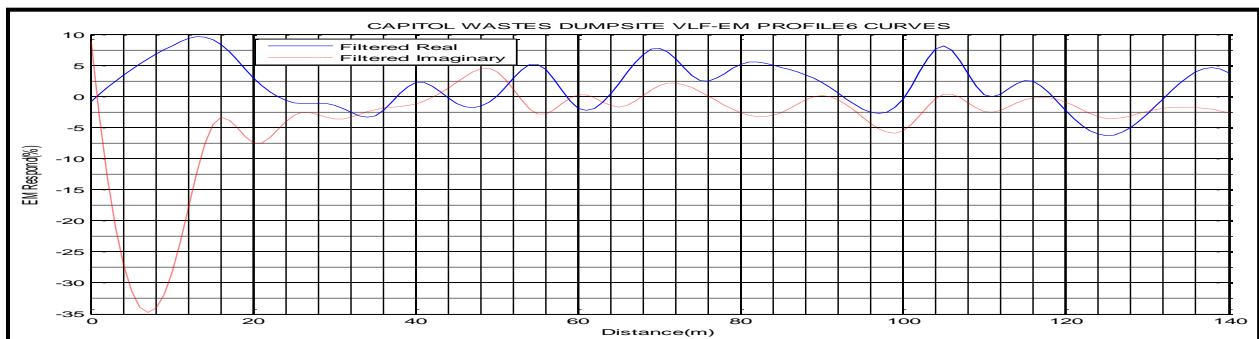


Fig. 4.20a: Capitol VLF-EM Curve (filtered real and filtered imaginary) of Profile (PL6)

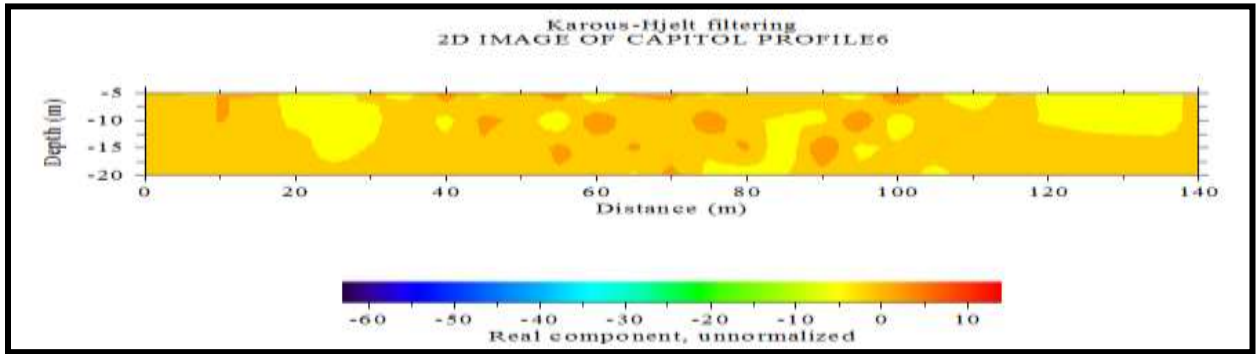


Fig. 4.20b: Capitol VLF-EM Image of Profile (PL6)

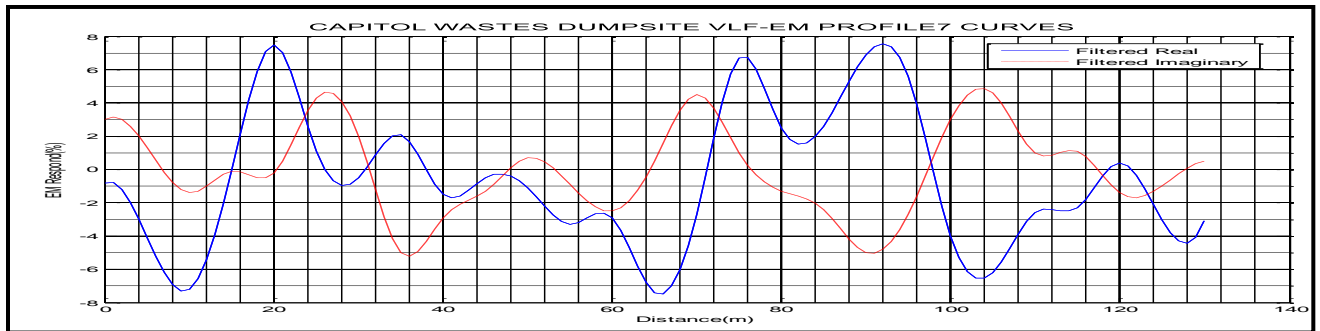


Fig. 4.21a: Capitol VLF-EM Image (filtered real and filtered imaginary) of Profile (PL7)

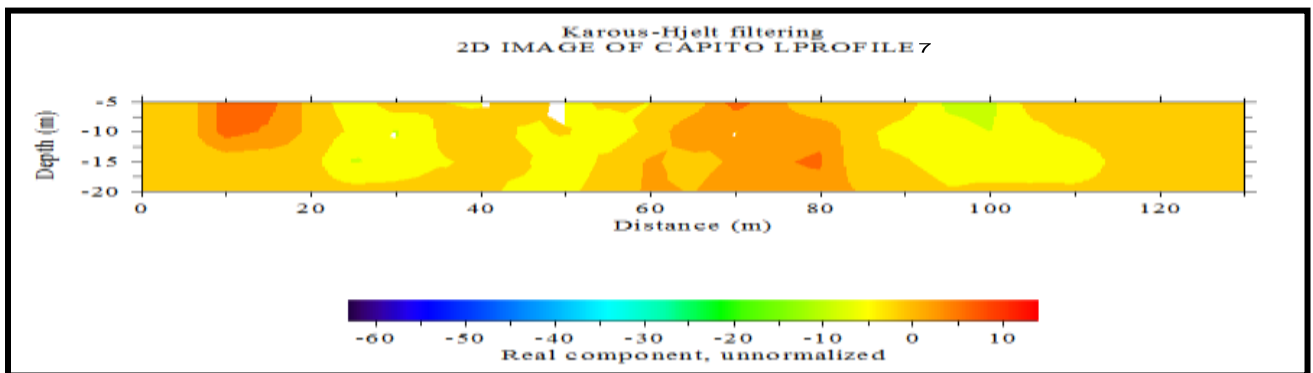


Fig. 4.21b: Capitol VLF-EM Image of Profile (PL7)

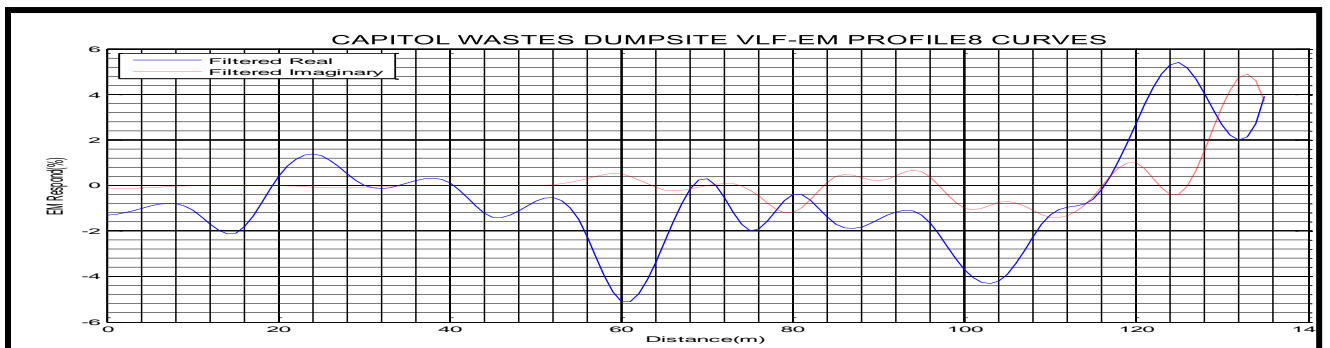


Fig. 4.22: Capitol VLF-EM Curve (filtered real and filtered imaginary) of Profile (PL8)

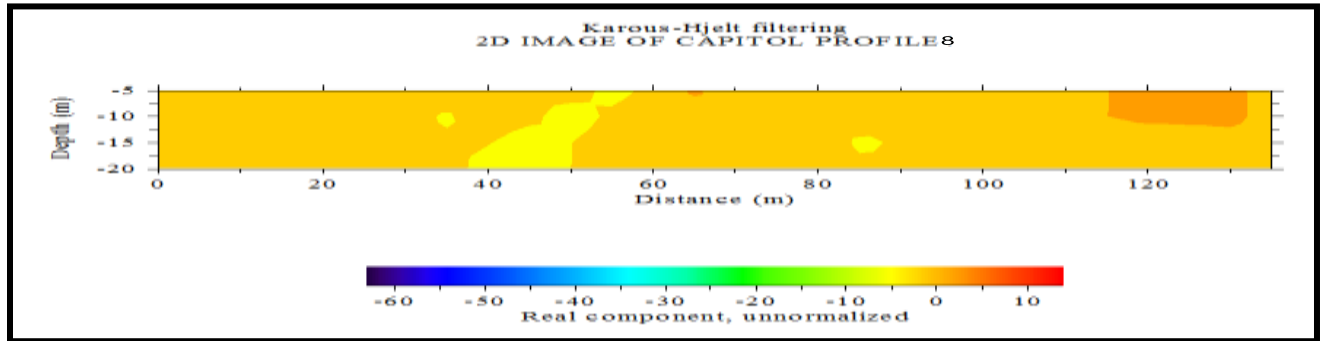


Fig. 4.22b: Capitol VLF-EM Image of Profile (PL8)

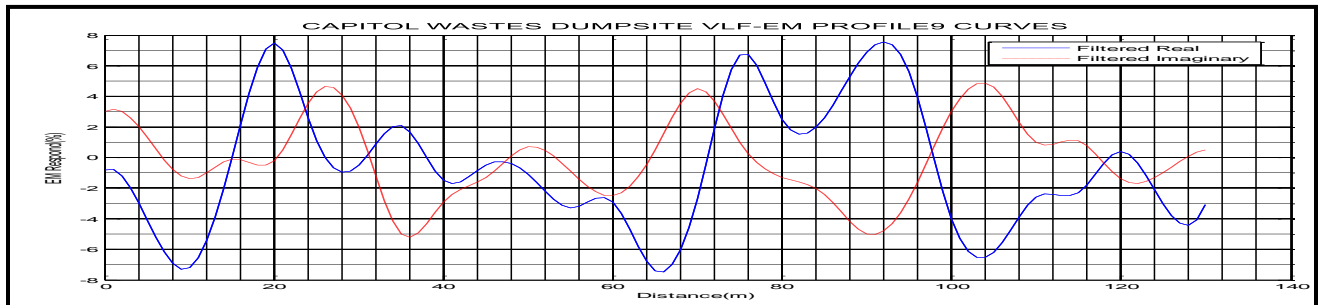


Fig. 4.23a: Capitol VLF-EM Curve (filtered real and filtered imaginary) of Profile (PL9)

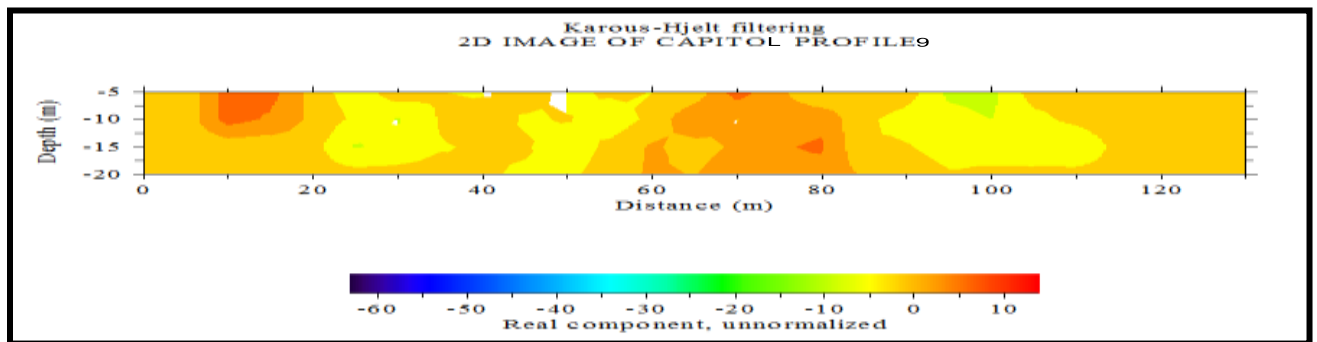


Fig. 4.23b: Capitol VLF-EM Image of Profile (PL9)

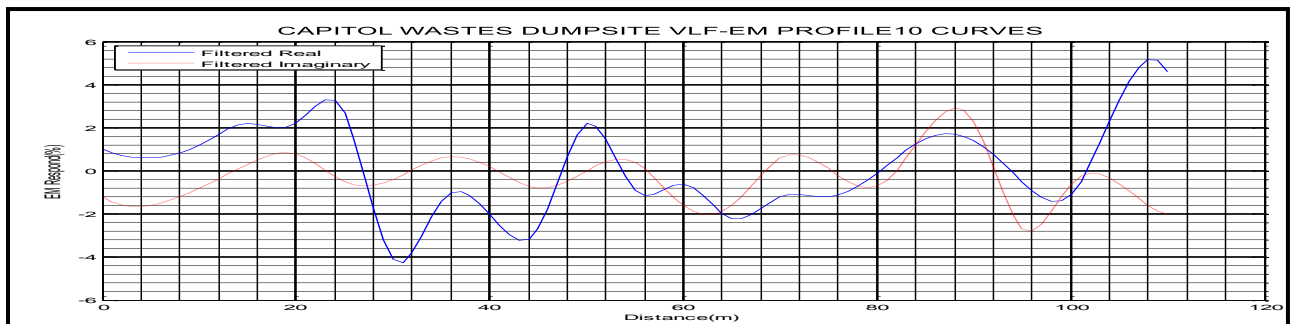


Fig. 4.24: Capitol VLF-EM Curve (filtered real and filtered imaginary) of Profile (PL10)

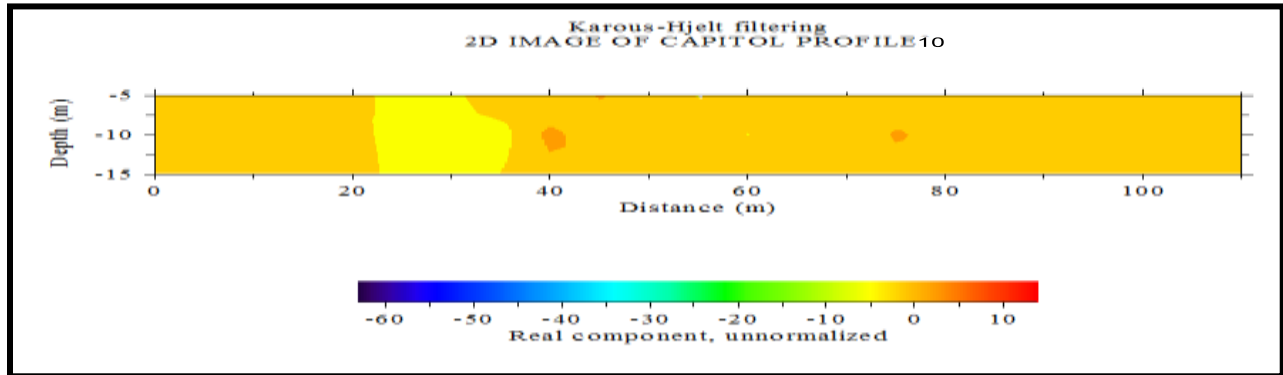


Fig. 4.24b: Capitol VLF-EM Image of Profile (PL10)

The Fraser filter or Karous and Hjelt transform the data into peaks enhancing the signals of the conductive structures. Figs. 4.15a – 4.24b shows the Karous and Hjelt filtered data (real and imaginary components). The in-phase profiles show positive peaks of different intensities and sharpness, suggesting the presence of shallow and deep conductors. These conductive zones may be due to leachate plumes, filled with contaminated water.

4.4.3 The Karous–Hjelt filtered pseudo-sections of Oluku Dumpsite

The Karous–Hjelt filter is used to obtain relative current density pseudosections. Lower values of relative current density correspond to higher values of resistivity. All the VLF-EM profiles in this study were oriented along N - S direction and processed using the Karous–Hjelt filter. Figs. 4.25a – 4.34b shows the computed relative current densities for ten VLF-EM profiles carried out in this site. The areas of high current density correspond to positive values. In Profile 1 (Figs. 4.25 - 4.25b) the current density values were observed at distance of 1m - 20m, 60 - 90m, 100m - 110m, 170m - 180m, 240m - 250m, 300m - 320m and 330m - 350m respectively, this indicates the presence of conductive zone. In Profile 2 (Figs. 4.26a - 4.26b) the current density values were observed at distance of 10m - 30m, 40 - 50m, 210m – 240m, and 310m - 320m respectively, this indicates the presence of conductive zone. In Profile 3 (Figs. 4.27a - 4.27b) the current density values were observed at distance of 1m - 40m, 60 - 100m, 80m - 150m, 170m - 230m, 250m - 260

and 310m - 330m respectively, this indicates the presence of conductive zone. In Profile 4 (Figs. 4.28a - 4.28b) the current density values were observed at distance of 1m - 10m and 20 - 40m respectively, this indicates the presence of conductive zone. In Profile 5 (Figs. 4.29a - 4.29b) the current density values were observed at distance of 30m - 50m, 110 - 130m and 180m respectively, this indicate presence of conductive zone. In Profile 6 (Figs. 4.30a - 4.30b) the current density values were observed at distance of 10m - 30m, 40m - 60m, 80m - 110m, 220m - 240m, 270m - 300m and 310m - 320m respectively, this indicates the presence of conductive zone. In Profile 7 (Figs. 4.31a - 4.31b) the current density values were observed at distance of 1m - 10m, 30m - 50m, and 190m - 220m respectively, this indicates the presence of conductive zone. In Profile 8 (Figs. 4.32a - 4.32b) the current density values were observed at distance of 20m - 40m, 80m - 110m and 120m - 140m respectively, this indicates the presence of conductive zone. In Profile 9 (Figs. 4.33a - 4.33b) the current density values were observed at distance of 10m - 30m, 40m - 60m and 80m - 130m respectively, this indicates the presence of conductive zone. In Profile 10 (Figs. 4.34a - 4.34b) the current density values were observed at distance of 40m - 60m, 80m - 95m and 110m - 130m respectively, this indicates the presence of conductive zone.

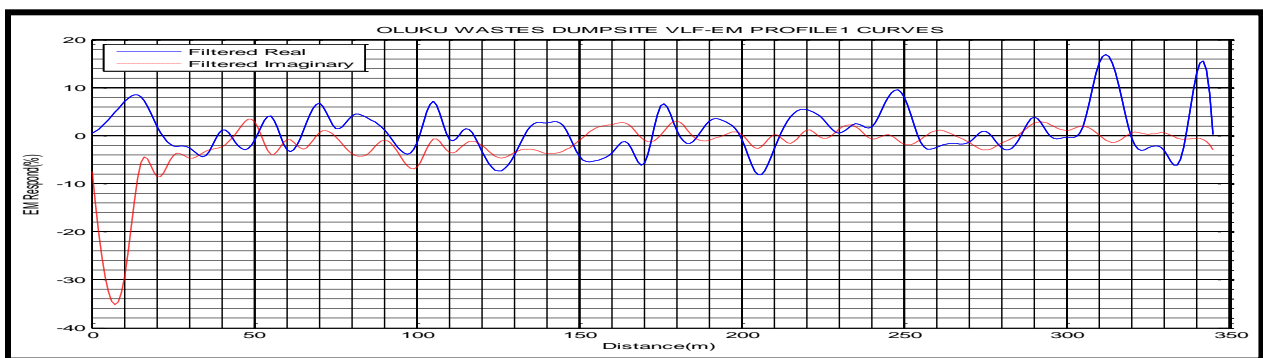


Fig. 4.25a: Oluku VLF-EM Curve (filtered real and filtered imaginary) of Profile (PL1)

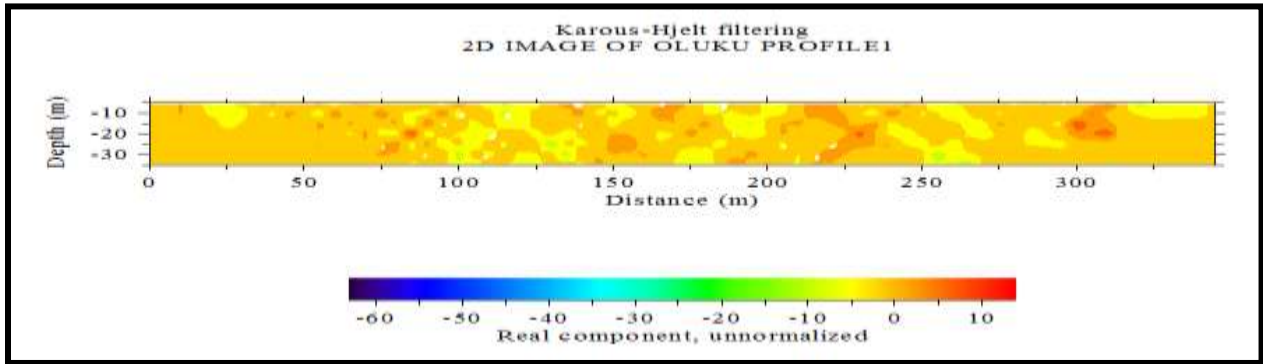


Fig. 4.25b: Oluku VLF-EM Image of Profile (PL1)

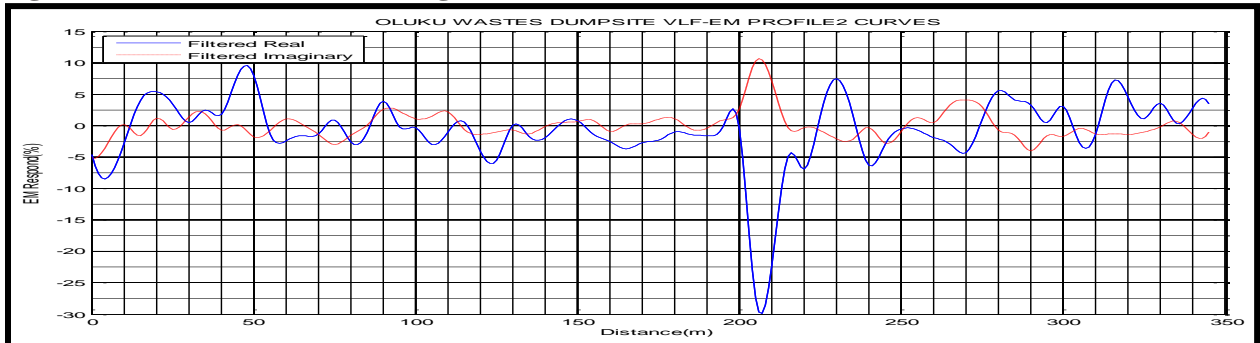


Fig. 4.26a: Oluku VLF-EM Curve (filtered real and filtered imaginary) of Profile (PL2)

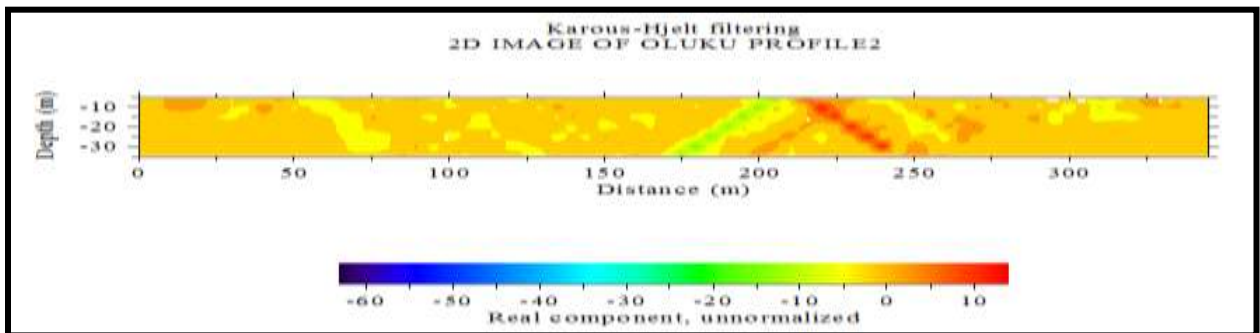


Fig. 4.26b: Oluku VLF-EM Image of Profile (PL2)

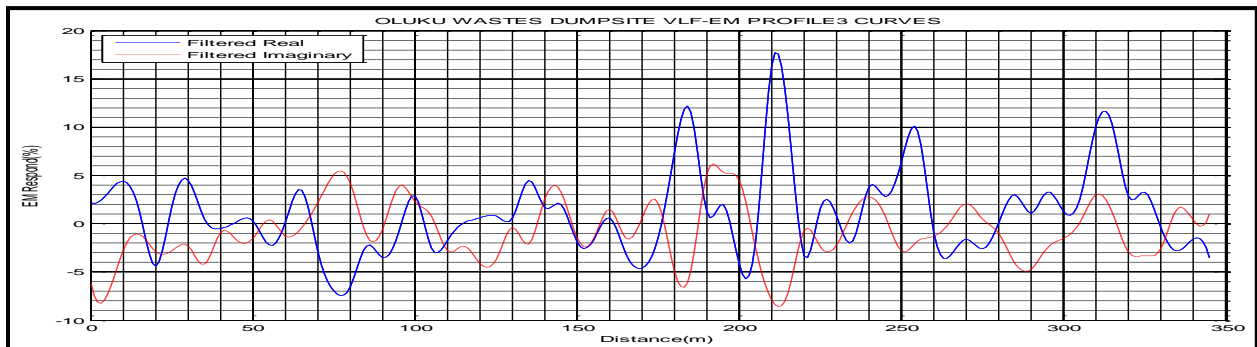


Fig. 4.27a: Oluku VLF-EM Curve (filtered real and filtered imaginary) of Profile (PL3)

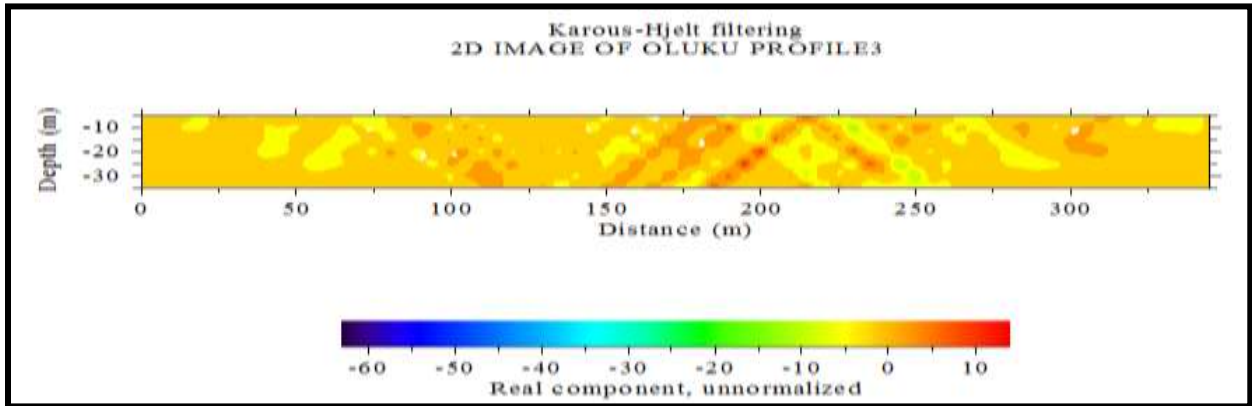


Fig. 4.27b: Oluku VLF-EM Image of Profile (PL3)

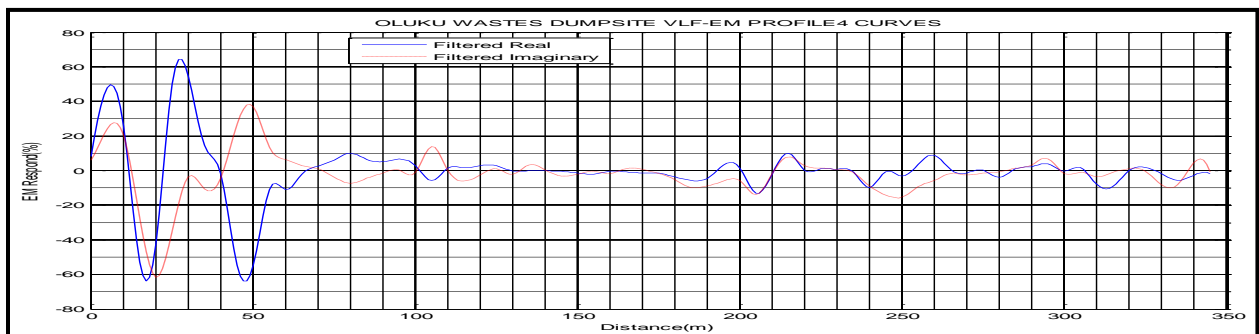


Fig. 4.28a: Oluku VLF-EM Curve (filtered real and filtered imaginary) of Profile (PL4)

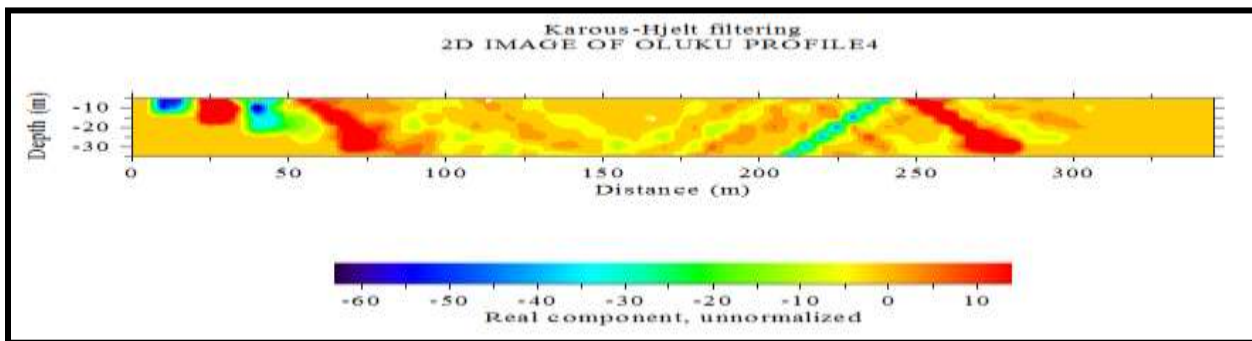


Fig. 4.28b: Oluku VLF-EM Image of Profile (PL4)

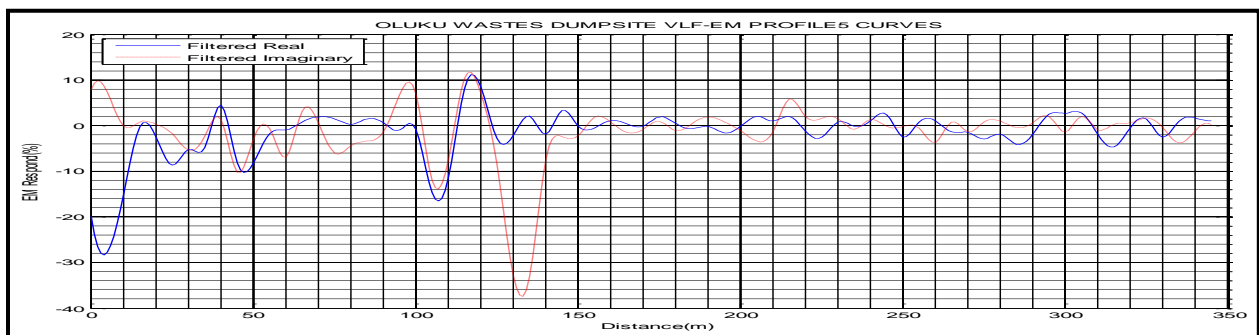


Fig. 4.29a: Oluku VLF-EM Curve (filtered real and filtered imaginary) of Profile (PL5)

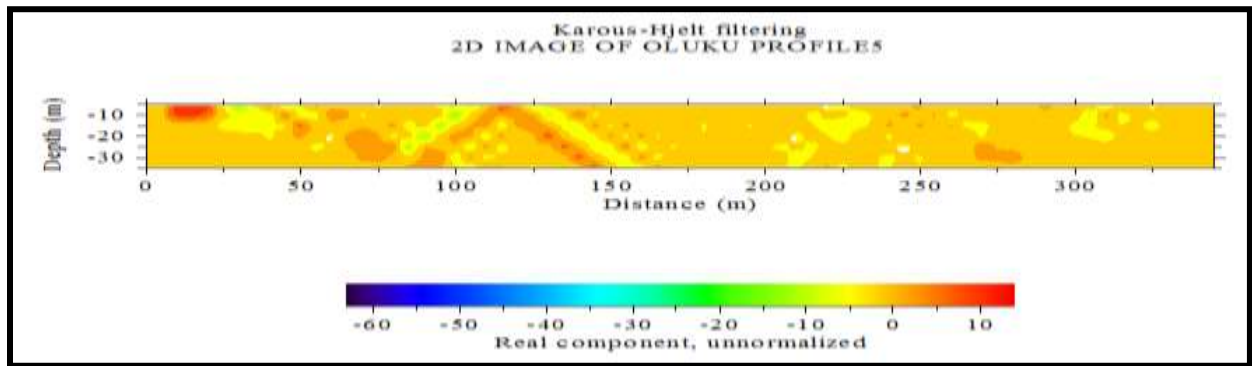


Fig. 4.29b: Oluku VLF-EM Image of Profile (PL5)

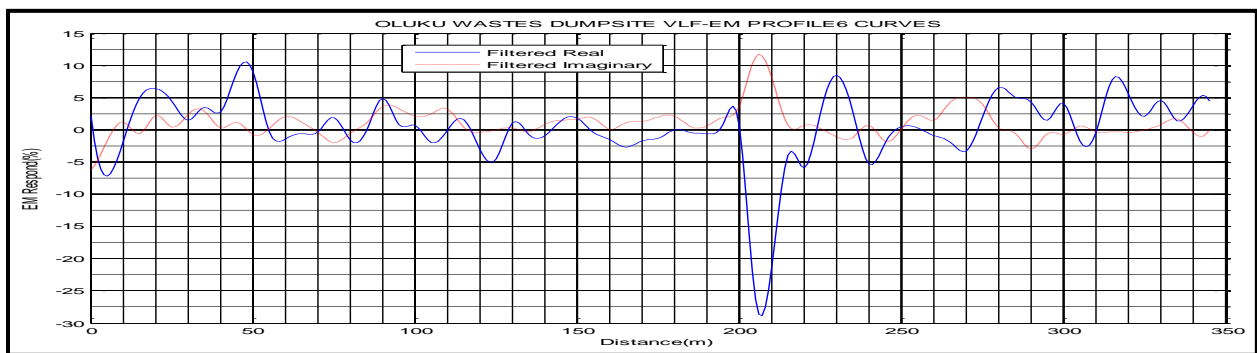


Fig. 4.30a: Oluku VLF-EM Curve (filtered real and filtered imaginary) of Profile (PL)6

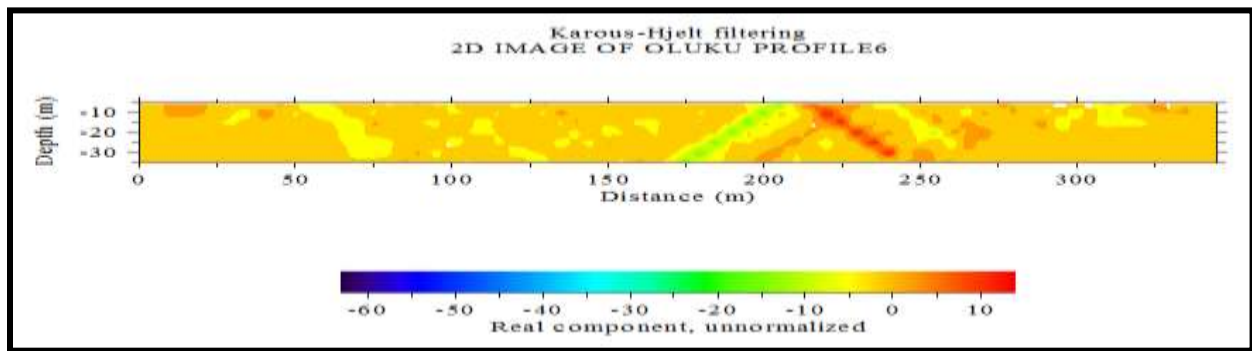


Fig. 4.30b: Oluku VLF-EM Image of Profile (PL6)

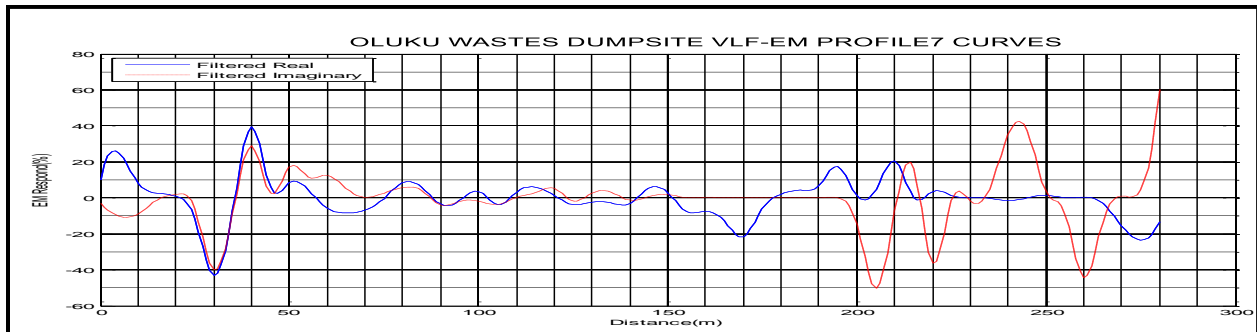


Fig. 4.31a: Oluku VLF-EM Curve (filtered real and filtered imaginary) of Profile (PL7)

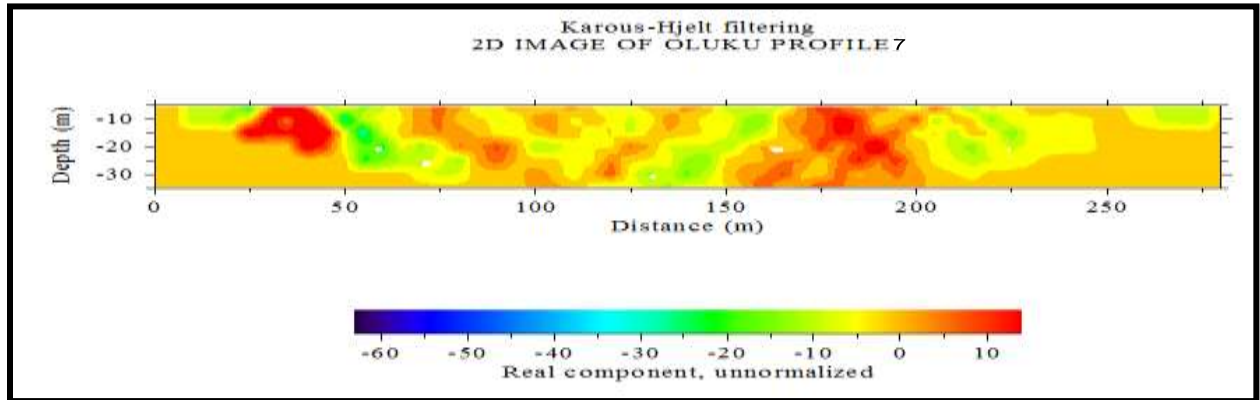


Fig. 4.31b: Oluku VLF-EM Image of Profile (PL7)

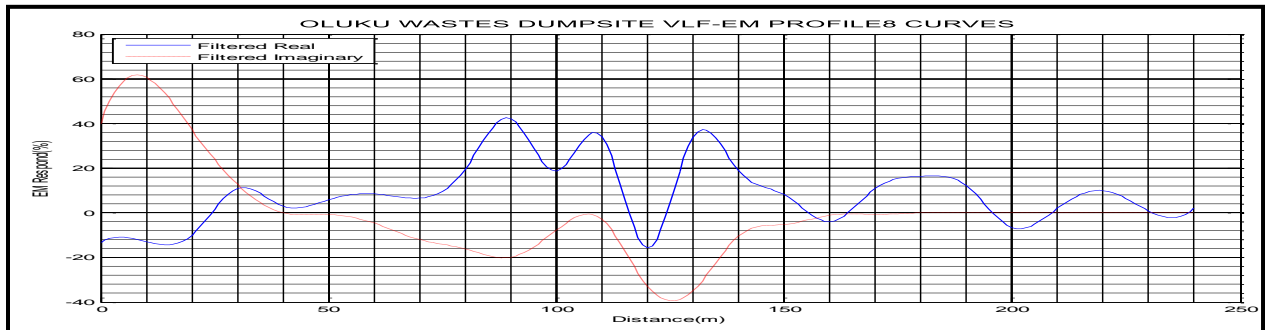


Fig. 4.32a: Oluku VLF-EM Curve (filtered real and filtered imaginary) of Profile (PL8)

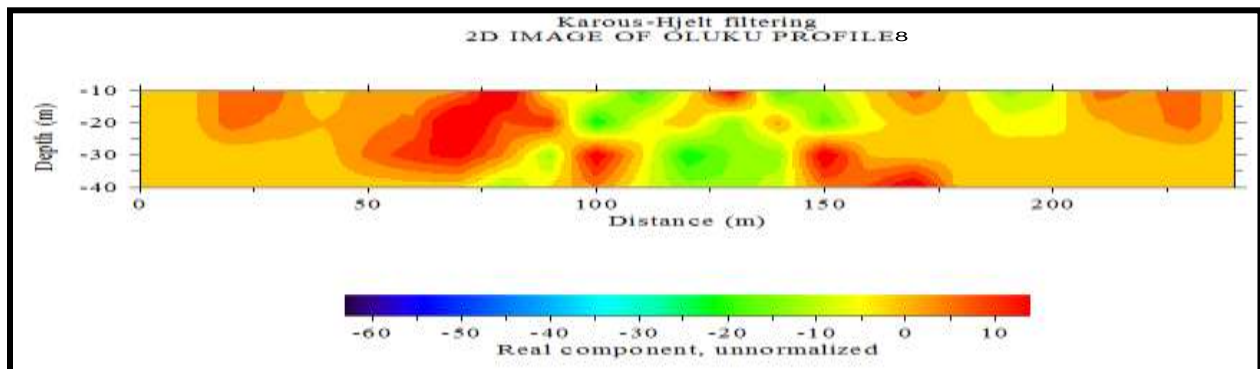


Fig. 4.32b: Oluku VLF-EM Image of Profile (PL8)

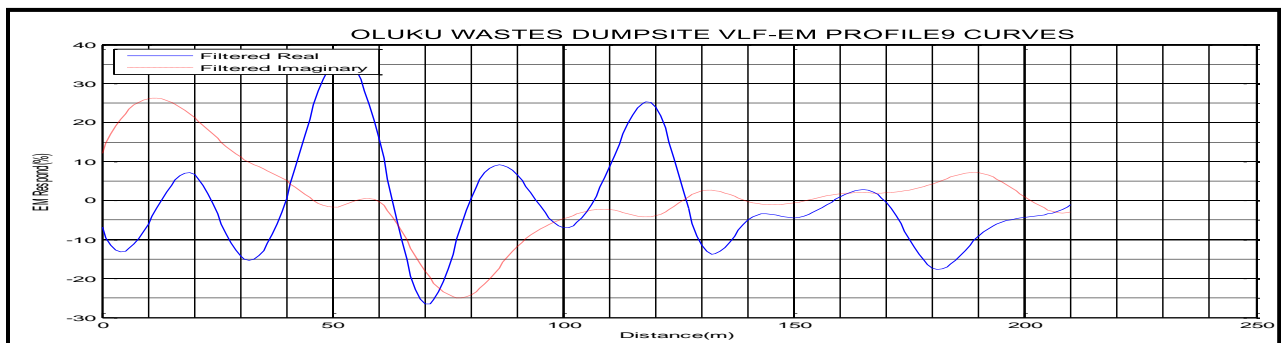


Fig. 4.33a: Oluku VLF-EM Curve (filtered real and filtered imaginary) of Profile (PL9)

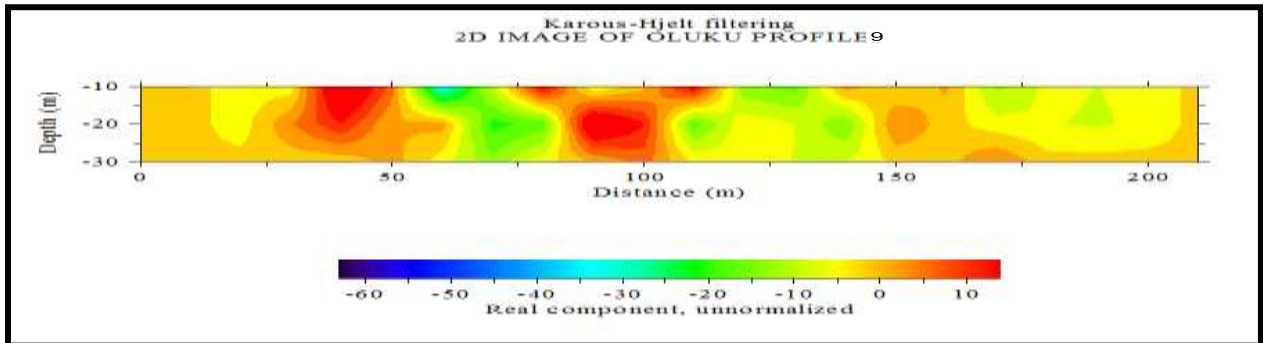


Fig. 4.33b: Oluku VLF-EM Image of Profile (PL9)

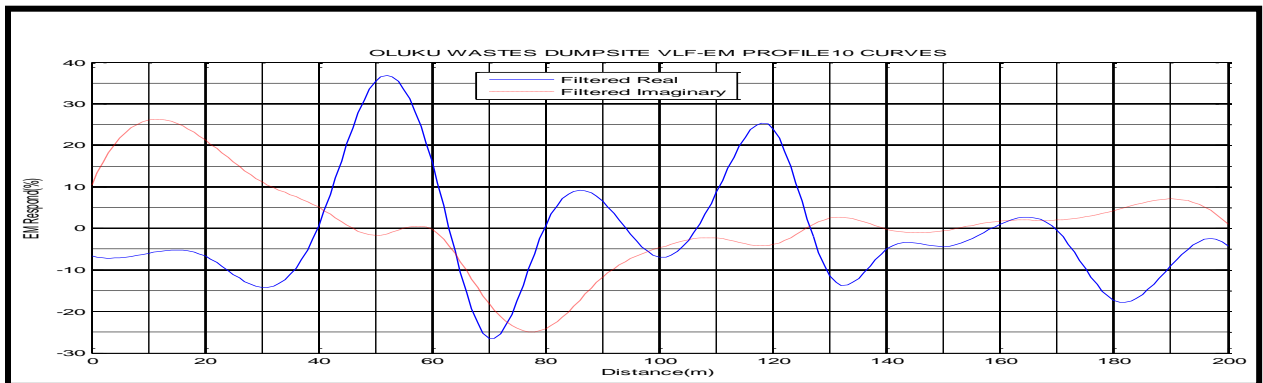


Fig. 4.34a: Oluku VLF-EM Curve (filtered real and filtered imaginary) of Profile (PL10)

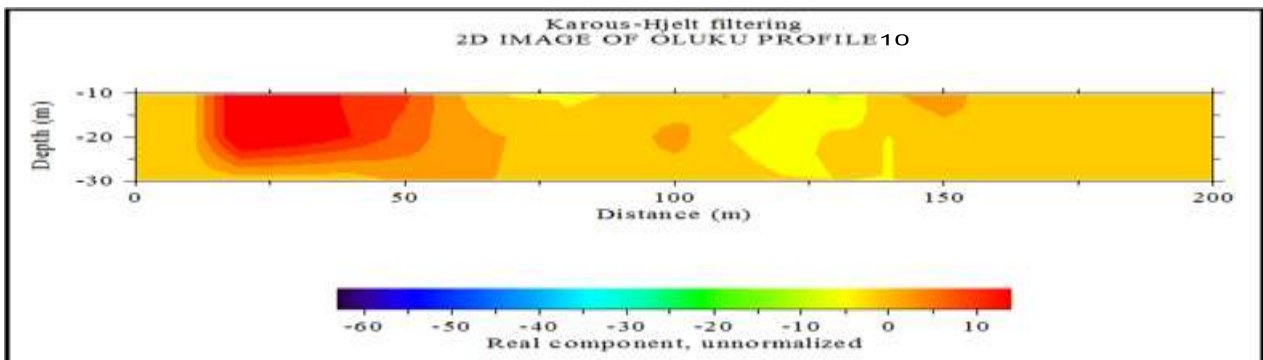


Fig. 4.34b: Oluku VLF-EM Image of Profile (PL10)

The Fraser filter or Karous and Hjelt transform the data into peaks enhancing the signals of the conductive structures. Figs. 4.25a - 4.34b show the Karous and Hjelt filtered data (real and imaginary components). The in-phase profiles show positive peaks of different intensities and sharpness, suggesting the presence of shallow and deep conductors. These conductive zones may be due to leachate plumes, artificial or presence of loose zone, filled with contaminated water.

4.5 Discussion of ERT of 2D Models

4.5.1 Results from Ikhueniro Dumpsite (ERT 1)

The profiles were oriented along the N - S direction of the dump. The ERT profiles were laid due to the appreciable results obtained from the anomaly maps of the conductive and non conductive zones from the VLF-EM survey. The electrode spacing was 2m which gave a total length of 168m, thus allowing depth of investigation down to 39.4m. The model shown in Fig. 4.35 indicated that the corresponding anomalies with low near surface resistivity from the top soil down to a depth of over 39m. The migrating pathways are suspected to be 112m and 144m marks on the profile. There is anomalous low resistivity value of $20\Omega\text{m}$ (Blue colour) which was observed between 96m - 112m mark on the profile to a depth of 39.4m. This is an indication that the surface soil down to 39m is contaminated as shown in Fig. 4.35. The true resistivity of the area is from $1\Omega\text{m}$ to $100000\Omega\text{m}$. Resistivities of $700\Omega\text{m}$ and $800\Omega\text{m}$ (Yellow colour) coincide with lateritic soil at a depth of 8m - 20m and also resistivity from $1000\Omega\text{m}$ (Purple colour) is composed of sandstone at a depth of 5m - 19.7m respectively. The resistivity of less than $100\Omega\text{m}$ (Green colour) is suspected to be clay formation at a depth of 5m - 39m. The resistivity of groundwater decreases as the concentration of salinity increases. Thus it appears that there is a correlation between the low resistivity values, along the pathways and increased ion concentration as a result of leachate contamination at these depths. The colour scaling changing from deep blue to light blue in all the profiles reflects the changes in the concentration of the leachate as it seep down due to infiltration by the sediments.

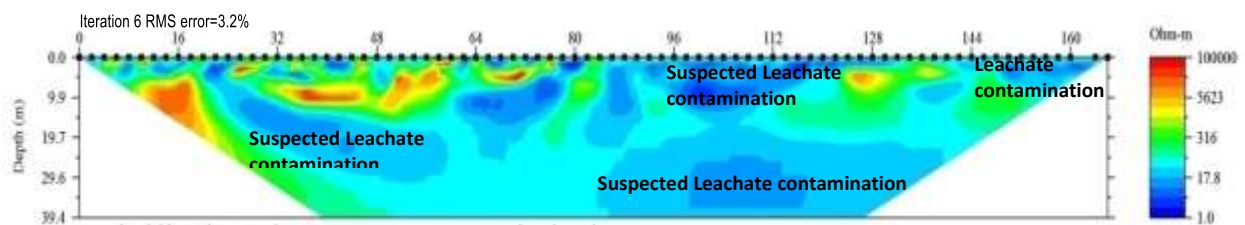


Fig. 4.35: Ikhueniro Inverse Resistivity Section of Profile ERT 1

4.5.2 Results from Ikhueniro Dumpsite (ERT 2)

This profile was oriented along the N - S direction of the dump. The electrode spacing was 2m which gave a total length of 168m, thus allowing depth of investigation down to 39.4m. The model shown in Fig. 4.36 indicates that the corresponding anomalies with low near surface resistivity from the top soil down to a depth of over 39m. The migrating pathways are suspected to be 112m and 144m marks on the profile. There is anomalous low resistivity value of $20\Omega\text{m}$ (Blue colour) which can be observed between 96m - 128m mark on the profile to a depth of 39.4m. This indicates that the surface soil down to 39m is contaminated as shown in Fig. 4.36. The “true” resistivity of the area from the inverse model is from $1\Omega\text{m}$ to $100000\Omega\text{m}$. Resistivities of $700\Omega\text{m}$ and $800\Omega\text{m}$ (Yellow colour) coincide with lateritic soil at a depth of 5m-19m and also resistivity from $1000\Omega\text{m}$ (Purple colour) is composed of sandstone respectively. The resistivity of less than $100\Omega\text{m}$ (Green colour) is suspected to be clay formation at a depth of 2m - 39.4m. Thus there is a correlation between the low resistivity values along the pathways. Because there is an increased in ion concentration as a result of leachate contamination within the depths penetrated.

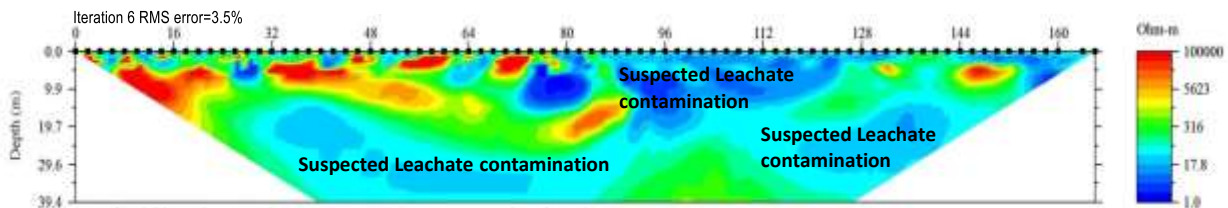


Fig. 4.36: Ikhueniro Inverse Resistivity Section of Profile ERT 2

4.5.3 Results from Ikhueniro Dumpsite (ERT 3)

This profile was oriented along the N - S direction of the dump. The electrode spacing was 2m which gave a total length of 168m, thus allowing depth of investigation down to 39.4m. The model shown in Fig. 4.37 indicates that the corresponding anomalies with low near surface resistivity from the top soil down to a depth of over 39m. The migrating pathways are suspected to be 112m

and 144m marks on the profile. There is anomalous low resistivity value of $20\Omega\text{m}$ (Blue colour) which can be observed between 98m-110m mark on the profile to a depth of 39.4m. This indicates that the surface soil down to 39m is contaminated as shown in Fig. 4.37. The “true” resistivity of the area from the inverse model is from $1.4\Omega\text{m}$ to $100000\Omega\text{m}$. Resistivities of $700\Omega\text{m}$ and $800\Omega\text{m}$ (Yellow colour) coincide with lateritic granite at a depth of 5m - 26m and also resistivity from $1000\Omega\text{m}$ (Purple colour) is composed of sandstone at a depth of 3m-25m respectively. The resistivity of less than $100\Omega\text{m}$ (Green colour) is suspected to be clay formation this is found at a depth of 2m - 39.4m. Thus there is a correlation between the low resistivity values along the pathways. Because there is an increased in ion concentration as a result of leachate contamination within the depths penetrated.

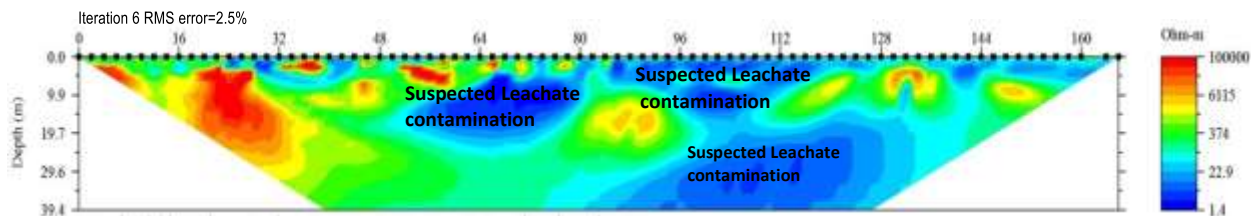


Fig. 4.37: Ikhueniro Inverse Resistivity Section of Profile ERT 3

4.5.4 Results from Capitol Dumpsite (ERT 1)

This profile was oriented along the N - S direction of the dump. The electrode spacing was 1m which gave a total length of 84m, thus allowing depth of investigation down to 17.4m. The model shown in Fig. 4.38 indicates that the corresponding anomalies with low near surface resistivity from the top soil down to a depth of over 13m. The migrating pathways are suspected to be 112m and 144m marks on the profile. There is anomalous low resistivity value of $20\Omega\text{m}$ (Blue colour) and this can be observed at 35m mark on the profile up to a depth of 10m. This indicates that the surface soil down to 13m is contaminated as shown in Fig. 4.38. The “true” resistivity of the area from the inverse model is from $1\Omega\text{m}$ to $100000\Omega\text{m}$. Resistivities of $700\Omega\text{m}$ and $800\Omega\text{m}$ (Yellow

colour) coincide with lateritic granite at a depth of 4m - 17.4m and also resistivity from 1000Ωm (Purple colour) is composed of sandstone at a depth of 4m - 17.4m respectively. The resistivity of less than 100Ωm (Green colour) is suspected to be clay formation at a depth of 2m - 17.4m. Thus there is a correlation between the low resistivity values, along the pathways. Because there is an increased in ion concentration as a result of leachate contamination within the depths penetrated.

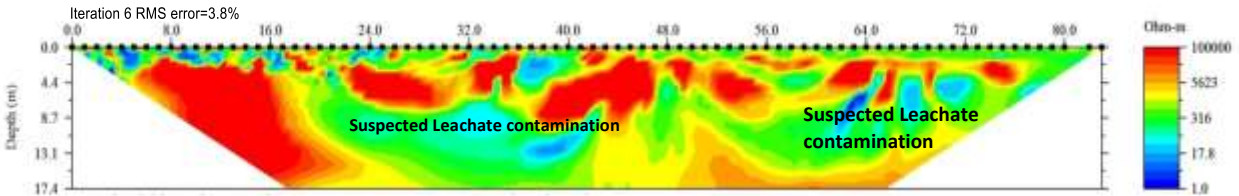


Fig. 4.38: Capitol Inverse Resistivity Section of Profile ERTI

4.5.5 Results from Capitol Dumpsite (ERT 2)

This profile was oriented along the N - S direction of the dump. The electrode spacing was 1m which gave a total length of 84m, thus allowing depth of investigation down to 17.4m. The model shown in Fig. 4.39 indicates the corresponding anomalies with low near surface resistivity from the top soil down to a depth of over 13m. The migrating pathways are suspected to be 112m and 144m marks on the profile. There is anomalous low resistivity value of 20Ωm (Blue colour) which can be observed between 24m - 32m mark on the profile to a depth of 5m. This indicates that the surface soil down to 10m is contaminated as shown in Fig. 4.39. The “true” resistivity of the area from the inverse model is from 1Ωm to 100000Ωm. Resistivities of 700Ωm and 800Ωm (Yellow colour) coincide with lateritic granite at a depth of 2m - 19m and also resistivity from 1000Ωm (Purple colour) is composed of sandstone at a depth of 2m - 12m respectively. The resistivity of less than 100Ωm (Green colour) is suspected to be clay formation.

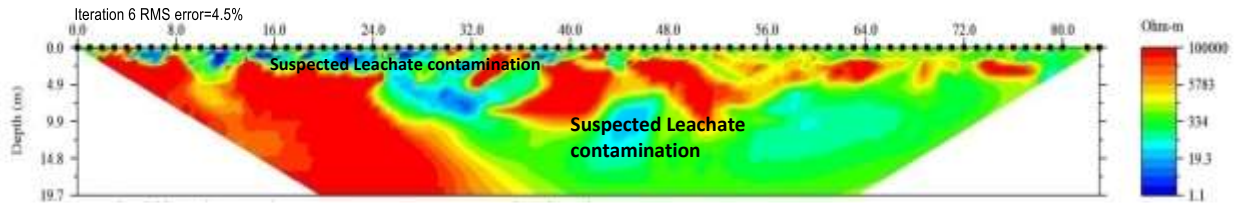


Fig. 4.39: Capitol Inverse Resistivity Section of Profile ERT2

4.5.6 Results from Capitol Dumpsite (ERT 3)

This profile was oriented along the N - S direction of the dump. The electrode spacing was 1m which gave a total length of 84m, thus allowing depth of investigation down to 17.4m. The model shown in Fig. 4.40 indicates that the corresponding anomalies with low near surface resistivity from the top soil down to a depth of 13m. There is anomalous low resistivity value of $20\Omega\text{m}$ (Blue colour) which can be observed between 24m and 64m mark on the profile to a depth of 10m. This indicates that the surface soil down to 13m is contaminated as shown in Fig. 4.40. The “true” resistivity of the area from the inverse model is from $1\Omega\text{m}$ to $100000\Omega\text{m}$. Resistivities of $700\Omega\text{m}$ and $800\Omega\text{m}$ (Yellow colour) coincide with lateritic granite at a depth of 4m - 17m and also resistivity from $1000\Omega\text{m}$ (Purple colour) is composed of sandstone at a depth of 3m - 17.4m respectively. The resistivity of less than $100\Omega\text{m}$ (Green colour) is suspected to be clay formation at a depth of 4m - 17.4m.

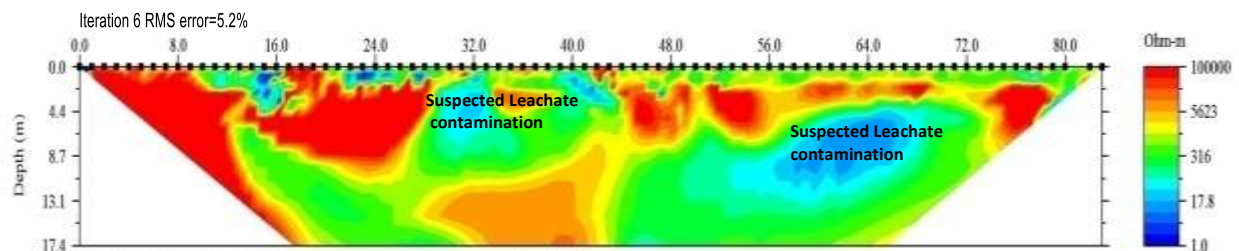


Fig. 4.40: Capitol Inverse Resistivity Section of Profile ERT

4.5.7 Results from Oluku Dumpsite (ERT 1)

This profile was oriented along the N - S direction of the dump. The electrode spacing was 2m which gave a total length of 168m, thus allowing depth of investigation down to 39.4m. The model

shown in Fig. 4.41 indicates that the corresponding anomalies with low near surface resistivity from the top soil down to a depth of 29m. The migrating pathways are suspected to be 32m and 80m marks on the profile. There is anomalous low resistivity value of $20\Omega\text{m}$ (Blue colour) which can be observed between 32m, 64m, 96m and 144m mark on the profile to a depth of 20m. This indicates that the surface soil down to 29m is contaminated as shown in Fig. 4.41. The “true” resistivity of the area from the inverse model is from $1\Omega\text{m}$ to $100000\Omega\text{m}$. Resistivities of $700\Omega\text{m}$ and $800\Omega\text{m}$ (Yellow colour) coincide with lateritic granite at a depth of 15m-39.4m and also resistivity from 1000 (Purple colour) is composed of sandstone at a depth of 5m-19m respectively. The resistivity of less than $100\Omega\text{m}$ (Green colour) is suspected to be clay formation at a depth of 4m - 39m. The resistivity of groundwater decreases as the concentration of salinity increases (Barker, 1990).

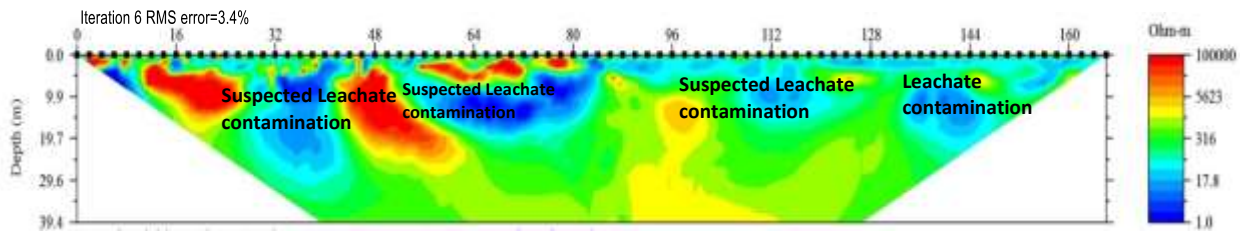


Fig. 4.41: Oluku Inverse Resistivity Section of Profile ERT 1

4.5.8 Results from Oluku Dumpsite (ERT 2)

This profile was oriented along the N-S direction of the dump. The electrode spacing was 2m which gave a total length of 168m, thus allowing depth of investigation down to 39.4m. The model shown in Fig. 4.42 indicates that the corresponding anomalies with low near surface resistivity from the top soil down to a depth of 10m. The migrating pathways are suspected to be 32m and 80m marks on the profile. There is anomalous low resistivity value of $20\Omega\text{m}$ (Blue colour) which can be observed between 64m, 96m and 112m mark on the profile to a depth of 17m. This indicates that the surface soil down to 10m is contaminated as shown in Fig. 4.42. The “true” resistivity of the area from the inverse

model is from $1\Omega\text{m}$ to $100000\Omega\text{m}$. Resistivities of $700\Omega\text{m}$ and $800\Omega\text{m}$ (Yellow colour) coincide with lateritic granite at a depth of 2m - 34m and also resistivity from 1000 (Purple colour) is composed of sandstone at a depth of 5m - 30m respectively. The resistivity of less than $100\Omega\text{m}$ (Green colour) is suspected to be clay formation at a depth of 5m - 34.8m.

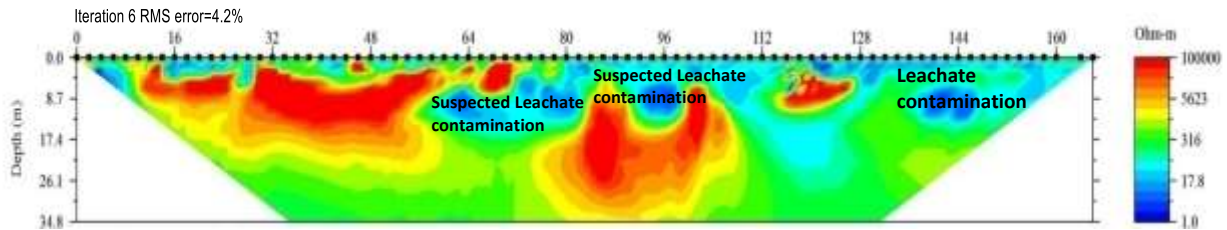


Fig. 4.42: Oluku Inverse Resistivity Section of Profile ETR 2

4.5.9 Results from Oluku Dumpsite (ERT 3)

This profile was oriented along the N - S direction of the dump. The electrode spacing was 2m which gave a total length of 168m, thus allowing depth of investigation down to 39.4m. The model shown in Fig. 4.43 indicates that the corresponding anomalies with low near surface resistivity from the top soil down to a depth of 19m. The migrating pathways are suspected to be 80m and 128m marks on the profile. There is anomalous low resistivity value of $20\Omega\text{m}$ (Blue colour) which can be observed between 64m, 96m and 112m mark on the profile to a depth of 17m. This indicates that the surface soil down to 10m is contaminated as shown in Fig. 4.43. The “true” resistivity of the area from the inverse model is from $1\Omega\text{m}$ to $100000\Omega\text{m}$. Resistivities of $700\Omega\text{m}$ and $800\Omega\text{m}$ (Yellow colour) coincide with lateritic granite at a depth of 10m - 34.8m and also resistivity from 1000 (Purple colour) is composed of sandstone at a depth of 5m - 34m respectively. The resistivity of less than $100\Omega\text{m}$ (Green colour) is suspected to be clay formation at a depth of 12m - 34.8m.

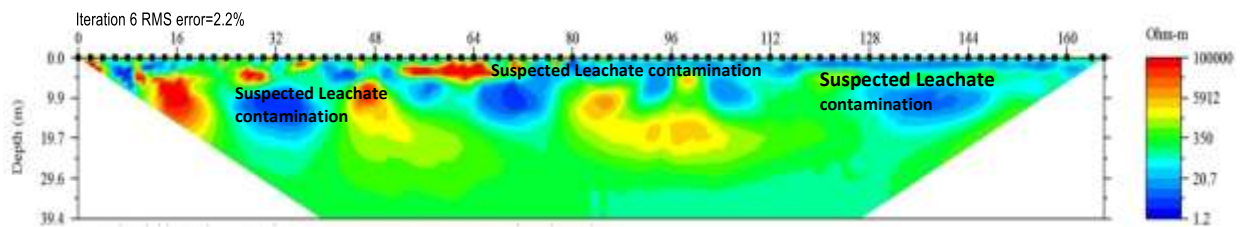


Fig. 4.43: Oluku Inverse Resistivity Section of Profile ERT3

4.6 Discussion of ERT of 3D Models

Nine 2D resistivity inversion results were used to plot a 3D resistivity map of the materials in the three dumpsites visited. The three parallel 2D profiles acquired from every site were combined to plot a 3D view of each site. The 3D plan views make use of the inversion data from the same depth in the individual 2D inversion results. The Easting and Northing in the 3D views represent the surface distance in metres and the contour showing the resistivity values at the particular depth. There are 3D views which represent the distribution of resistivity at different depths as shown in Fig. 4.44 - 4.46. The same resistivity data used for 2D inversion was combined for the 2D slices.

a). From the resistivity results there are two ranges of values which may be related to the contamination occurring at the sites. The first range is less than $20\Omega\text{m}$ which is related to the existing contamination (leachate) at the site and interrelated to existing soil moisture and any surface water. It is represented by the dark red colour on the plan views. The distribution of low resistivity values at the three depth slices of (1m - 38m) is quite obvious at the study area.

b). The second range of resistivity value is within $200\Omega\text{m}$, from 5m mark on the profile (Fig. 4.44). The low resistivity value decreased but the resistivity value range from $200 - 1000\Omega\text{m}$ (yellow to purple colours) appearing as most dominant in some areas. According to Atekwana *et al.*, (1998) these values are likely to be a representative of hydrocarbon contamination in the soil. The resistivity value of the area (Fig. 4.44 - 4.49) from the inverse model is from $1\Omega\text{m}$ to $1000\Omega\text{m}$. The resistivity of less than $100\Omega\text{m}$ (light red colour) is suspected to be clay formation. The resistivities of $700\Omega\text{m} - 800\Omega\text{m}$ (Blue colour) coincide with lateritic granite and also resistivity from $1000\Omega\text{m}$ (Purple colour) is composed of sandstone respectively.

4.6.1 Results from Ikhueniro dumpsite

The 3D models obtained from the inversion of the resistivity data set are displayed as horizontal slices as shown in Fig. 4.44 - 4.45. The three profiles obtained at Ikhueniro dumpsite were used to interpret slice A, B and C. The inverse section of slice A shows several anomalies at depths of about 5.8m as shown in Fig. 4.45. We interpret these low resistivity ($20\Omega\text{m}$) anomalies (Red colour) to be the effect from conductor (leachate) at the subsurface. The high resistivity area near the surface is due to the drier upper sandy layers. At a depth of about 5.8m, the anomalies with low resistivity values are believed to be the presence of loosed sandy zone. Thus, the anomalies at 5.8m depths indicate that the soil is contaminated beyond 5.8m as shown in Fig. 4.45. The slice (B) shows almost similar anomalies at a depth of about 18m as shown in Fig. 4.45. There is anomalous low resistivity value of $20\Omega\text{m}$ (red colour) were observed between 80m - 160m mark on the profile to a depth of 38m of slice (C). This indicates that the surface soil down to 38m is contaminated as shown in Figures 4.45. A comparison of the results from the 3D slices A, B and C (Fig. 4.45) shows anomalies with resistivity value of less than $20\Omega\text{m}$. This is suspected to be leachate seeping down (38m) with similar profile range from ERT (2D) and VLF-EM images.

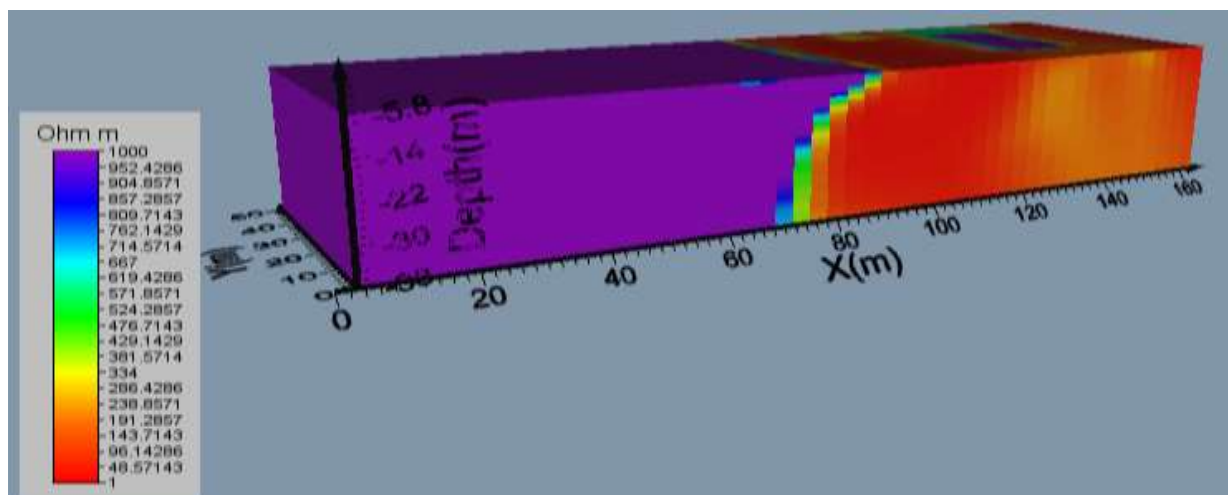


Fig. 4.44: 3D Slices of Ikhueniro Dumpsite

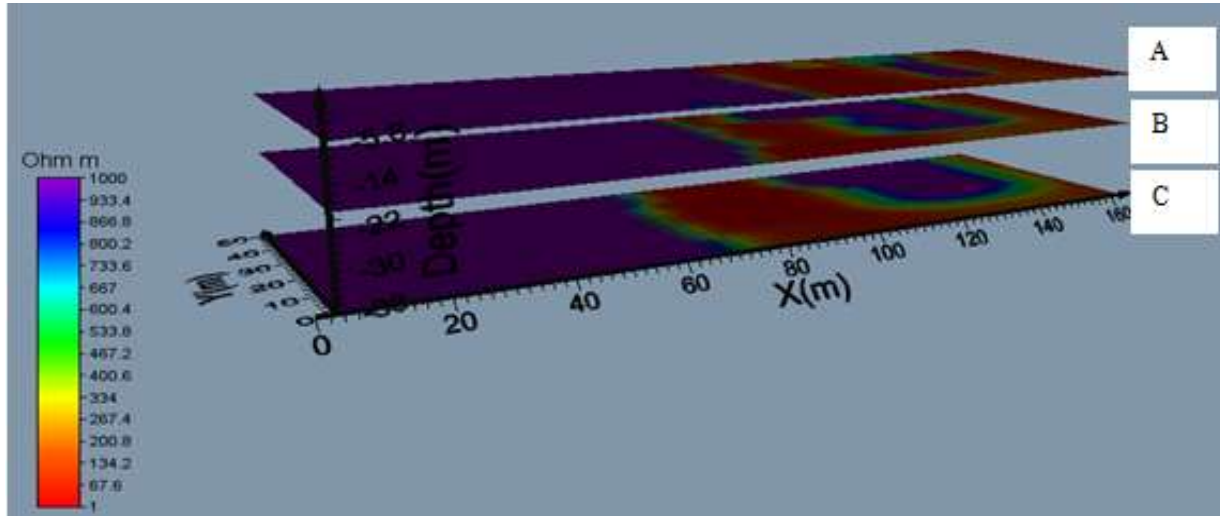


Fig. 4.45: 3D Slice of Ikheuniro Dumpsite at 5m, 18m and 38m depth

4.6.2 Results from Capitol Dumpsite (CA 1)

The 3D models obtained from the inversion of the resistivity data set are displayed as horizontal slices as shown in Figs. 4.46 - 4.47. The three profiles obtained at Capitol dumpsite were used to interpret slices A, B and C. The inverse section of slice A shows several anomalies at depths of about 1m and this is shown in Fig. 4.46. We interpret these low resistivity ($20\Omega\text{m}$) anomalies (Red colour) to be the effect from conductor (leachate) at the subsurface. The high resistivity area near the surface is due to the drier upper sandy layers. At a depth of about 1m, the anomalies with low resistivity values are believed to be the presence of loosed sandy zone. Thus, the anomaly at 1m depths indicates that the soil is contaminated beyond 1m (Fig. 4.47). The slice (B) shows almost similar anomalies at a depth of about 22m and is as shown in Fig. 4.47. There is anomalous low resistivity value of $20\Omega\text{m}$ (red colour) which can be observed between 40m-84m mark on the profile to a depth of 38m of slice (C). This suggests that the surface soil down to 38m is contaminated this is shown in Fig. 4.46. A comparison of the results from the 3D slices A, B and C (Fig. 4.47) shows anomalies with resistivity value of less than $20\Omega\text{m}$ which is suspected to be leachate seeping down (38m) with similar profile range from ERT (2D) and VLF-EM images.

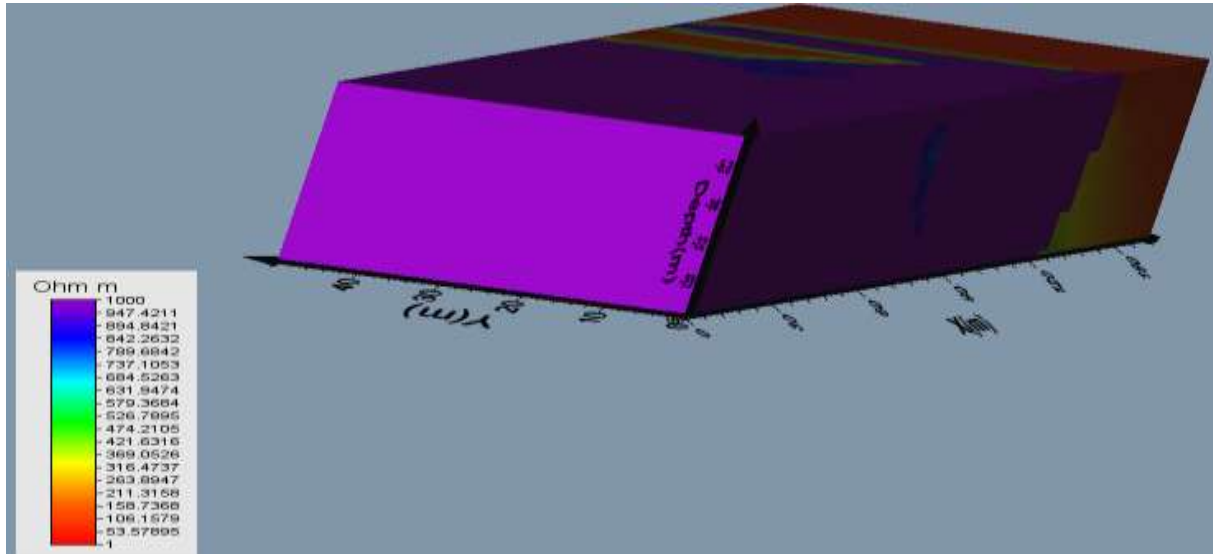


Fig. 4.46: 2D Slice of Capitol Dumpsite

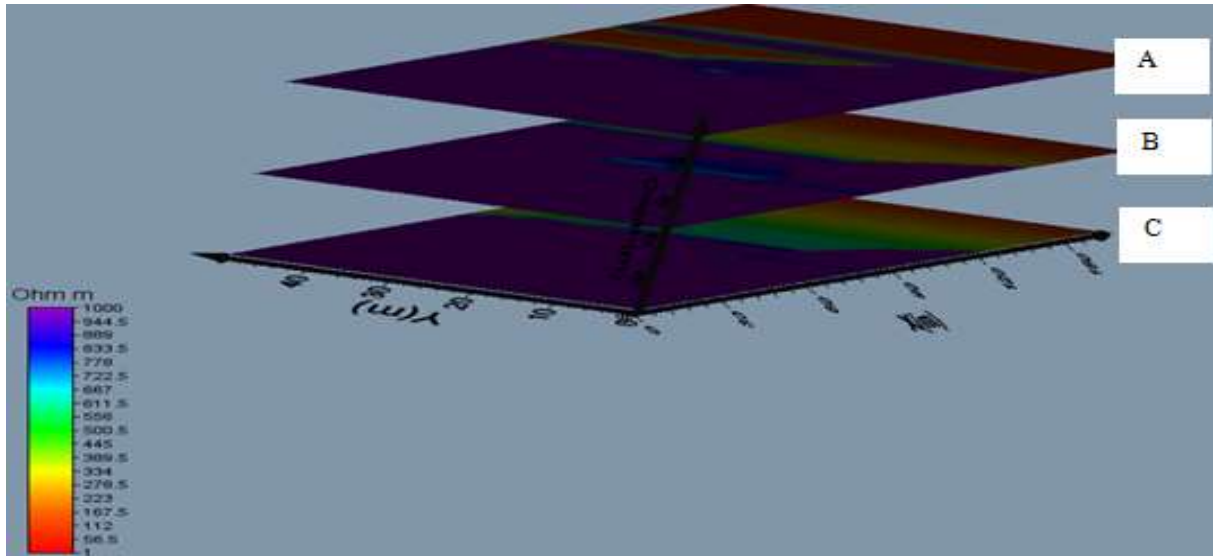


Fig. 4.47: 3D Slice of Capitol Dumpsite at 1m, 22m and 38m depth

4.6.3 Results from Oluku dumpsite

The 3D models obtained from the inversion of the resistivity data set are displayed as horizontal slices as shown in Figs. 4.48 - 4.49. The three profiles obtained at Oluku dumpsite were used to interpret slice A, B and C. The inverse section of slice A shows several anomalies at depths of about 8m as shown in Fig. 4.49. We interpret these low resistivity ($20\Omega\text{m}$) anomalies (Red colour) to be the effect from conductor (leachate) at the subsurface. The high resistivity area near the

surface is due to the drier upper sandy layers. At a depth of about 8m, the anomalies with low resistivity values are believed to be the presence of loosed sandy zone. Thus, the anomalies at 8m depths indicate that the soil is contaminated beyond 8m as shown in Fig. 4.49. The slice (B) shows almost similar anomalies at a depth of about 23m as shown in Fig. 4.49. There is anomalous low resistivity value of $20\Omega\text{m}$ (red colour) which can be observed between 80m - 160m mark on the profile to a depth of 38m of slice (C). This indicates that the surface soil down to 38m is contaminated as shown in Fig. 4.46. A comparison of the results from the 3D slices A, B and C (Fig. 4.49) shows anomalies with resistivity value of less than $20\Omega\text{m}$. This is suspected to be leachate seeping down (38m) with similar profile range from ERT (2D) and VLF-EM images.

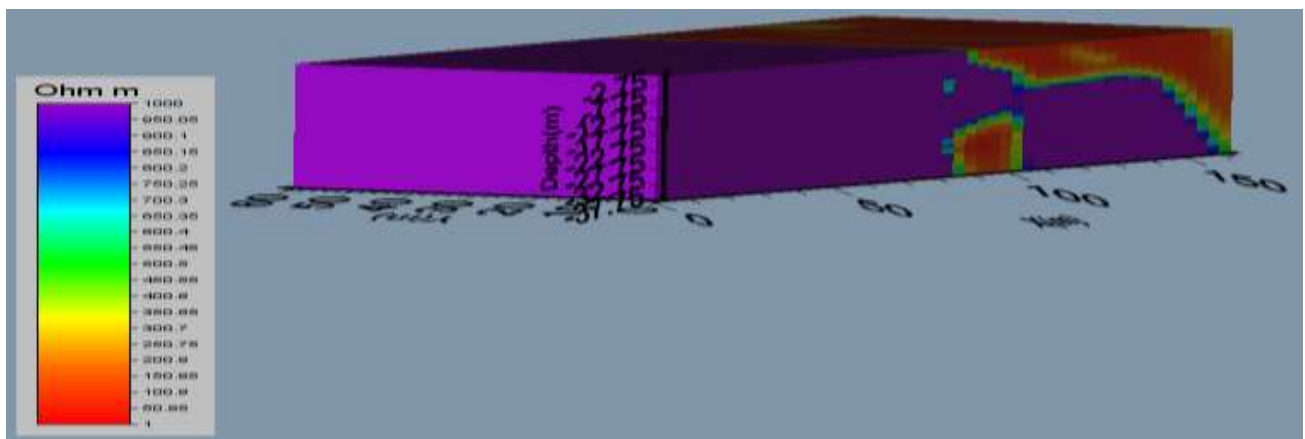


Fig. 4.48: 3D Slices of Oluku Dumpsite

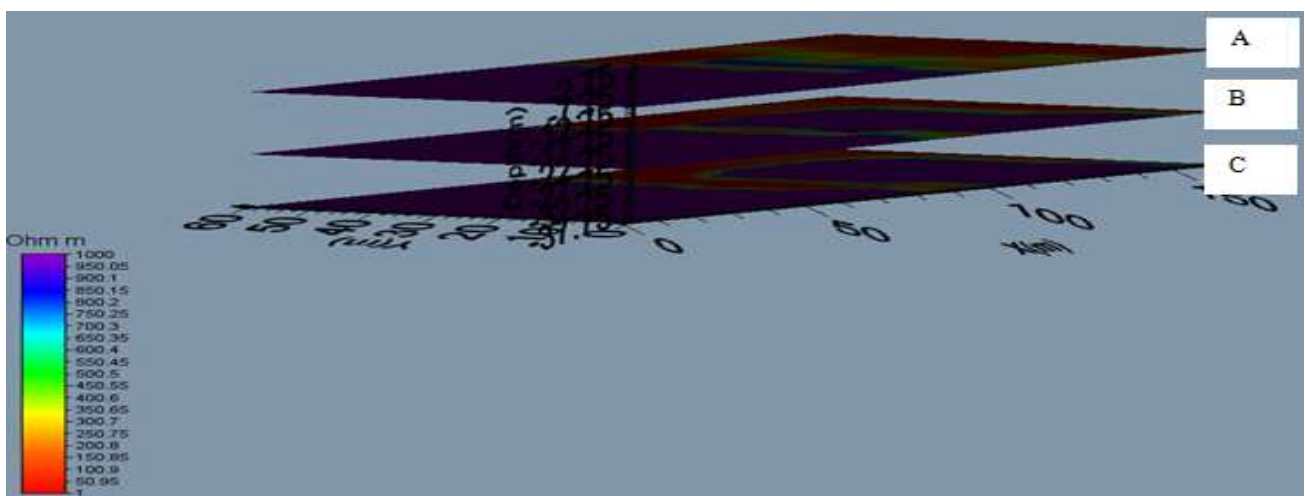


Fig. 4.49: 3D Slice of Oluku Dumpsite at 8m, 23m and 38m depth

4.7 Combination of research output

This study revealed that there are possible qualitative correlations that can be established between the geophysical results. The resistivity information used for the correlation only at 39.4m depth (from 2D plan view) and ABEM Wadi survey which included the electromagnetic wave with a high/low frequency (given information for shallower/deeper layer). Generally a good correlation between them has been observed in the shallower layer. Listed here are some of the observations: The VLF profile along PL7 (Fig. 4.11b) at Ikhueniro which corresponds to ERT 1 (Fig. 4.35) shows a very strong correlation of the contaminant plume within surface location 75m - 100m. Also the VLF profile along PL8 (Fig. 4.12b) at Ikhueniro which corresponds to ERT 2 (Fig. 4.36) shows a very strong correlation of contaminant plume within surface location 20m - 50m and weak zone at 125m. The VLF profile along PL9 (Fig. 4.13b) at Ikhueniro which corresponds to ERT 3 (Fig. 4.37) shows a very strong correlation of the contaminant plume within surface locations 20m - 50m and 100m - 130m. The VLF profile along PL5 (Fig. 4.19b) at Capitol which corresponds to ERT 1 (Fig. 4.38) shows a very strong correlation of subsurface contaminant plume within 20m - 50m, 35m - 45m and 60m - 70m. Also the VLF profile along PL6 (Fig. 4.20b) at Capitol which corresponds to ERT 2 (Figure 4.39) shows a very strong correlation of subsurface contaminant plume within 8m - 12m, 35m - 40m and 50m - 65m. The VLF profile along PL7 (Fig. 4.21b) at Capitol which corresponds to ERT 3 (Fig. 4.40) shows a very strong correlation of subsurface contaminant plume within 10m - 20m and 60m - 70m. The VLF profile along PL7 (Fig. 4.31b) at Oluku which corresponds to ERT 1 (Fig. 4.40) shows a very strong correlation of subsurface contaminant plume within 20m - 50m, 70m - 140m and 150m - 160m. Also the VLF profile along PL8 (Fig. 4.32b) at Oluku which corresponds to ERT 2 (Fig. 4.41) shows a very strong correlation of subsurface contaminant plume

between 16m - 45m, 50m - 110m and slightly fractured zone at 160m. The VLF profile along PL9 (Fig. 4.33b) at Oluku which corresponds to ERT 3 (Fig. 4.42) shows a very strong correlation of subsurface contaminant plume within 25m - 55m and slightly fractured zone at 160m. The electromagnetic results show an excellent correlation with the 2D resistivity profile. The images show a good correlation in dispersion of contaminant at the sites.

CHAPTER FIVE

SUMMARY, CONCLUSION AND RECOMMENDATION

5.1 Summary and Conclusion

Integration of geophysical methods has been used to assess the subsurface conditions of some municipal dumpsites in Benin City. Geophysical survey have been employed to obtain a 2D and 3D view of the current contamination scenario found at each dumpsite in Benin City. The existing boreholes data gives information regarding the lithological layers, expected depth of groundwater table. The geophysical methods employed in this study were able to map and delineate the contaminated plume (leachate) within the dumpsites. The integrated methods have proven to be tool for environmental assessment of waste site. The VLF and ERT revealed highly conductive zones with low resistivity (1 - 20 Ω m) of leachate to the depth of 39.4m (Figs. 4.4a - 4.45) beneath the surface which coincide with the upper section of the first aquifer in the area, an indication of complete submerge of the first groundwater aquifer harnessed by majority through shallow wells.

In the geophysical interpretation, the data was related to the deeper geological properties in the sites due to the presence of boreholes at Ikhueniro and Oluku at a distance of less than 40m and Capitol 400m from the dumpsites. The true resistivity model revealed anomalies with low near surface resistivity from the top soil down to a maximum depth of 39.4m. This study revealed that very low resistivity values may be associated with leachate. These low resistivities were prominent in locations within Ikhueniro and Oluku environs. The high resistivity values at the top soil correspond to the compacted dried nature of the unsaturated sandy formation as well as the decomposed organic materials within the formation.

The surface run off (flow direction) elevation contour map of the study areas revealed that the surface run off at Ikhueniro is toward the North and Northwestern part of the region. Based on the flow pattern of the surface run off system in Ikhueniro, borehole should be sited in the South and

Southwestern part of the area and not in the North and West regions in order to minimize groundwater contamination.

The surface run off elevation contour map of Capitol revealed that surface run off direction is toward the North and Northeastern region. Based on the flow pattern of the surface run off system in Capitol dumpsite, borehole should be sited in the South and Southeastern part of the area and not in the North and Eastern regions in order to minimize groundwater contamination.

The surface run off elevation contour map of Oluku dumpsite revealed that surface run off direction is toward the South and Southwestern region. Based on the flow pattern of the surface run off system in Oluku dumpsite, borehole should be sited in the North and Northwestern part of the area and not in the South and Western regions in order to minimize groundwater contamination.

This research did not only pave way for a clear picture of the hydrological knowledge of Benin land in other to create awareness on the productive and prolific aquifer for sustainable groundwater supply but act as guides to both the government and the individuals especially those involved in groundwater development and environmental management.

5.2 Recommendation

It is therefore recommended based on the appreciable results obtained from the study that boreholes for portable and sustainable water supply in the study areas should be drilled to a depth of above 40m to minimize surface water pollution. Furthermore, based on the flow direction/pattern of the surface run off system in the study areas, boreholes should be sited in the South and Southwestern parts of Ikhueniro, South and Southeastern parts of Capitol and South and Southwestern parts of Oluku in order to minimize groundwater contamination by the dumpsites. Finally, proper borehole location and construction of seal to prevent leachate from entering water

body is the key to avoiding contamination of drinking water. It is evident that water borne diseases are due to improper disposal of refuse, contamination of water by sewage and surface runoff. Therefore, programmes must be organized to educate the general populace on the proper disposal of refuse, treatment of sewage and the need to purify our water to make it fit for drinking. In areas lacking in tap water as in rural dwelling, educative programmes must be organized by researchers and government agencies to enlighten the villagers on the proper use and treatment of surface water. Finally, it is recommended that a groundwater monitoring programme to determine groundwater quality status of wells in the neighborhood of the study area be implemented by stakeholders to safeguard the health of innocent residents.

REFERENCES

- Adeoti L, Alilie O.M, Uchegbulam, O. (2010): Geophysical investigation of saline water intrusion into freshwater aquifers: A case study of Oniru, Lagos state. *Sci. Res. Essays*, 5: 248-259
- Alkali, S. C. (1995): "Resistivity measurement of the upper aquifer system around Lake Alau area. *Water Resources Journal*. 6 (1 & 2). 26-30.
- Alile O. M. Ujuanbi O. and Iyoha A. (2012): Geoelectrical Investigation of Groundwater Resources at Ikpoba Okha Local Government Area, Edo State, Nigeria. *Journal of Science and Technology*, 2(1) 41-46.
- Allen R.N. (2004): GLE 594: Introduction to Applied Geophysics. Retrieved from http://seismo.berkeley.edu/~rallen/teaching/F04_GE0594_IntroAppGeophys/Lectures/L10.pdf. (accessed on 12/11/2013)
- Anon, S. (2009): "Hydrogeological Implications in Solid Waste Disposal," *Bull. International Association Hydrogeol*, 146 - 158.
- Arlena Kowalska, Marta Kondracka and Maciej Jan Mendecki (2012): VLF Mapping and Resistivity Imaging of Contaminated Quaternary Formations Near To "Panewniki" Coal Waste Disposal (Southern Poland). *Acta Geodyn. Geomater.* 9, 4 (168). 473–480.
- Akujieze, C.N. (2004): Effects of Anthropogenic Activities (Sand Quarrying and Waste Disposal) on Urban Groundwater System and Aquifer Vulnerability Assessment in Benin City, Edo State, Nigeria. PhD Thesis, University of Benin, Benin City, Nigeria.
- Apkokoje, E. G. (1979): "The importance of engineering geological mapping" in the development of the Niger Delta Basin. *Bull.1 in Assoc. Eng. Geol.* 19 102-108.
- Archie, G. E. (1942): The electrical resistivity log as an aid in determining some reservoir characteristics. *Transactions of the American Institute of Mining and Metallurgical Engineers*. 146, 54-61.
- Arcone, S. A., Lawson, D. E., Delaney, A. J., Strasser, J. C. and Strasser, J. D. (1998): Ground penetrating radar, reflection profiling of groundwater and bedrock in an area of discontinuous permafrost: *Geophysics*, 63 (5). 1573-1584.
- Ariyo, S. O., Omosanya, K. O and Oshinloye, B. A. (2013): Electrical resistivity imaging of contaminant zone at Sotubo dumpsite along Sagamu-Ikorodu Road, Southwestern Nigeria. *African Journal of Environmental Science and Technology*. <http://www.academicjournals.org/AJEST>. 7(5). 312-320,
- Asseez, L. O. (1976): "Review of the stratigraphy, Sedimentation and Structure of the Niger Delta in geology of Nigeria" Elizabethan Publishing Co., Lagos Nigeria.

- Atekwana, E. A; Werkema, D. D. Duris, J. W; Rossbach, S; Atekwana, E. A; Sauck, W. A; Cassidy, D. P; Means J; & Legall, F. D. (1998): In situ apparent conductivity measurements and microbial population distribution at a hydrocarbon-contaminated site. *Geophysics* 69 (1). 56–63.
- Avbovbo, A. A. (1970): “Tertiary Lithostratigraphy of the Niger Delta Bull. American Association of Petroleum Geology 63. 295-306.
- Baines C.D. (2001): Electrical Resistivity Ground Imaging (ERGI): Field Experiments to Develop Methods for Investigating Fluvial Sediments, M.Sc. Thesis, Department of Geography, University of Calgary, Alberta. 20.
- Bentley L. R; Gharibi, M. (2004): Two- and three-dimensional electrical resistivity imaging at a heterogeneous remediation site. *Geophysics* 69 (3). 674–680.
- Beres, M; Green. A.G; & Pugin, A. (2000): Diapiric origin of the Chessel-Noville hills of the Rhone valley interpreted from georadar mapping: *Environ. Eng. Geoscience*. 6. 141-153.
- Burke, K. K. (1972): “long stone drift, Submarine Canyons and Submarine fans in the development of the Niger Delta A.A.P.G. Bull. 56. 1975-1983.
- Dahlin, T, & Zhou, B. (2002): Gradient and Mid-point referred measurements for multichannel 2-D resistivity imaging, *Procs. 8th meeting of the Environmental and engineering Geophysics, Aveiro, Portugal* 8 (12). 157-160.
- Depountist, N; Harris, C; Davics, M. C. R; Koukis, G; & Sabatakakis, N.(2005): Application of electrical imaging to leachate plume evolution studies under in-situ and model conditions. *Environmental Geo* 47. 907-914
- Dharmadhikari N.P, Meshram D.C, Kulkarni S.D, Kharat A.G, Sorate R.R, Pimplikar S.S. Narang Girish, Rajkumar Deshmukh, Dheeraj Sunil and Bangal C.B (2012): Use of Dowsing and Geo-Resistivity meter For Detection of Geopathic Stress Zone. *International Journal of Modern Engineering Research (IJMER)*. www.ijmer.com 1, (2). 609-614
- Dijkstra J, W. Broere and Van Tol, A. F (2012): Electrical resistivity method for the measurement of density changes near a probe *Geotechnique* 62 (8). 721–725
- Dingman, S. L. (2002): *Physical hydrology*, Second edition. New Jersey, Prentice Hall, Upper Saddle River
- Doran, J.W; Sarrantonio, M. and Liebig M, (1996): Soil Health and Sustainability. In: Sparks, D.L. (Ed.), *Advances in Agronomy*. Academic Press, San Diego, 56. 1-54.
- Doran, J.W. and Zeiss, M.R. (2000): Soil health and sustainability: managing the biotic component of soil quality. *Appl. Soil Ecol.* 15(3). 11.

- Edo State Ministry of Water Resources, (2012): Borehole Lithology in Benin City, Edo State Library, number 1240 Sapele Road, Benin City.
- Elijah Adebawale Ayolabi, Adetayo Femi Folorunso, Ayodele Franklin Eleyinmi, and Esther O. Anuyah (2009): Applications of 1D and 2D Electrical Resistivity Methods to Map Aquifers in a Complex Geologic Terrain of Foursquare Camp, Ajebo, Southwestern Nigeria. *The Pacific Journal of Science and Technology*. 10 (2).
- Environmental Protection Agency, UK (2011): What is contaminated land? Online available http://www.environmentalprotection.org.uk/land_quality/contaminated-land [Accessed 23 November 2011]
- Eswaran, H. R., Almaraz, E. van den Berg and Reich P. (1997): An assessment of the soil resources of Africa in relation to productivity. *Geoderma*, 77. 1-18.
- Etu-Efeotor, J.O. (1997): *Fundamentals of Petroleum Geology*. 111-123.
- Ewusi, A. (2006): *Groundwater Exploration and Management using Geophysics: Northern Region of Ghana*, Ph. D. Thesis, Faculty of Environmental Sciences and Process Engineering. International Course of Study: Environment and Resource Management, Brandenburg Technical University of Cottbus.16-27
- Ezeigbo, H. I; and Obiefuwa, G. I. (1995): “An Evaluation of the groundwater resources of Ogbunike area and environs, Anambra State, South - Eastern Nigeria. *Water Resources*. 6 (1). 31-42.
- Forté, S. (2011): *Mapping Organic Contaminant Plumes in Groundwater Using Spontaneous Potentials*, Ph. D. Thesis, Department of Geoscience, University of Calgary, Alberta. 132.
- Foster A. R; Veath, M. D. & Baird, S. L. (1986): *Hazardous waste geophysics. The Leading Edge*. 6. 8 - 13.
- Froese, D. G; and Clement, D. T. (2005): *Characterizing large river history with Shallow geophysics: Middle Yukon river, Yukon territory and Alaska. Geomorphology* 67. 391-406
- George V, Panayiotis T, Alexandros S, Ilias F, Dimitrios B and Nikolaos P. (2012): *A focusing approach to ground water detection by means of electrical and EM methods: The case of Paliouri, Northern Greece. Stud. Geophys. Geod.*, 56.
- Green, A. G; Lanz, E; Maurer, H; and Boerner, D. (1999): *A template for geophysical investigations of small landfills: The Leading Edge*, 18. 248 - 254.
- Herman, R. (2001): *An introduction to electrical resistivity in geophysics: Department of chemistry and physics. Radford University, Radford, Virginia* 24(1). 42.
- Hospers, J. (1965): “Gravity field and Structure of Niger-Delta” *Nigeria Geological Society American Bulletin*. 76. 407–422.

- Hussein H. Karim (2013): Characteristics of 2-D Electrical Resistivity Imaging Survey for Soil. Eng. & Tech. Journal, 31(19).
- Ibitola, M. N; Ehinola, O. A; and Akinigbagbe, A. E. (2011): Electrical Resistivity Method in Delineating Vadose and Saturated Zone in some Selected Dumpsites in Ibadan Part of South-Western, Nigeria. International Journal of Geomatics and Geosciences. 2(1).
- Iyoha, A; Akhirevbulu, O.E; Amadasun C.V.O and Evboumwan I.A. (2013): 2D Resistivity Imaging Investigation of Solid Waste Landfill Sites in Ikhueniro Municipality, Ikpoba Okha Local Government Area, Edo State, Nigeria. Journal of Resources Development and Management.1. 65–69.
- Karous, M; Hjelt, S.E. (1983): Linear-filtering of VLF dip-angle measurements. Geophysical Prospecting 31. 782–894.
- Kearey, P; Brooks, M; and Hill, Ian (2002): An Introduction to Geophysical Prospecting (3rd Ed.) Blackwell Scientific Publications, London, UK.
- Keller, G. V. and Frischknecht, F. C. (1970): “Electrical methods of geophysical prospecting” Pergamon press, New York. 96–517.
- Kirschmann, I. D. and Dunne, L. J. (1984): Nutrition Almanac. 2nd edition. New York. McGraw-Hill
- Klaassen, C. D. (2001): Ed. Casarett and Doull’s Toxicology: The Basic Science of Poison, 6th edition McGraw-Hill Publishing New York.
- Kogbe, C. A. and Assez, L. O. (1979) :”Geology of Nigeria, the Stratigraphy and Sedimentation of the Niger Delta” Elizabethan Publication, Lagos. 311-323.
- Lehmann, F. and Green, A. G. (2000): Topographic migration of georadar data: Implications for acquisition and processing. Geophysics 65. 836-848.
- Loke M.H. (1999): Electrical Imaging Surveys for Environmental and Engineering Studies: A Practical Guide to 2-D and 3-D Surveys.
- Loke, M. H. (2000): Electrical Imaging Surveys for environmental and engineering studies: A practical guide to 2-D and 3-D surveys. www.heritagegeophysics.com
- Loke,M.H.(2001):Tutorial:2-Dand3-DImaging Surveys.<https://pangea.stanford.edu/research/groups/sfmf/docs/DCResistivityNotes.pdf>. Accessed in Jan. 2012
- Loke, M. H. (2004): Electrical Imaging Surveys for environmental and engineering studies. <http://www.abem.sc>

- Maron, P. (1969): "Stratigraphical aspects of the Niger Delta" Nigeria Journal of Mining and Geology. 4(1 & 2). 3-12.
- McCurry, P. (1976): "The geology of the Precambrian to Lower paleogenic rocks of Northern Nigeria". A review in Kogbe, C. (ED) Geology of Nigeria. Elizabethan Publication Company, Ibadan Nigeria. (15-38).
- Majumdar, R. K, and Das, D. (2011): Hydrological characterization and estimation of aquifer properties from electrical sounding data in Saga Island region, South 24 Parganas, West Bengal, India Asian J. Earth Scie., 4. 60-74
- Martinho E, Almeida F, and Matias M. J. S. (2006): An experimental study of organic pollutant effects on some domain induced polarization measurements. Journal of Applied Geophysics. 60(1). 27- 40.
- McNeill, J. D., (1990): "Use of Electromagnetic Methods for Groundwater Studies," In Geotechnical and Environmental Geophysics, Vol. I, Review and Tutorial, Ward, S. H. (ed.) Soc. Explor. Geophy., Tulsa, OK. 191-218.
- Meju, A. (2000): Geoelectrical investigation of old abandoned covered landfill sites in urban areas: Modelled development with a generic diagnosis approach. Journal of Exploration Geophysics 44.
- Nasir Khalid Abdullahi, Isaac Babatunde Osazuwa, Abraham Onugba (2010): Detecting Municipal Solid Waste Leachate Plumes Through Electrical Resistivity Survey and Physio-Chemical Analysis of Groundwater Samples. Journal of American Science. 6(8). 540-548.
- Nielsen F. H., Hunt, C. D. Mullen, L. M. & Hunt, J. R. (1987): Effect of Dietary Boron on Mineral, Estrogen, and Testosterone and Metabolism in Postmenopausal Women. 394-397.
- Nwankwo, L. I. (2011): 2D resistivity survey for groundwater exploration in a hard rock terrain: A case study of MAGDAS observatory, UNILORIN, Nigeria. Asian J. Earth Sci., 4. 46-53
- Ogungbe A.S, Ogabi C.O. and Umar A.A. (2012): Assessment of the Impact of Municipal Solid Waste Landfill on Groundwater using Neighbouring, Opposite and Cross Methods of Electrical Impedance Tomography (EIT): Case study of Solous III, Lagos, Nigeria New York Science Journal. 5(9). 44
- Okoronkwo, N. Igwe, J. C. and Onwuchekwa, E. C. (2005): "Risk and health implications of polluted soils for crop production. 'Africa Journal of Biotechnology' 4 (13), P. 1521-1524
- Olawofela J.A, Akinyemi. O.D and Ogungbe A.S (2012): Imaging and Detecting Underground Contaminants in Landfill Sites Using Electrical Impedance Tomography (EIT): A Case Study of Lagos, Southwestern, Nigeria Research Journal of Environmental and Earth Sciences 4(3). 270-281

- Oomkens, E. C. (1974): "Lithofacies relation in late Quaternary Niger Delta Complex" 21. 115-222.
- Oseji, J. O; Asokhia, M. B. and Okolie, E. C. (2006): "Determination of groundwater potential in Obiaruku and Environs using surface geoelectric sounding". The environmentalist Springer Science Business Media Netherlands, 26. 301-308.
- Osemeikhian J.E.A & Asokhia M.B. (1994): Applied Geophysics. Samtos Services LTD, 26 Ilupeju Rd., Palm-Grove, Lagos, Nigeria.
- Otobo Egwebe; Aigbogun, C O; Ifedili, S. O (2007): Geoelectrical Evaluation of Waste Dump Sites at Warri and its Environ, Delta State, Nigeria J. Appl. Sci. Environ. Manage. 11 (2). 61-64.
- Oyedele, K. F. (2001): "Hydro geophysical and hydro geochemical investigation of groundwater quality in some parts of Lagos, Nigeria. African Journal of Environmental studies, 1(4). 31-37.
- Ozegin K.O, Ataman O. J and Jegede S. I (2017): Dumpsite Characterisation in Ekpoma from Integrated Surface Geophysical Methods. Physical Science International Journal. 15(4).1-11
- Pantelis S, Nikos P, Ilias P, Maria K, Filippou V, Apostolos S and Thrassyvoulos M (2007): Application of integrated methods in mapping waste disposal areas Springer-Verlag
- Powers, C. J; Hacni, F. P. and Smith, S., (1999): Integrated use of continuous seismic reflection profiling and ground-penetrating radar methods at John's Pond, Cape Cod. Massachusetts: Ann. Symp. Environ. Engin. Geophys. Soc. (SAGEEP), Proceedings. 359 - 368.
- Reyment, R.A (1965): Aspects of the Geology of Nigeria. University of Ibadan Press. Nigeria.
- Samouelian A., Cousin I., Tabbagh A., Bruand A., Richard G. (2007): Electrical Resistivity Survey in Soil Science: a review. Web accessed 16th August 2010. [http://www.hal.insu.achives-ouvertes.fr/docs/00/06/69/p2/PDF/Ary.Bruan-2006-soil Tillage Research.pdf](http://www.hal.insu.achives-ouvertes.fr/docs/00/06/69/p2/PDF/Ary.Bruan-2006-soil_Tillage_Research.pdf).
- Senos M. M; Marques da Silva. M; Eerreira, P., & Ramalho, E., (1994): A geophysical and hydrogeological study of aquifer contamination by a landfill: J. Appl. Geophys., 32. 155-162."
- Short K. C., Stauble AJ (1967): Outline of the Geology of the Niger Delta. AAPG Bull. 51. 761-779.

- Smith, D.V; Wright, D. L. and Abraham, J. D. (2000): Advances in early time electromagnetic (VETEM) system data analysis and image proceedings. Ann. Symp. Environ. Engin. Geopys. Soc. (SAGEEP), Proceedings. 469-475
- Sunmonu L.A, Olafisoye E.R., Adagunodo T.A., Ojoawo I.A. And Oladejo O.P. (2012): Integrated Geophysical Survey In A Refuse Dumpsite Of Aarada, Ogbomoso, Southwestern Nigeria. IOSR Journal of Applied Physics (IOSRJAP). 2(5). 11- 20.
- Tattam, C.M. (1943) A Review of Nigerian Stratigraphy. Research and Educational Development of the Geological Survey of Nigeria. 26-27.
- Telford W.M; Geldart L.P. and Sheriff R.E. (1990): *Applied Geophysics*. Shahrood University Central Library.
- Todd D. K. and Mays L. W. (2005): Groundwater Hydrogeology (3rd edition) New York, John Wiley and Son Inc.
- Triantafilis J, RoeJ.A.E, Monteiro F. A, and Santos F. (2006): Detecting a leachate plume in an aeolian sand landscape using a DUALEM-421 induction probe to measure electrical conductivity followed by inversion modelling. Soil Use and Management Journal, 27. 357-366.
- Ufuah, M. E; Odin, E. M. & Edokpolo, O.O. (2004): Analysis of Chemical Substances Affecting Water Quality Along Ikpoba River in Edo State, Nigeria. Zuma Journal of Pure and Applied Sciences. 6 (1).
- Ward, S.H. (1990): "Resistivity and Induced Polarization Methods," Geotechnical and Environmental Geophysics, 4(12). 147-190.
- Wisén, R; Dahlin, T. and Bernstone, C, (1999): Resistivity and inductive electromagnetic for delineation studies of Leakage from a waste deposit in southern Sweden: 5th Ann. Mtg., Environ. Engin. Geophys. Soc, Europ. Sect. Proceedings. [www.google](http://www.google.com) earth com retrieved March, 2014
- Wynn, J. and Gettings, M. (2000): An Airborne Electromagnetic (EM) Survey Used to Map the Upper San Pedro River Aquifer, Near Fort Huachuca in Southeastern Arizona
- Yalo Nicaise, Lawson Messan and Adihou Consolas (2013): Geophysical Contribution for Mapping the Contaminant Plume of Leachate from Rubbish Dumpsite of Hevie, Benin. British Journal of Applied Science & Technology 4(1). 127-143
- Zhou W; Beck B.F. & Stephenson J. B. (2000): Reliability of Dipole-Dipole Electrical Resistivity Tomography for Defining Depth to Bedrock in Covered Karst Terranes. Environmental Geology 37(7).
- Zume, J.T; Tarhule, A. and Christenson, S. (2006): Subsurface imaging of an abandoned solid waste landfill site in Norman, Oklahoma. Groundwater Monitoring and Remediation, 26. 62–69.